



University of Kentucky
UKnowledge

Theses and Dissertations--Mining Engineering

Mining Engineering

2015

KOREAN ANTHRACITE COAL CLEANING BY MEANS OF DRY AND WET BASED SEPARATION TECHNOLOGIES

Majid Mahmoodabadi
University of Kentucky, mma258@g.uky.edu

[Right click to open a feedback form in a new tab to let us know how this document benefits you.](#)

Recommended Citation

Mahmoodabadi, Majid, "KOREAN ANTHRACITE COAL CLEANING BY MEANS OF DRY AND WET BASED SEPARATION TECHNOLOGIES" (2015). *Theses and Dissertations--Mining Engineering*. 18.
https://uknowledge.uky.edu/mng_etds/18

This Master's Thesis is brought to you for free and open access by the Mining Engineering at UKnowledge. It has been accepted for inclusion in Theses and Dissertations--Mining Engineering by an authorized administrator of UKnowledge. For more information, please contact UKnowledge@lsv.uky.edu.

STUDENT AGREEMENT:

I represent that my thesis or dissertation and abstract are my original work. Proper attribution has been given to all outside sources. I understand that I am solely responsible for obtaining any needed copyright permissions. I have obtained needed written permission statement(s) from the owner(s) of each third-party copyrighted matter to be included in my work, allowing electronic distribution (if such use is not permitted by the fair use doctrine) which will be submitted to UKnowledge as Additional File.

I hereby grant to The University of Kentucky and its agents the irrevocable, non-exclusive, and royalty-free license to archive and make accessible my work in whole or in part in all forms of media, now or hereafter known. I agree that the document mentioned above may be made available immediately for worldwide access unless an embargo applies.

I retain all other ownership rights to the copyright of my work. I also retain the right to use in future works (such as articles or books) all or part of my work. I understand that I am free to register the copyright to my work.

REVIEW, APPROVAL AND ACCEPTANCE

The document mentioned above has been reviewed and accepted by the student's advisor, on behalf of the advisory committee, and by the Director of Graduate Studies (DGS), on behalf of the program; we verify that this is the final, approved version of the student's thesis including all changes required by the advisory committee. The undersigned agree to abide by the statements above.

Majid Mahmoodabadi, Student

Dr. Rick Honaker, Major Professor

Dr. Thomas Novak, Director of Graduate Studies

KOREAN ANTHRACITE
COAL CLEANING BY MEANS OF DRY
AND WET BASED SEPARATION TECHNOLOGIES

THESIS

A thesis submitted in partial fulfillment of the
requirements for the degree of Master of Science in Mining
Engineering in the College of Engineering
at the University of Kentucky

By

Majid Mahmoodabadi

Lexington, Kentucky

Director: Dr. Rick Q. Honaker, Professor of Mining Engineering

Lexington, Kentucky

2014

Copyright © Majid Mahmoodabadi 2014

ABSTRACT OF THESIS

KOREAN ANTHRACITE COAL CLEANING BY MEANS OF DRY AND WET BASED SEPARATION TECHNOLOGIES

Korean coals are typically high rank anthracite characterized by high ash content and difficult cleaning characteristics. The main objective of the study was to evaluate the feasibility of treating various size fractions within the coal using an assortment of physical coal cleaning technologies. Dry cleaning is preferred due to the friability of the coal. As such, three pneumatic processes were tested including Ore Sorting for the plus 10 mm material, Air Table Separation for 10 x 1 mm fraction and Tribo-electric Separator for - 1 mm fraction. The Dense Medium Cyclone is known to be one of the most efficient separation processes and thus was evaluated for the cleaning of 10 x 1 mm coal.

To realize the optimum performances from the Air Table and Rotary Tribo-electric Separator, their operational variables were systematically studied using a parametric experimental design. In addition, the dense medium cyclone and X-ray Transmission Sorting trials were performed under various medium densities and separation settings, respectively. A comparison of the cleaning performance revealed that the Dense Medium Cyclone and X-ray Transmission Sorting proved to provide the most effective results

with maximum ash rejection and combustible recovery. The tribo-electric separation process was ineffective while the air table provided modest ash reduction potential.

Key words: dense medium cyclone, pneumatic riffle table, X-ray transmission sorter, Rotary tribo-electric separator, Coal cleaning.

Majid Mahmoodabadi

Date

KOREAN ANTHRACITE COAL
CLEANING BY MEANS OF DRY AND
WET BASED SEPARATION TECHNOLOGIES

By

Majid Mahmoodabadi

Dr. Rick Q. Honaker
Director of Thesis

Dr. Thomas Novak
Director of Graduate Studies

DEDICATION

I dedicate this work to my father Ahmad Mahmoodabadi and my mother Zahra Mollaei who have supported me all the way since I was born. Also, this thesis is dedicated to my sister Marjan who has been a great source of motivation and inspiration. Without my family and their great supports, this work would not have seen the light of the day.

ACKNOWLEDGEMENTS

I would like to express my gratitude to Dr. Rick Q. Honaker for his valuable guidance and motivation throughout the course of this study. Gratitude is also extended to Dr. B. K. Parekh and Dr. Thomas. Novak from Department of Mining Engineering of University of Kentucky for their time, assistance and suggestions for their research.

I would like to extend my thanks to KIGAM (Korean Institute of Geoscience and Mineral Resources) for the financial and technical support which made this work possible.

Special appreciation is given to Ed Thompson due to his guidance and technical support in this project. I would also like to acknowledge Kathy Kitora, Megan Doyle, Joy McDonald and other department staff for their assistance.

Special thanks are given to all my friends, Hassan Amini, Mohammad Rezaee, Omid Omid, Abraham Najjar Zadeh, Tathagata Ghosh, and other graduate students for their support and friendship.

TABLE OF CONTENTS

ACKNOWLEDGEMENTS	III
TABLE OF CONTENTS.....	IV
LIST OF TABLES	VIII
LIST OF FIGURES	XI
CHAPTER 1 INTRODUCTION	1
1.1 Preface.....	1
1.2 Goals and Objectives	3
1.3 Thesis Outline	5
CHAPTER 2 LITERATURE REVIEW	6
2.1 Introduction.....	6
2.2 Dry Based Anthracite Cleaning Technologies.....	7
2.2.1 Introduction.....	7
2.2.2 Pickers.....	9
2.2.2.1 Pickers Applying Shape Differences	9
2.2.2.2 Pickers Applying Friction Coefficient Differences	11
2.2.2.3 Pickers Applying Specific Gravity and Friction Coefficient	12
2.2.2.4 Pickers Applying Shape and Friction Coefficient Differences.....	13
2.2.3 Air gravity Separators.....	14
2.2.3.1 Air Table	15

2.2.3.2	Air - Sand Process.....	16
2.2.3.3	Stump Air Flow Jig.....	17
2.2.3.4	AllAir Jig	19
2.2.4	Magnetic Separators.....	23
2.2.4.1	High gradient magnetic separator (HGMS).....	24
2.2.4.2	Open gradient magnetic separator (OGMS).....	25
2.2.4.3	Induced Roll Magnetic Separator	26
2.2.5	Electrostatic Separators.....	28
2.2.5.1	Conductive - Induction Separator	29
2.2.5.2	Corona Charging / Ion Bombardment.....	31
2.2.5.3	Tribo-Electrostatic Separator	32
2.2.5.3.1	Double Drum Separator	37
2.2.5.3.2	Rotary Tribo-electrostatic Separator.....	39
2.2.6	Dual Energy X-ray Transmission Sorting Technology	40
2.3	Wet Based Anthracite Cleaning Technologies	51
2.3.1	Introduction.....	51
2.3.2	Gravity Separators	52
2.3.2.1	Teeter Bed Separator (TBS).....	52
2.3.2.2	Wet Jig	57
2.3.2.3	Wet Concentration Table	59
2.3.2.4	Humphreys Spiral	62

2.3.2.5	Water Only Cyclone (WOC)	68
2.3.2.6	Heavy Media Separation.....	70
2.3.2.6.1	Introduction.....	70
2.3.2.6.2	Static Separators.....	71
2.3.2.6.3	Dynamic Separators	76
2.3.3	Froth Flotation	84
CHAPTER 3 EXPERIMENTAL.....		89
3.1	Introduction.....	89
3.2	Experimental Procedure of air table and dense medium cyclone	89
3.2.1	Particle Size and Washability Analysis	89
3.2.2	Experimental Approach, Dense Medium Cyclone	97
3.2.3	Experimental Approach, Air table	101
3.3	Experimental Procedure of Rotary Tribo-electric Separator (RTS) and Dual Energy X-ray Transmission Sorting Technology (DE-XRT)	106
3.3.1	Particle Size and Washability Analysis	106
3.3.2	Experimental Approach, Rotary Tribo-electric Separator (RTS).....	112
3.3.3	Experimental Approach, X-ray Transmission Sorting (XRT).....	115
CHAPTER 4 RESULT AND DISCUSSION		118
4.1	Introduction.....	118
4.2	Dense Medium Cyclone.....	120
4.2.1	Introduction.....	120
4.2.2	Phase 1	120

4.2.3	Phase 2	122
4.3	Air Table	123
4.4	Rotary Tribo-electric Separator	137
4.5	Dual Energy X-ray Transmission Sorting Technology	139
4.5.1	31.75 mm x 19 mm size fraction of raw feed	140
4.5.1.1	Rougher Unit.....	140
4.5.1.2	Cleaner Unit	142
4.5.1.3	Overall circuit	145
CHAPTER 5	SUMMARY AND CONCLUSION	150
APPENDICES	155
REFERENCES	172
VITA	177

LIST OF TABLES

Table 2.1 Cleaning performance of AllAir jig.....	23
Table 2.2 Mean size of magnetite samples used for evaluating effect of magnetite size on medium stability and viscosity	82
Table 3.1 Particle size and ash distribution of nominally coarse (8 x 4 mm) Korean anthracite coal sample	90
Table 3.2 Particle size and ash distribution of nominally fine (5 x 1 mm) Korean anthracite coal sample	91
Table 3.3 Density-by-density weight and ash distribution data of the obtained coarse (+ 0.6 mm) Korean anthracite coal sample	93
Table 3.4 Density-by-density weight and ash distribution data of the obtained fine (+ 0.212 mm) Korean anthracite coal sample	93
Table 3.5 Operating parameters and their respective value ranges evaluated in the statistically-designed test program conducted on the air table for the treatment of the 8 x 4 mm Korean coal sample.....	103
Table 3.6 Operating parameters and their respective value ranges evaluated in the statistically-designed test program conducted on the air table for the treatment of the 5 x 1 mm Korean coal sample.....	104
Table 3.7 Particle size and ash distribution for coal sample treated by Rotary Tribo-electric Separator (RTS) and Dual Energy X-ray Transmission Sorting Technology (DE-XRT).....	107
Table 3.8 Washability data for the 63.5 x 31.75 mm size fraction used to assess the Dual Energy X-ray Transmission Sorting (DE-XRT) process	108
Table 3.9 Washability data for the 31.75 x 19 mm size fraction used to assess the Dual X-ray Transmission Sorting (DE-XRT) process	108

Table 3.10 Washability data for the 63.5 x 19 mm size fraction used to assess the Dual Energy X-ray Transmission Sorting (DE-XRT) process	109
Table 3.11 Washability data for the 1 x 0.15 mm size fraction used to assess the Rotary Tribo-electric Separator (RTS) process.....	109
Table 3.12 Operating parameters and their respective value ranges evaluated in the statistically-designed test program conducted on the Rotary Tribo-electric Separator (RTS) for the treatment of fine size fraction of Korean Anthracite coal sample	113
Table 4.1 Dense medium cyclone analytical data achieved on 1.70, 1.75, 1.85 and 1.90 specific gravities.....	121
Table 4.2 Separation performance summary achieved by a dense medium cyclone treating 6 x 1 mm Korean coal	123
Table 4.3 Analysis of variance of product yield for coarse sample cleaned by Air Table.....	125
Table 4.4 Analysis of variance of combustible recovery for coarse sample cleaned by Air Table	125
Table 4.5 Analysis of variance of product ash for coarse sample cleaned by Air Table.....	126
Table 4.6 Optimum operational parameters and their effect on Product Yield of coarse sample cleaned by Air Table.....	130
Table 4.7 Optimum operational parameters and their effect on Product Ash content of coarse sample cleaned by Air Table	130
Table 4.8 Optimum operational parameters and their effect on Combustible Recovery of coarse sample cleaned by Air Table	131
Table 4.9 Analysis of variance of product ash for fine sample cleaned by Air Table.....	132
Table 4.10 Analysis of variance of combustible recovery for fine sample cleaned by Air Table	132

Table 4.11 Analysis of variance of product ash for fine sample cleaned by Air Table.....	133
Table 4.12 Optimum operational parameters and analytical results of fine sample cleaned by Air Table.....	137
Table 4.13 Analytical results achieved in rougher stage of DE-XRT over three separation settings	140
Table 4.14 Partition curves parameters obtained from performances of rougher stage of DE-XRT over three separation settings	142
Table 4.15 Analytical results achieved by DE-XRT cleaner stage over three separation settings.....	144
Table 4.16 Partition curves parameters obtained from performances of cleaner stage of DE-XRT over three separation settings.....	144
Table 4.17 Analytical results achieved by DE-XRT overall circuit over three separation settings.....	147
Table 4.18 Partition curves parameters obtained from performance of DE-XRT overall circuit over three separation settings.....	148

LIST OF FIGURES

Figure 1.1 Simulation of dry separation circuit used for cleaning Korean Anthracite coal.....	3
Figure 2.1 Flat Picker.....	10
Figure 2.2 Roller Picker.....	10
Figure 2.3 Ayers Picker	11
Figure 2.4 Spiral Picker	13
Figure 2.5 Berrisford Separator	14
Figure 2.6 Typical Air Table Separator	16
Figure 2.7 Fraser Air Sand Process.....	17
Figure 2.8 Stump Air Flow Jig	18
Figure 2.9 Four classical stages of jig strokes	20
Figure 2.10 Allair jig.....	21
Figure 2.11 Schematic exposition of the Allair jig.....	22
Figure 2.12 High Gradient Magnetic Separator.....	25
Figure 2.13 Operational principles of Open Gradient Magnetic Separator	26
Figure 2.14 Operational principles of Induced Roll Magnetic Separator	27
Figure 2.15 Structure of induced roll magnetic separator.....	27
Figure 2.16 Tilting angle induced roll magnetic separator	28
Figure 2.17 Different particles charging mechanisms: conductive-insulator separation process (a) and conductive-conductive separation process (b).....	30
Figure 2.18 Conductive-Induction Separators: Roll type (a) and Plate type (b)	31
Figure 2.19 Corona charging mechanism	32

Figure 2.20 Tribo-charging mechanisms: particle-particle charging (a) and particle-plate charging (b).....	33
Figure 2.21 Process of coal cleaning by use of tribo-electrostatic separator.....	34
Figure 2.22 Structure of Double Drum Electrostatic Separator.....	38
Figure 2.23 Process of coal cleaning by means of Rotary Tribo-electrostatic Separator.....	40
Figure 2.24 Operational principles of a belt type XRT based sorter	42
Figure 2.25 Transmission curve of mixtures with different PbS Grades at 83kV/50kV	44
Figure 2.26 Screenshot of Brightness Value Extraction from the Image by GIMP.....	46
Figure 2.27 Typical Dual Energy X-Ray Transmission Sorting calibration curve.....	47
Figure 2.28 Determination of high and low density zones of XRT calibration curve.....	48
Figure 2.29 Simulation of coal and shale representative sample by XRT calibration curve	49
Figure 2.30 Separation settings used in XRT experiments in manual preparation method.....	50
Figure 2.31 Operational fundamental of Teeter bed separator	54
Figure 2.32 Modified teeter bed separator	57
Figure 2.33 Baum Jig.....	59
Figure 2.34 Arrangement of particles with different size and density under effect of flowing film	60
Figure 2.35 Separation zones on wet concentration table.....	61
Figure 2.36 Humphreys spiral separator: cross section of rim (a) and full body of structure (b).....	63

Figure 2.37 Two stage circuit including: rougher-scavenger (a) and rougher-cleaner (b)	66
Figure 2.38 Compound cleaner spiral	67
Figure 2.39 Particles distribution inside the water only cyclone	68
Figure 2.40 Chance Cone separation machine.....	73
Figure 2.41 Conklin Process Separator.....	74
Figure 2.42 Teska vessel.....	76
Figure 2.43 Dynawhirlpool coal cleaner.....	78
Figure 2.44 Dense Medium Cyclone	80
Figure 2.45 Several parts of Dense Medium Cyclone	80
Figure 2.46 The effect of magnetite particle size on density differential of dense medium separation technologies.....	82
Figure 2.47 Effect of magnetite particle size on E_p of dense medium separation technologies.....	83
Figure 2.48 Typical separation process of flotation cell.....	85
Figure 2.49 Schematic representation of the equilibrium contact between an air bubble and a solid immersed in a liquid. The contact angle is the angle between the liquid/gas and the liquid/ solid interfaces, measured through the liquid	86
Figure 3.1 Near gravity curve for coarse size fraction of Korean Anthracite coal sample.....	94
Figure 3.2 Cumulative float yield and combustible recovery curves for coarse size fraction of Korean Anthracite coal sample	95
Figure 3.3 Amount of near-gravity curve material as a function of medium specific gravity for the fine Korean Anthracite coal sample.....	96
Figure 3.4 Cumulative float yield and combustible recovery curves for the fine size fraction of Korean Anthracite coal sample	96

Figure 3.5 Closed-loop dense medium cyclone circuit.....	98
Figure 3.6 Fifteen centimeter diameter Krebs dense medium cyclone.....	99
Figure 3.7 Dense medium cyclone circuit	99
Figure 3.8 Changes in the feed cleanability characteristics resulting from particle size degradation during feed recirculation in the dense medium circuit.....	100
Figure 3.9 Laboratory-scale air table separator with vibratory feeder and various other components	102
Figure 3.10 Modified air table with 1 mm aperture screen deck and discharge gates.....	102
Figure 3.11 Sample collection points, A, B, C, D and E located along the edge of air table	105
Figure 3.12 Cumulative float curves obtained from the coarse size fractions of the coal sample used for the tests involving the Dual Energy X-ray Transmission Sorting Technology (DE-XRT)	111
Figure 3.13 Recovery curve obtained from the coarse size fractions of the coal sample used for the tests involving the Dual energy X-ray Transmission Sorting Technology (XRT)	111
Figure 3.14 Cumulative float curve and recovery curve from washability analysis of the fine size fraction (1 x 0.15 mm) of coal sample used in the tests involving the Rotary Tribo- electric Separator (RTS)	112
Figure 3.15 Schematic of the separation zone in the Rotary Tribo-electric Separator showing the charged electrode plates and the direction of charged particles	114
Figure 3.16 Methodology used in the XRT sorting test program.....	116
Figure 3.17 Different DE-XRT settings used for cleaning coarse size fraction of Korean Anthracite coal sample.....	116
Figure 4.1 Separation efficiency factors as revealed by partition curves: (a) comparison of ideal separation and actual separation and (b) partition curve showing low density bypass to the high density stream.	119

Figure 4.2 Theoretical combustible recovery curve vs. practical combustible recovery curve for dense medium cyclone test.....	121
Figure 4.3 Partition curves obtained from dense medium cyclone performances when using medium specific gravity value.....	122
Figure 4.4 Effect of fan frequency (air flow rate) and transverse angle on product yield achieved from coarse sample by using Air Table.....	127
Figure 4.5 Effect of blower frequency (air flow rate) and transverse angle on achieved combustible recovery from coarse sample by using Air Table.....	128
Figure 4.6 Effect of blower frequency (air flow rate) and transverse angle on product ash content of clean coal of coarse sample cleaned by Air Table.	129
Figure 4.7 Effect of blower frequency (air flow rate) and table frequency on product yield achieved from fine sample using Air Table.....	134
Figure 4.8 Effect of blower frequency (air flow rate) and table frequency on combustible recovery achieved from fine sample using Air Table.....	135
Figure 4.9 Effect of blower frequency (air flow rate) and table frequency on product ash content of clean coal achieved from fine sample using Air table.	136
Figure 4.10 Partition curves obtained from performances of rougher stage of DE-XRT over three separation settings.....	142
Figure 4.11 Partition curves obtained from performances of cleaner stage of DE-XRT over three separation settings.....	145
Figure 4.12 Partition curves parameters obtained from performances of DE-XRT overall circuit over three separation settings.....	149

CHAPTER 1

INTRODUCTION

1.1 Preface

Anthracite is a high ranked coal distinguished from other type of coal by its brittle composition, great hardness, higher density, the most fixed carbon and calorific content, as well as the lowest moisture and volatile percentage. The lower amounts of volatile constituents demonstrate that anthracite formed during the process of bituminous to graphite conversion, through which the coal undergoes high degree of metamorphism and volatile matters partially removed. Therefore, high amount of fixed carbon results in an increase of hard grove index up to 110. The anthracite structure consists of approximately 5 percent moisture, 10 percent ash, 4 percent volatile matter, 1 percent sulfur, and 80 percent fixed carbon. In addition, the heating value varies from 12000 to 14000 Btu/lb, on an as-received basis containing both inherent moisture and mineral matter (Officer & Hamlin, 1993). Anthracite deposits contain more or less 1% of total earth coal reserves and principally used in either power generation or metallurgy industry, regarding their carbon content (Wilson, 2012).

Anthracite coal mining has played a significant role in US industry development due to potentially generating a great deal of energy. The Anthracite seam was initially discovered in 1760 in the Wyoming valley of Pennsylvania, but the mining and marketing did not become industrially utilized until the early 19th century, by when Wurtz brothers, Smith brothers, Beach, and Boyd, all known as pioneer companies in anthracite mining, started surface coal extraction at a continuous and industrial scale (Eckerd and Spencer 1971). The US ranks 7th internationally as the largest anthracite source with an estimated 60 billion tons of recoverable coal. These resources would remain around 38 years, considering 1.6 billion tons of production per year (Meister, 2009). China and Vietnam additionally produce 67 % of 500 million tons of total anthracite which annually is consumed worldwide (Wilson, 2012).

As countries develop and the amount of energy resources decline, the demand for high coal quality satisfying industrial and environmental requirements increases. Run - of - mine (Rom) coal contained incombustible minerals substantially reduce the coal quality and the amount of energy emitted per each pound of weight of product. Coal preparation is used as a separation stage between the raw coal and the market in order to minimize the amount of impurities by means of difference in the material physical properties e.g. specific gravity. Hence, the final achieved product would have upgraded quality and more combustible value compared to run - of -mine materials.

As a general procedure, raw coals are preliminary classified based on particle size, and then treated employing several wet and /or dry - based separators. An example of the dry separation potential is the X-ray transmission sorter which is widely utilized at a pre-separation stage to beneficiate the 60 mm to 6 mm particle size fraction in the preparation plant feed to avoid the costs of wet classification, separation, and dewatering. In this technique, particles are individually exposed to various energy levels of X-ray and separated based on their ability in attenuation intensity of radiated ray (Strydom, 2010). Another option is the air table which exploits density differences between coal and mineral matter to clean 75 mm to 6 mm coal using air as the medium. To pneumatically treat -1 mm, differences in tribo-electric charging between the coal and mineral matter can be exploited to achieve an effective separation.

Cleaning processes using water as a medium achieve efficient coal upgrading utilizing differences in particle density for particles greater than 0.15 mm and in hydrophobicity for particles smaller than 0.15 mm. Similar to dry coal treating processes, raw materials initially categorized based on their size are fed into the preparation plant. The coarsest fraction, has nominal size over +10 mm, is directed to Dense Medium Vessel. The intermediate size fraction which ranges between 10 mm and 1 mm in size is treated by Dense Medium Cyclones (DMC). The Spiral concentrator cleans the third largest particles sizing from 1 mm to 0.15 mm, while the finest size fraction (- 0.15 mm) is

purified by means of froth flotation process. The first three separators employ particles' settling direction and velocity differences, which is directly associated to their specific gravity, whereas the floatation process applies hydrophobic characteristic of particles to separate mineral matter from valuable particles.

1.2 Goals and Objectives

The aim of projected research has been established on investigating the feasibility of treating Korean anthracite coal by means of both dry and wet based lab scale processing technologies including: Air table (10 x 1 mm), Dense Medium Cyclone (10 x 1 mm), Rotary Tribo-electric separator (- 1 mm), and Dual Energy X-ray Transmission Sorting technology (+10 mm). The entire dry separation process could be simulated by a circuit drawn in the Figure 1.1. The trials were carried out in four different stages involving the treatment of several Korean coal samples possessing different particle size distribution and washability characteristics.

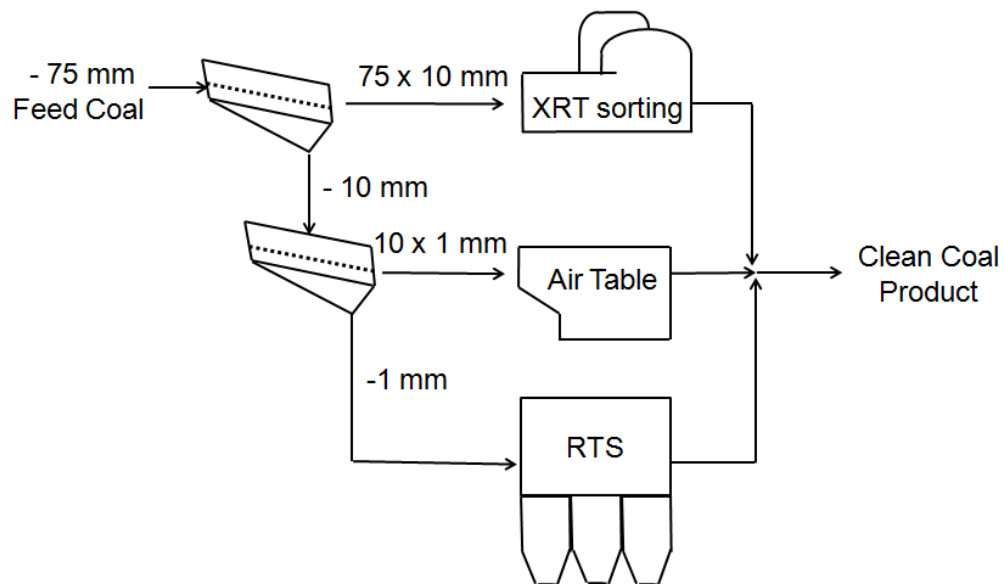


Figure 1.1 Simulation of dry separation circuit used for cleaning Korean Anthracite coal

The specific objectives of the research program are:

- To corroborate the laboratory applicability of the recently modified air table for enriching Korean coal. A series of tests, designed based on statistical method, were performed to study air flow rate, longitudinal and transverse angles, table frequency, and feed rate, to determine the optimum operational parameter values that provide the best separation performance.
- To demonstrate the potential of cleaning – 1 mm Korean anthracite coal using the Rotary Tribo-electric Separator (RTS). Similar to the above-described procedure, the operational factors of each test are determined by means of statistical design in which feed rate, charger rotation speed, charger voltage, and air flow velocity were studied. The ultimate objective was to identify the optimum conditions providing low ash content and high yield product.
- To evaluate the significance of performance-based empirical models attained from laboratory scale tests (regarding 95% statistical confidence) in order to determine whether any correlation existed between achieved data and operational parameters.
- To study the feasibility of upgrading Korean coal employing dense medium cyclone and Dual X-ray Transmission Sorter at several densities and settings, respectively.

Successful achievement of the objectives will provide the data needed to technically and economically assess the potential of the technologies to clean Korean anthracite coal. Ultimate outcome of the project will identify the technologies most favorable for upgrading Korean coal.

1.3 Thesis Outline

First chapter of this thesis discusses the properties of anthracite coal, and significant role of coal preparation in enhancing coal quality. The cleaning performance and operational principles of the most frequently used anthracite cleaning machines have been comprehensively discussed in chapter two. The procedure of analyzing raw feed materials, and conducting experiments were introduced throughout chapter three. The following chapter focuses on providing analytical results obtained by each of aforementioned devices. In addition, the achieved data have been thoroughly studied based on the operational principles of each associated machine. The last chapter summarizes the conducted study and briefly draws conclusions from experimental results.

CHAPTER 2

LITERATURE REVIEW

2.1 Introduction

The anthracite cleaning, from the beginning till now, has developed with introduction of new technologies for classification, separation and crushing. The early stages of anthracite preparation generally involved crushing particles by using hammer, as well as size classifying, and separating from slate by means of hand, rake (4.4 cm opening), and revolving screens. The major progresses of crushing made during 50 years period from mid to late 19th century, when coal breaker with circular screens, and several types of single and double rolls such as fluke, fluted, and teeth came into coal processing industry and greatly improved speed and efficiency of the breakage process.

There had been such a developing trend in anthracite crushing, size classifying and beneficiating by 1950, through which use of man power gradually was displaced with semi-machinery processes. The typical procedure of semi-machinery operation included separating coarse size particles from raw coal, and then breaking them down to finer fractions. Thereafter, the combination of crushed particles with rest of materials were passed through a set of screens (rotary, pentagon, gyratory, and shaker screens were invented and employed chronologically) for sizing. Finally, along the chutes, coal particles were separated from slates by hand picking (Ashmead, 1920) .Modern preparation plants for anthracite, of course, were greatly different from those of which were operated during 1840's. These sorts of plants employed semi-automated and continuous process systems, which were capable to produce clean coal with wide variety of size and quality. Since now, crushing and screening processes of anthracite cleaning have been remarkably improved, parallel with introduction of new versions of crushers and screens to coal preparation industry.

The need for apply a specific size specification which best fits the consumption necessities persuaded anthracite comity to approve a general size characterization on 1974(this classification is still being used). In this category, particles are classified into: Egg the top size in scale (3 inch), stove (2 inch), chestnut (1 inch), pea (3/4 inch); and buckwheat which is individually divided into 5 subgroups including No.1 (1/2 inch); No.2 (1/4 inch) known as rice; No.3 (1/8 inch), that commercially called barley; No. 4 (1/16 inch); and No.5 (1/32 inch) (Eckerd & Spencer, 1971). Buckwheat No.3 and No.4 are utilized as foamy slag or injection carbon for electric arc furnaces, Chestnut and Pea are used in carbon additive situations such as re- carbonization, ladle addition, and open hearth; while the coarsest size is consumed for charge carbon uses (Atlantic Coal plc., 2012). The prices of all sizes are more or less similar due their specialized utilization in specific industries. Each application accepted clean coal possessing a particular size and quality which established the importance of coal preparation.

Throughout this chapter, dry and wet-based coal preparation technologies, which have been most frequently used in anthracite beneficiation industry, will be discussed. The operational principles and cleaning performance of the processing devices are comprehensively reviewed in two separate sections. The first section discusses units belonging to the dry based separators category, while the following section focuses on machines classified into wet-based separators category.

2.2 Dry Based Anthracite Cleaning Technologies

2.2.1 Introduction

In spite of the fact that wet cleaning has dominated coal purification industry, due to conducting considerably high efficient separation, alternatively some modern types of dry based separators have recently been deployed in coal beneficiation industry. The reason is attributed to the fact that this sorts of separators provides coal producers with lower moisture content product, as well as more cost-effective and environmentally friendly

preparation processes. More clarification, dry cleaning becomes remarkably preferable to wet cleaning on several conditions, listed as:

1. Dry cleaning beneficially exploited in arid or semi-arid areas such as Africa, where lack of water resources limits or makes infeasible the use of wet separation.
2. Dry processes avoid the operational cost which is associated specifically to wet cleaning processes, such as solid filtration, flotation chemicals consumption, and waste water treatment.
3. Tailings generated in wet treatment process contain trace elements which pollute underground water resources. These elements are normally released after being oxidized.
4. In arctic areas such as Alaska where temperature falls down the water freezing point, the water absorbed by porous holes of coal is frozen and arise enormous handling difficulties (Houwelingen & De Jong, 2004).

The early days of anthracite beneficiation initiated by hand picking and screening as primary dry based sorting mechanisms. Since then, various dry separators have been employed in anthracite cleaning industry, which work based on different characteristics of particles. For instance, X-ray transmission sorter widely utilized as pre-separation stage to treat 6 mm to 60 mm size fraction of preparation feed plant in favor of declining subsequent classifying, separating, and dewatering cost. In this technique, particles are individually exposed to various energy levels of X-ray and separated based on their ability in attenuation of intensity of radiated ray (Strydom 2010). Air table applies density difference between coal and mineral matter to clean medium size fraction of coal (6-75 mm) using air as medium (Ghosh, 2013), while Tribo-electrostatic separator generally treats particles finer than 1 mm exploiting surface charge properties (Tao, Fan, & Jiang,

2008). Throughout the following sentences, several dry anthracite cleaning devices will be studied based on their operational fundamentals.

2.2.2 Pickers

The first attempts of dry separation involved in treat coal from slate by use of pickers. Several types of this machine were developed, which they employed differential friction coefficient, resiliency, specific gravity, and shape of particles to purify raw materials. Various versions of this machine apply one, two, or all aforementioned properties to treat coal particles. The First group relates to those machines which uses particles' shape differences as a mean of separation.

2.2.2.1 Pickers Applying Shape Differences

Naturally, coal and slate particles could be simply distinguished from each other based on their basic shape. The coal particles normally have cubical shape, while the following slate particles are flatter in appearance. Thus, the difference of shape can be applied as a well way to separate slate from coal. Flat pickers (Figure 2.1), as pioneer of shape based separators, were widely used to treat flat coal / slate from nut coal. These separators were installed at the discharged end of shaking screen, conveyers, or chutes. The separation principles of all of those were the same, in which flat coal / slate passed through openings, while the cubic coal particle rolled over the bars. Different types of flat pickers were categorized based on the arrangement and angle of slots / bars (Mitchell & Hewes, 1943).

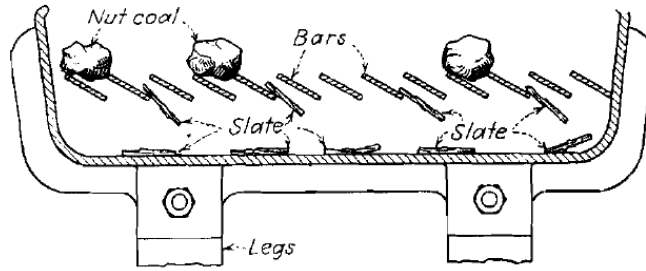


Figure 2.1 Flat Picker (Mitchell & Hewes, 1943)

Roller and Fredrick flat-slate pickers are identified as two other machines using the shape differences to upgrading anthracite nut size. The mentioned machines consist of several rotary rollers revolving in the same direction. The distance of rolls from each other was adjusted corresponding to thickness of slate particles which existed in raw feed. Figure 2.2 illustrates a roller picker in which the direction of flow is perpendicular to long axis of rolls. As the mixture of coal and slate particles were introduced to the machine, the flatter ones (slate) passed through openings, while the cubical particles rolled down towards the product discharge which located at lower end of machine. However, the Fredrick picker contained parallel inclined rolls. In this unit, raw materials flowed in the same direction as long axis of rolls and well dispersed on the deck, hence they were separated more efficiently from each other.

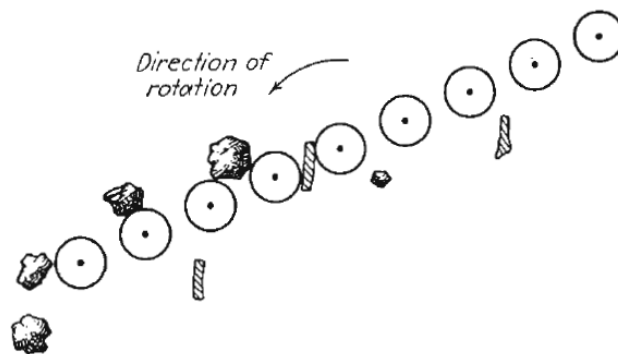


Figure 2.2 Roller Picker (Mitchell & Hewes, 1943)

2.2.2.2 Pickers Applying Friction Coefficient Differences

Second group of pickers are characterized by machines which only use frictional resistance to separate valuable particles from gangue. The first member of this group is known as Ziegler picker. The main part of machine is a sloping chute which contains several openings locating perpendicular to chute length. As particles travel along the chute, the slate ones move slowly and drop through slots, since they are exerted higher frictional resistance. Whereas, rounded coal particles jump over the gaps and move towards the discharge end (Mitchell & Hewes, 1943).

Ayers pickers, the other member of this family, employs an inclined belt moving in upward direction, to purify coal particle from accompanying tailings. Since slate particle are subjected to stronger fractional force, they stick to the surface of belt and are carried toward the top discharge. On the other hand, coal-lighter particles have less friction coefficient; hence they easily roll over the slates ones and travel to lower discharge end. (Ayres, 1909). This unit has been schematically depicted on the following figure.

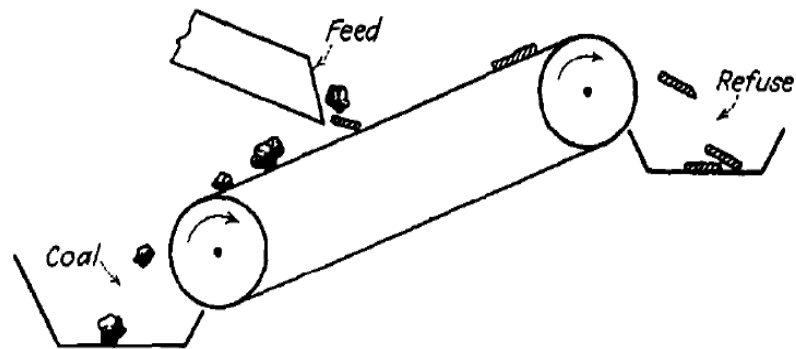


Figure 2.3 Ayers Picker (Mitchell & Hewes, 1943)

2.2.2.3 Pickers Applying Specific Gravity and Friction Coefficient

Spiral picker was the first dry gravity based separator introduced to anthracite cleaning industry (Figure 2.4). Structurally, the machine consists of a helical rout expanding along vertical axis. As particles travel along the spiral path, the lighter-low ash content particles are affected by more centrifugal force and less frictional force. Thus, these sorts of particles travel through the helical rout at higher speed and are shifted towards outer wall of spiral. However, heavier particles (slate) are exerted higher frictional force and moves at lower rate. Hence, these particles are inclined to inner wall. Thereby, two particles are separated based on their specific gravity and friction coefficient. Major advantages of spiral separator could be listed as high capacity and low operating cost (Ashmead, 1920).

The applicability of the mentioned unit was primary assessed through running laboratory scale experiments. The analytical results indicated that this machine managed to efficiently decrease the total ash content from 15 % to 1 %. In addition, approximately, 1 % of coal particles bypassed to slate stream. During experiment, clean coal particle were concentrated in right box mounted near outer wall of spiral. However, the slate particles were mostly gathered in left box which was installed close to inner wall (Ashmead, 1920).

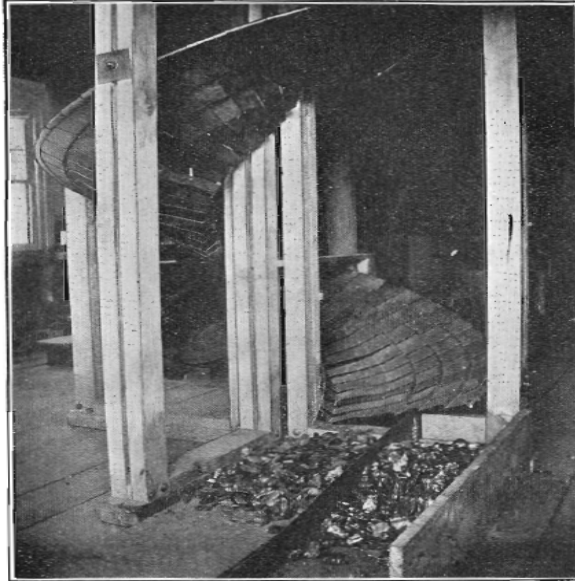


Figure 2.4 Spiral Picker (Ashmead, 1920)

2.2.2.4 Pickers Applying Shape and Friction Coefficient Differences

Berrisford separator, the most well-known member of this group, employs particles differential shape and friction coefficient/resiliency. The unit contains an inclined polished glass plate which the coal and slate are fed onto it and separated based on their resiliency. As shown on Figure 2.5, the flat slate particles tend to slip slowly towards the discharge end. During their journey, a specific gap is made between slates; due to these particles have more friction with plate, and thus fewer resiliencies. However, the coal particles have more resiliency and travel more rapidly along the length of plate. As these particles hit the plate, they jump off and travel more distance than slate while leaving the plate. Therefore, slate particles simply slide off the discharge end close by, whereas coal particles bounce off the plate and are reported to the gap which is located far away from discharge end (Alderman & Snoby, 2001).

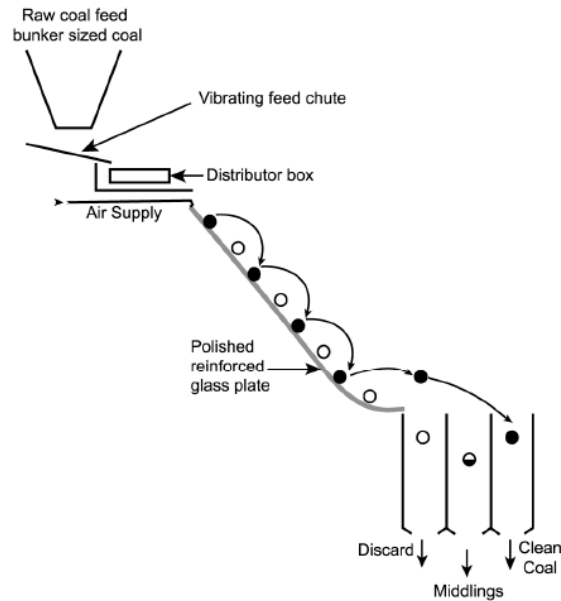


Figure 2.5 Berrisford Separator (Alderman & Snoby, 2001)

2.2.3 Air gravity Separators

A large group of concentrating devices use air as the separating medium to beneficiate valuable minerals from gangues. The first cleaning air gravity separating unit was American pneumatic separator, or table that initially developed in purpose of seed preparation. Thereafter, Henry M. Sutton, Walter L. Steele and E. G. Steele introduced the prime industrial scale air table which was capable of treating coal. Several types of machines that use air as mean of separation were developed by 1930 (Mitchell D. R., 1942). These devices are classified generally into four groups:

1. Stationary devices with pulsating air currents. The separating zone is usually riffled and air is supplied either by fans or compressors e.g. Air Jigs.
2. Stationary devices with continuous upward air currents. These machines submit the material to a continuous current of air, either horizontal or vertical. E.g. chaff is blown from wheat by such a device.

3. Reciprocating or vibrating devices with pulsating air. A small group in which the pulsating air is supplied by a fan and some motion provided in the separating surface to move the stratified material to various discharge points.
4. Reciprocating or vibrating devices with a continuous air supply, e.g. the American Pneumatic Separator (Houwelingen & De Jong, 2004).

The fundamentals of the above-named groups have been established on using combination of air, resiliency, friction, vibration, and specific gravity to facilitate treatment of coal from impurities (Mitchell D. R., 1942).

2.2.3.1 Air Table

Concentration table is the first dry gravity based anthracite separators which treats raw materials sizing finer than buckwheat. The machine contains of vibrating deck that has some openings which air produced by fan comes through. Particles are fed from a corner of deck and stratified by riffles located perpendicular to materials' flow direction. Riffles are also responsible for channeling high ash content particles to reject discharge end.

Principally, this unit applies upward continues air flow and vibrating motion to separate particles based on their differential specific gravity, resiliency, and friction coefficient. Air flow exerts a pushing upward force on raw materials which causes low ash-light particles to be lifted up. This type of materials jump over riffles and would not be affected by vibratory motion, hence they travel along the length of deck. However, the denser particles settle on the deck and are exposed to higher inertia (due to existence of high friction force between them and riffles). Consequently, the high ash content particles settle inside the gaps formed by riffles, are greatly affected by vibrating force (eccentric

force), and are pushed along the width of table (Ghosh, 2013). A typical version of this unit has been shown on Figure 2.6.

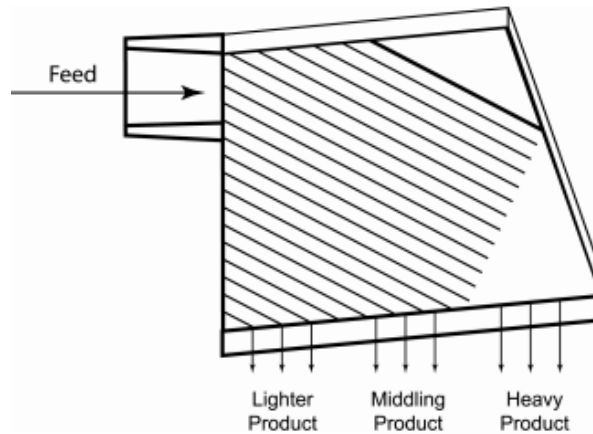


Figure 2.6 Typical Air Table Separator (Ghosh, 2013)

2.2.3.2 Air - Sand Process

In 1930, Fraser and Yancey developed a dry gravity separator known as Air - Sand Process which fundamentally resembles separation principles of heavy medium separators. The air flow is continuously blown from the bottom of machine through a perforated surface into separation chamber. The air upward velocity is set on a value as equal as settling velocity of sand particles, finer than 12 mesh size. Hence, air flow fluidizes sands particles and generates a teetered heavy bed. The bed density is more and less uniform throughout fluidization region, and relies between density of coal particles and impurities. Thus, low ash content coal particles are not able to pass through bed and are reported to overflow discharge, while tailings simply penetrates through the bed and sink at the bottom of machine (Figure 2.7). The medium density could be changed by varying air flow rate (Alderman & Snoby, 2001).

This machine initially designed to treat nut size anthracite coal in two separation stages including rougher and scavenger, so that the greater portion of coal particles to be

recovered. In 1935, air sand process unit was applied in a different arrangement in which raw materials primary were fed into a rougher compartment, and then product stream was directed to a cleaner device to be retreated. Tailing streams provided from these two machines were combined together and introduced to third compartment working as scavenger which recovered misplaced coal particles. The product of scavenger was recycled back to rougher, while the reject streams were completely discarded (Hall, Given, Edwards, Wooton, & McCarthy, 1936). During the process of separation, the machine typically circulates 3 tons of sand per every tons of cleaned coal, as well as losses 1.5 kg sand for each ton of raw feed being treated (Alderman & Snoby, 2001).

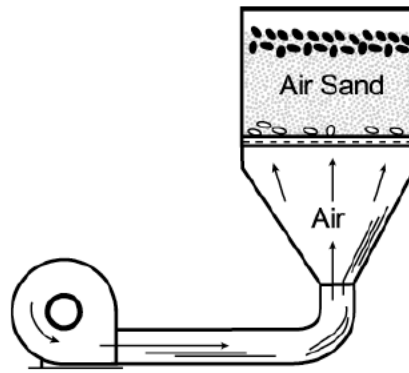


Figure 2.7 Fraser Air Sand Process (Alderman & Snoby, 2001)

2.2.3.3 Stump Air Flow Jig

In the early 1930's, the first stump air flow cleaner was introduced by Earl Stump, which was initially employed in pilot plant. At the same period, the prime industrial scale machine installed at the Barnes Coal Co., in central Pennsylvania. The separation region of machine typically consists of a reciprocating, inclined, porous deck, set over a bed of marbles to get air distribution facilitated throughout the deck (Figure 2.8). The pulsating air pass through openings up and repeatedly raise light particles, hence form a stratified bed in which coal is located on the top layer whereas high density, generally high ash

content particles settle on the lower layer. The refuse portion of feed is removed through three withdrawal lips, distributed along the deck at equal intervals and the middling part is removed by the fourth draw mounted at discharge end of deck (Mitchell D. R., 1942).

As thickness of refuse on the deck of the machine gradually increases towards the lower point, differential air resistance made over length of the deck which results in air short - circuiting. In order to keep resistance of the bed approximately constant, the marble pack progressively decreases in thickness from the feed to the discharge end. The first Stump Air Jigs were only 18 x 24 inch wide and able to clean low amount of materials. The design of machines has rapidly improved annually and resulted in wider devices with more capacity. The state - of - the - art model of this jig, known as ‘Super Air Flow’, is a 2.4 m wide deck machine with a capacity of up to 135 ton per hour of 50 mm x 0 feed per unit (Alderman & Snoby, 2001; Mitchell D. R., 1942). Among all industrial dry based beneficiating machines, the application of air Flow jig were outstandingly deployed comparing to other available separators due to the facts that this technology had high capacity and were capable of treating broad range size of materials with high efficiency.

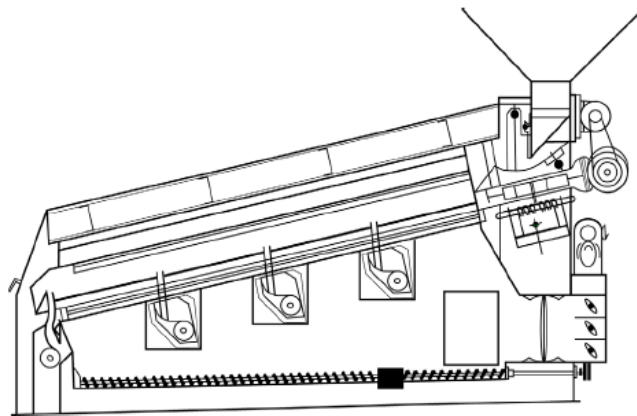


Figure 2.8 Stump Air Flow Jig (Alderman & Snoby, 2001)

2.2.3.4 AllAir Jig

The historical evidences demonstrate that the trend of developing new type of wet based separators were expedited rather than dry processing technologies, between mid-1930's and 2000. During this period, the conventional air gravity separators were modified while new types of these machines were never came into existence in coal processing industry. On early 21's, the high efficiency of wet jig in processing coal particles have motivated "All mineral company" to manufactures a dry based jig that exploits as same principles as applied in wet jigging. These principles are listed as:

- Differential Acceleration
- Free Settling
- Hindered Settling
- Consolidation Trickling
- Superimposed Pulsation Stroke

The total process of preparation is implemented via four sequent stages including:

1. Differential acceleration: Having particles thrown up from the surface of perforated deck, they initiate settling based on their density rather than their size. The reason is completely associated with the effect of drag force which is approximately deactivated at the beginning of settling motion. Thus, denser particles move same vertical distance than the lighter ones, regardless of their size.
2. Free settling: As particles travel more distance along the height of separation chamber, the drag force raises and effect of size difference becomes prominent. Hence, the falling velocity of the coarser particles increases more than finer ones.

3. **Hindered settling:** As the bed begins to compact, the particles collide and impede free settling. As a result, the effect of size differences on the particles' settling velocity is significantly exceeded.
4. **Consolidation trickling:** As the last stage of jigging process, fine, typically high-density particles pass through the voids made by coarser particles.

The aforementioned stages have been schematically illustrated on the following figure, in which the red spots representing low density materials, while the white one are corresponded to high density particles (Alderman & Snoby, 2001).

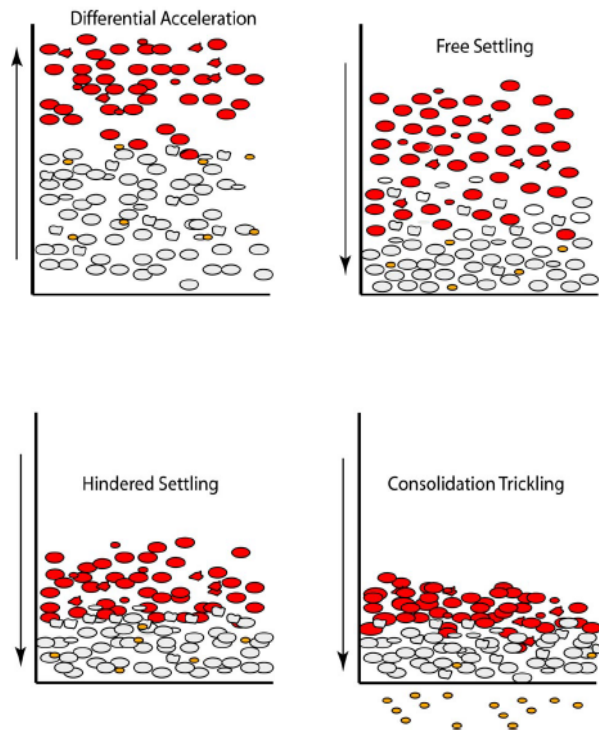


Figure 2.9 Four classical stages of jig strokes (Alderman & Snoby, 2001)

The engineered design of the AllAir jig has enabled the machine to properly employ the combination of aforementioned factors; hence it can effectively clean various sizes of particles ranging from wide to close. Particles are fed to a perforated deck through the surge hopper coupled with a variable speed star gate. This part could provide different volumetric feed rates, and uniformly distribute materials across width of the deck. Air, as the medium of cleaning, is imported to the separation area in two different forms including continuous flow, and a pulsated air flow. The supplied air is responsible for facilitating bed stratification and consolidation trickling. In order to prevent short-circuiting and bypass of coal to the refuse stream, the machine is equipped with a hutch design which work in conjunction with perforated deck. The cooperation of these parts provides uniform distribution of air throughout the deck by declining air turbulence, and number of dead spots. A pulsed air stroke is superimposed upon a constant stream of rising air currents, which allows the jig to control stroke amplitude, frequency and acceleration. Thus, stratification of the feed material is greatly enhanced (Alderman & Snoby, 2001) .

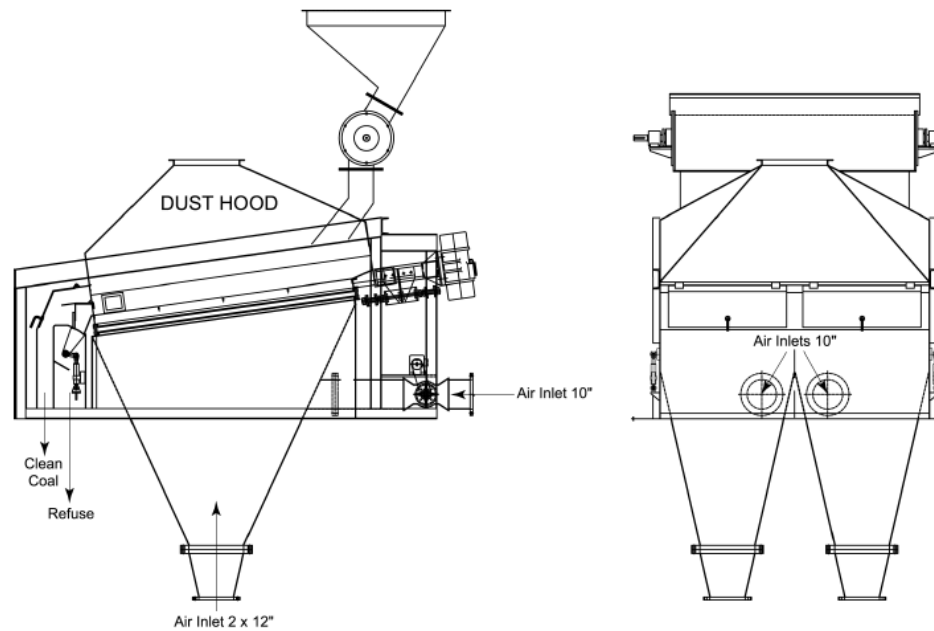


Figure 2.10 Allair jig (Alderman & Snoby, 2001)

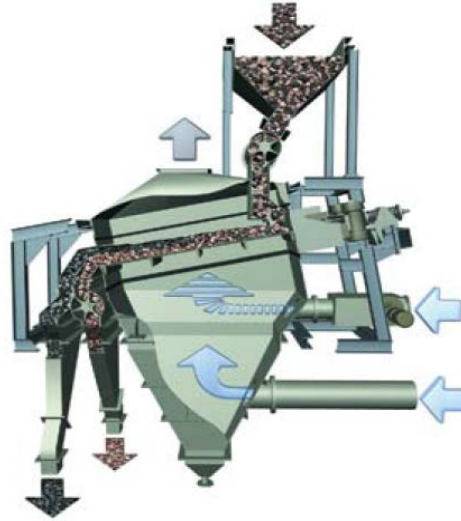


Figure 2.11 Schematic exposition of the Allair jig
(Weitkaemper & Wotruba, 2010)

One set of 50 t/hr AllAir jig has been employed at the OCL plant located in Rajgangpur, India to examine the applicability of the machine in beneficiation of high ash coal. Having conducted analysis tests, the feed material ranged between 40 to 5 mm and contained 40 % ash, 7.8 % moisture, and calorific value of 2,850 kcal/kg. In order to discover the correlation between the feed size and separation performance, the overall feed has been divided into two narrower size ranges varying from 40 mm to 13 mm and from 13 mm to 5 mm. Then, each size fraction was individually cleaned and the associated separation efficiencies were evaluated applying partition curve factors (generated through float-sink tests). Referring Table 2.1, the achieved data clearly indicates that the equipment managed to conduct more efficient treatment on finer size fraction, due to providing higher mass yield, and lower E_p value. Regarding the feed high ash percentage, difficulties of processing this type of coal, and obtained results, the AllAir jig has proved to treat the entire size fraction in an acceptable manner (Charan et al., 2011).

Table 2.1 Cleaning performance of AllAir jig (Charan et al., 2011)

Size, (mm)	40 - 13	13 - 5	Overall
Feed Ash (%)	41.30	37.60	39.60
Product Ash (%)	31.70	34.10	32.70
Tailings Ash (%)	61.20	62.50	61.20
Mass Yield (%)	67.50	86.90	75.80
Relative density of separation (d_{50})	1.82	1.62	1.87
Probable error (E_p)	0.12	0.08	0.18

2.2.4 Magnetic Separators

The immediate objective of coal magnetic beneficiation is set on lessening sulfur percentage of feed by extracting pyrite minerals mixed with coal particles. In industry, this process is called desulfurization. The principle of magnetic separation entirely established on applying differential magnetic characteristics of particles to conduct separation process. Naturally, coal is identified as diamagnetic material possessing weak magnetic susceptibility, which is repelled from magnetic field. On the contrary, some types of minerals matters (e.g. pyrite) consist of more and less amount of iron, which enhances their magnetization capability. Pyrite is a paramagnetic substance that would be attracted towards the poles if is exposed to high intensity magnetic field. As a result, pyrite is captured by magnetic field, while coal is repulsed from poles. In some minor cases, the extracted coal would be diluted with paramagnetic / ferromagnetic impurities, if the coal seam lies on between two hematite or magnetite layers. Regarding magnetic

specification of mineral matter, either high or low intensity magnetic separator is employed to purify coal from the followed rock.

Among all magnetic separators applied in mineral beneficiation industry, open gradient, induced roll, and high gradient magnetic separators have proved to produce more satisfactory results in coal beneficiation processes. Two first mentioned technologies particularly work on dry basis while the last one is capable of treating materials in both wet and dry conditions. Magnetic field gradient is defined as the number of lines moving from surface of one pole to the opposite magnet per unit of area. Thus, particles are exerted more attraction force when located in higher magnetic field gradient (Dwari & Rao, 2007).

2.2.4.1 High gradient magnetic separator (HGMS)

High gradient magnetic separator (HGMS), as conceive from its name, applies magnetic field changes (across the separation zone) to capture magnetic particles. A bunch of data was acquired from the several plants equipped with this technology, in order to evaluate the performance of unit in treating coal particles. Different materials with specific characteristics have been prepared by this machine that the maximum sulfur content of which reaches approximately 6.5 %, and ash content varying from 10 to 28 %. The HGMS has been able to decline materials' ash content 15 to 85 %, with 14 to 94 % sulfur removal. Likewise, the performance of machine has been found to be deeply depended on particle size range. Providing further clarification, excessive magnitude of fine particles in feed creates negative impact on separation efficiency due to enhancement of probability of particles agglomeration. To elucidate the correlation between particle size and HGMS treatment efficiency, feed materials containing various quantities of fine particles were cleaned. Comparing the obtained data, the highest efficiency would be achieved if the amount of fine particles ($-150\mu\text{m}$) is minimized (Dwari & Rao, 2007).

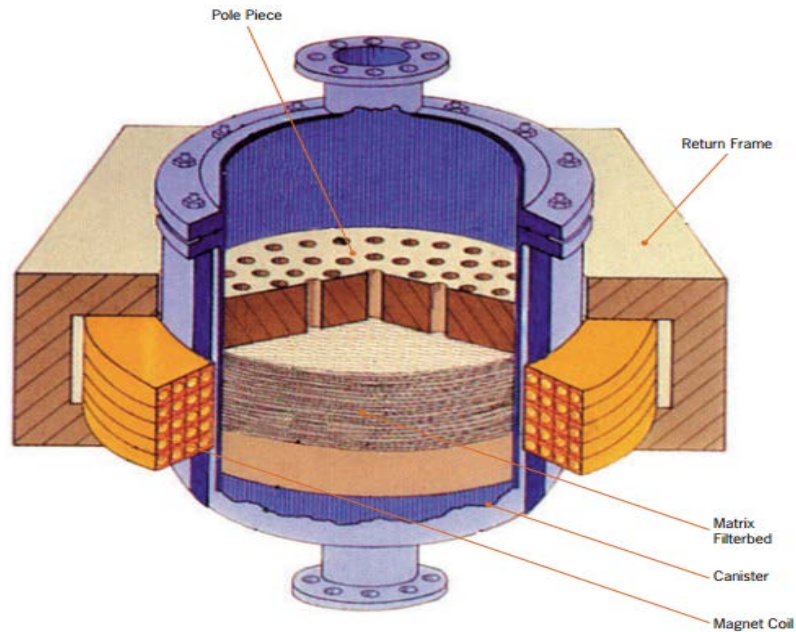


Figure 2.12 High Gradient Magnetic Separator (Metso Minerals Industries, Inc, 2006)

2.2.4.2 Open gradient magnetic separator (OGMS)

The principle of operation of Open gradient magnetic separator (OGMS) almost resembles the aforementioned device by this difference that OGMS provides a weak force and deeply distributes it along the separation zone, whereas HGMS exerts a powerful magnetic force in a small distance. Consequently, the distance of particles from collection points directly determines the magnetic force. The application of this unit in pulverized coal desulfurization process indicates that this technology has capability of decreasing sulfur content by 24 % (Dwari & Rao, 2007).

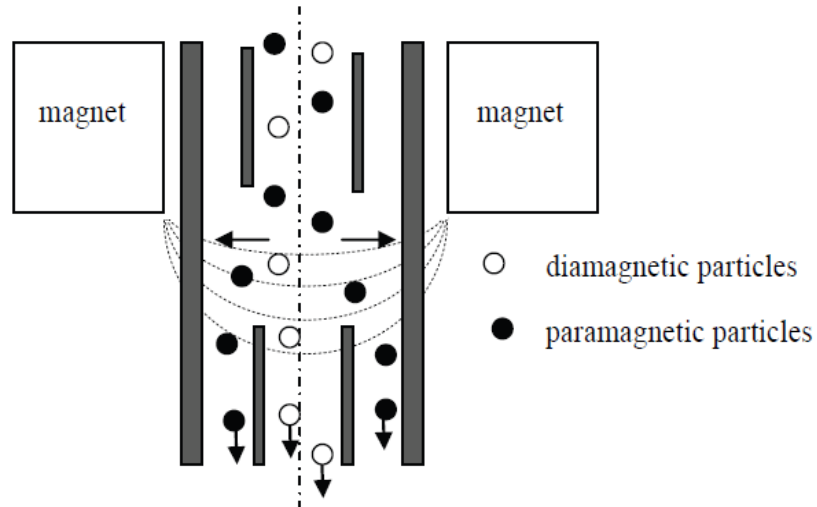


Figure 2.13 Operational principles of Open Gradient Magnetic Separator (CIEŚLA, 2012)

2.2.4.3 Induced Roll Magnetic Separator

This unit consists of a stationary north magnet pole installed on top of the machine, and a rotating roll coupled with a south magnet pole which is mounted on the inside surface of roll. The magnetic field is generated between stationary and rotating magnets located opposite to each other in which flux lines moves from fixed pole to revolving one. Mixtures of pyrite and coal particles are fed by a vibratory feeder installed on the stationary magnet. Raw feed is treated along the interval made between roll and magnet pole, as called cleaning zone. Having carried out separation process, non-magnetic coal materials are thrown away from the surface of drum by centrifugal force, and travel towards their corresponded stream, while magnetic pyrite materials stick to roll and are detached from its surface by a brush located beneath of the drum. In addition, one set of movable splitter is used to separate coal and pyrite streams from each other, which could change the amount of coal recovery and grade, regarding its position (Figures 2.15 and 2.16) (Knuutila, 2006).

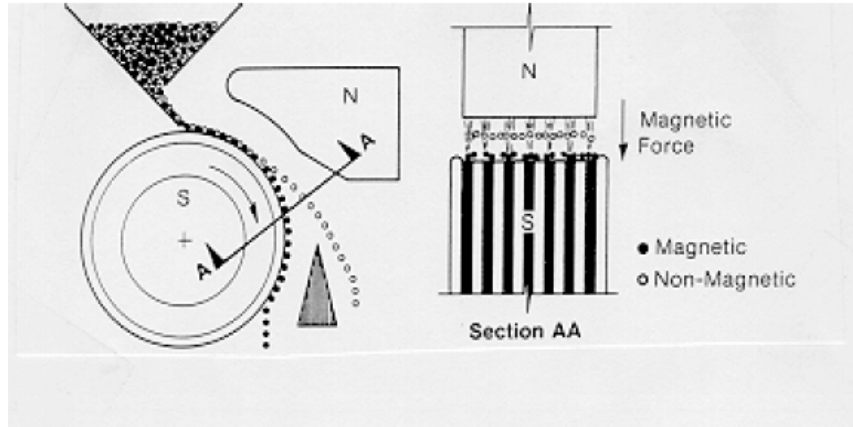


Figure 2.14 Operational principles of Induced Roll Magnetic Separator (Knuutila, 2006)

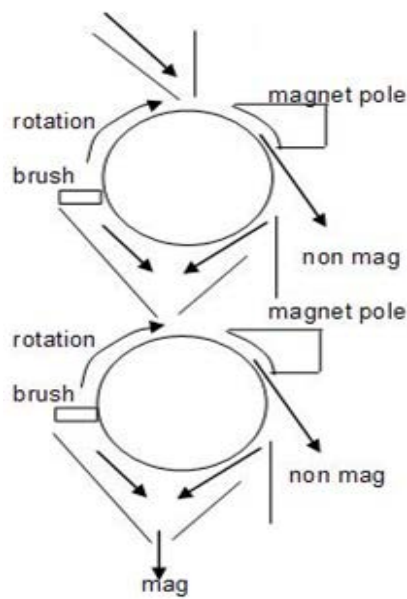


Figure 2.15 Structure of induced roll magnetic separator (Gaber, 1969)

Moreover, the machine is equipped with a hinge base that provides the roll with the ability of moving along the vertical axis. Depending on the drum position, a certain angle (named as tilting angle) is formed between the horizon axis and the line connecting center of roll to bottom of magnet pole (Figure 2.16). The magnetic intensity is measured in

seven positions on the surface of drum which varies from one to seven. The numbers written under cycles demonstrates the magnetic intensity corresponded to that specific position. Equal quantities of pulverized coal were processed by the unit in various tilting angle and collected products were analyzed in order to discover the effect of mounting angle on coal grade. The acquired results indicate that the recovery of magnetic particles dramatically boosts with each degree raise of tilting angle. The reason is attributed to this fact that high intensity positions are located in separation zone, thus time of treatment enhances. Therefore, the product stream is increasingly refined from pyrite particles (Gaber, 1969).

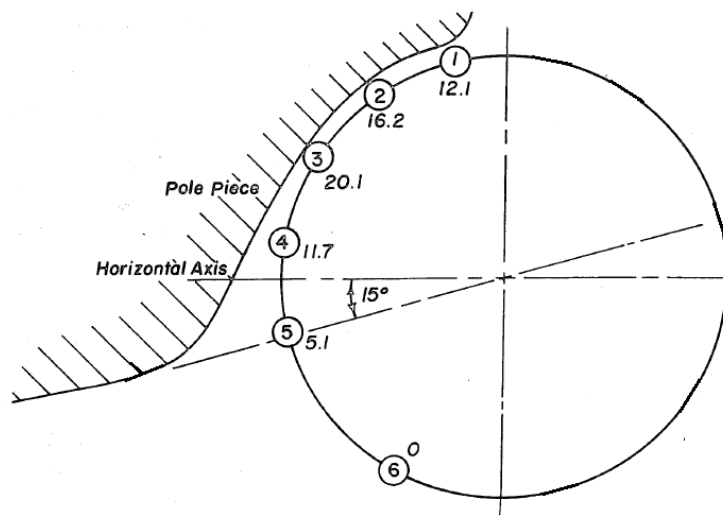


Figure 2.16 Tilting angle induced roll magnetic separator (Gaber, 1969)

2.2.5 Electrostatic Separators

The fundamental of this method of preparation relies on employing a high voltage electric field to separate particles based on their differential electric properties. According to electrical conductivity, minerals are classified into three general groups including conductive, semi conductive and insulator (dielectric), in which there is increasing order of magnitude of electrical resistance from first mentioned class to the last one (Manouchehri et al., 2000). Several electrostatic separators have been introduced to the

mineral processing industry that the principles of each of which are proportional to specifications of raw materials. Some types of machines have been designed to clean conductive materials from non-conductive ones, while others are able to prepare insulator particles. Each electrostatic separator employs a particular mechanism of particle charging which differs from the other types. Among all machines applied for anthracite coal cleaning, conductive-induction, tribo-electrostatic, and corona charging have proved to perform more efficient treatments. The raw feed consists of coal (known as weak conductive mineral / almost insulator), and impurities which may either be insulator or conductive. Thus, the electrical characteristics of coal and mineral matter directly determine what aforementioned machines should be employed. The tribo-electrostatic separator is capable of treating non-conductive materials, while corona charging is used to separate insulator particles from conductive ones. The conductive-induction machine is able to perform both conductive-insulator and conductive-conductive separation, however only the first mentioned application has been employed in anthracite preparation (Dwari & Rao, 2007).

2.2.5.1 Conductive - Induction Separator

The electrical field is generated between an inclined charged surface that materials are fed on and a grounded plate mounted superimposed upon the charge surface. The basic of separation is established on the materials' polarization rate / capability of attaining voltage of charge plate. Having particles fed and contacted to the charged plate, the conductive minerals are quickly polarized and obtain as equal potential as charged surface has. Because, their high conductivity make them unable to distribute acquired charge over their entire surface. The non-conductive particles also acquire polarity, by this difference which only that side of the particle located away from the charged plate acquires surface polarity (as same polarity as charged plate). The other side of mineral which meets the plate, approximately, assumes the same quantity of negative and positive charge; hence this surface of particle possesses no polarity (Figure 2.18). This phenomenon is caused by high electrical resistant of dielectrics which delays distribution

of charge throughout particles' surface. As a result, the conductive minerals (impurities) are attracted towards the ground plate, while the insulators (coal) move down the charged surface, due to not being exerted by any attracting force. The other version of this technology includes a charging roll and a grounded one that follows exactly the same fundamental of separation (Figure 2.18 (a)) (Dwari & Rao, 2007; Manouchehri, Hanumantha Rao, & Forssberg, 2000).

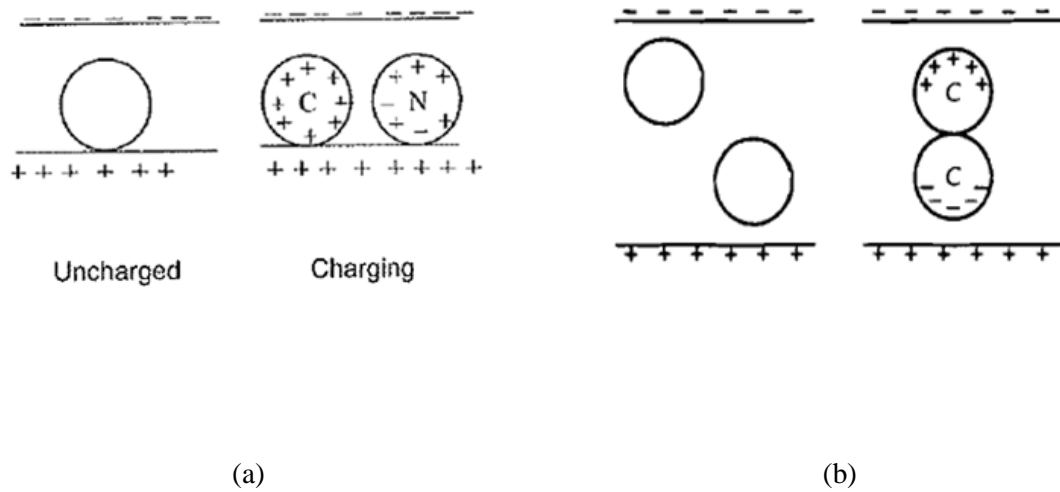


Figure 2.17 Different particles charging mechanisms: conductive-insulator separation process (a) and conductive-conductive separation process (b) (Manouchehri et al., 2000)

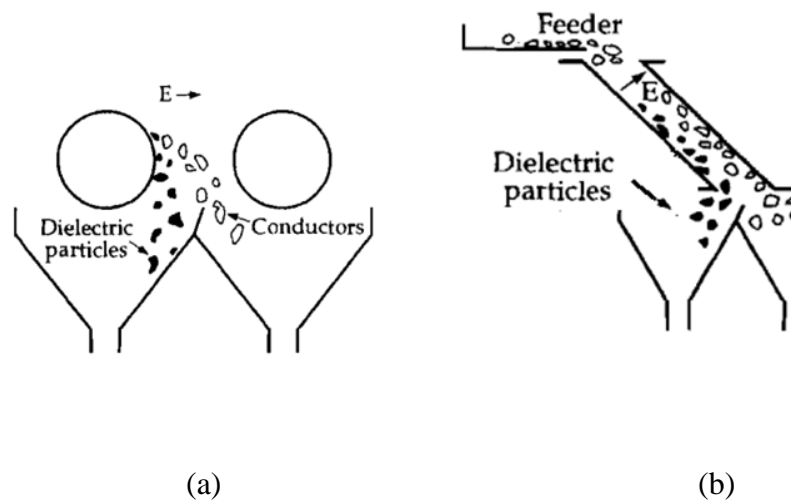


Figure 2.18 Conductive-Induction Separators: Roll type (a) and Plate type (b) (Manouchehri et al., 2000)

2.2.5.2 Corona Charging / Ion Bombardment

The corona charging has been proved to be able of treating various types of mineral on the high efficient manner (Bada, Falcon, & Falcon, 2010). This technology applies a revolving grounded roll, and a thin wire connected to a high voltage supplier with the aim of producing electrical filed, charging particles and finally separating them. The high potential field generated between two electrodes ionizes the enclosed air of wire and provides an ions flow / bombardment towards the rolling electrode. As particles fed on the roll and exposed to the field, their surface are coated by ions, thus attain electrical charge. The conductive particles instantly discharge the received ions on the surface of roll, whereas insulators sustain the achieved ions on their surface and stick to the roll. Therefore, the conductive minerals are thrown away by centrifugal force generated by rotating motion, while non-conductive ones are carried, and finally detached by AC discharge and brush scarper (Figure 2.20) (Lawver, Taylor, & Knoll, 1986).

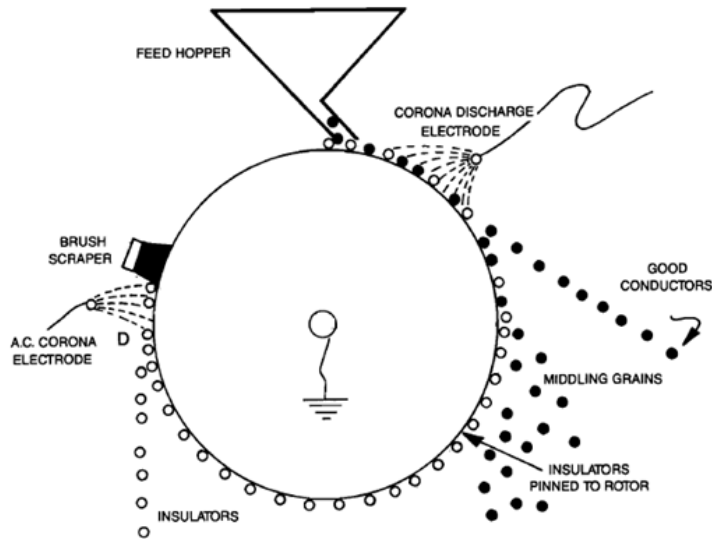


Figure 2.19 Corona charging mechanism (Lawver, Taylor, & Knoll, 1986)

2.2.5.3 Tribo-Electrostatic Separator

The preparation mechanism of tribo-electrostatic separator has been designed on the basis of insulators' differential work function (Jiang et al., 1999). Work function is defined as the minimum amount of energy that should be applied to extract an electron from Fermi level and carry it to vacuum level. After being contacted objects, the one that has lower work function releases electron and would become positively charged, while the particle possessing higher work function captures the electron and attains negative polarity. Due to this fact, coal obtains positive surface charge; however mineral matter will be negatively charged (Utz, 1993). The fundamental of charging involves in particle-particle and particle-charged plate contacting / friction, through which minerals attain positive or negative charge depending on their work function, as shown on Figure 2.21 (Manouchehri et al., 2000).

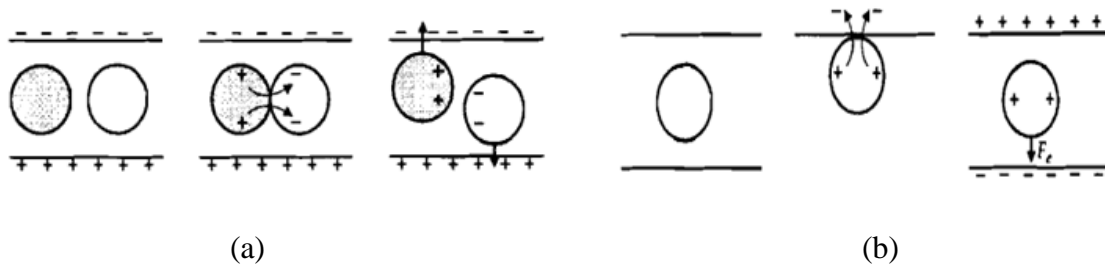


Figure 2.20 Tribo-charging mechanisms: particle-particle charging (a) and particle-plate charging (b) (Manouchehri et al., 2000).

The machine includes a horizontal tube that provides continuous flow of minerals and air into the Tribo-charger (friction / charging section) in which particles are polarized by either rubbing to each other or contacting to plates of tribo-charger. Thereafter, minerals are passed through a nozzle and led towards the high voltage separation / processing zone, which consists of negative and positive plates generating electrical field (Figure 2.22). The trajectory of particles inside the separation zone is dependent on two factors: 1) the sign of surface charge, and 2) the amount of surface charge per unit of mass (charge - mass ratio). The positive charge particles are deflected towards the negative plate, while the negatively charged minerals are attracted by positive plate. But, particles with more charge - mass ratio are exerted stronger electrical force, hence move faster towards the associated plate. As a result, various charge - mass ratios direct particles to different points of plate. On the other hand, there are some sorts of particles which proportion of surface charge over mass will provide too low value. These minerals would be misplaced to either positively charged particles stream or the other one (Zhang et al., 2010).

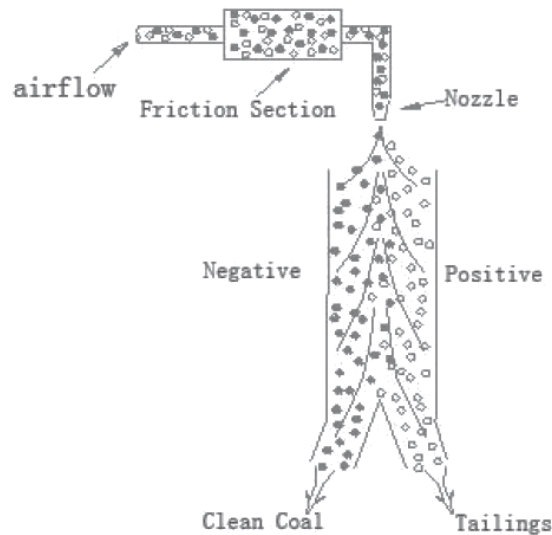


Figure 2.21 Process of coal cleaning by use of tribo-electrostatic separator (Zhang et al., 2010).

The ability of this technology in beneficiating high rank coal has been examined by processing representative samples of ultra-fine anthracite coal having a particle size finer than 43 micro- meter. The procedure of test established on varying different parameters which are involved in separation process, in order to discover the effect of each factor on processing efficiency. The experimental factors include: air flow, separation voltage, separation zone length, humidity of air flow, position of splitter, and flow sheet experiment. Each set of experiment includes different trials (4, 8, etc.) in which one parameter is continuously changed, while the others kept constant. Thereafter, ash and weight analysis is individually carried on each clean coal product. Next, all achieved results are compared to each other to find what trial provides the most efficient separation. The effect of all aforementioned parameters on treatment process will be separately discussed in the following sentences.

- Air Flow: This parameter plays a significant role during charging and separation processes. As air flow sequentially increases towards a specific value, product yield percent raises, while the ash content decreases. More air flow increases

beyond the optimum point will result in ash increase and yield decline. The reason could be explained by this fact that the energy of friction / contact is directly related to magnitude of air flow. As air flow enhances, it carries particles with higher velocity, thus particle-particle or particle-plate rubbing intensity will increase which provides more charge - mass ratio. On the other hand, the separation mechanism inside the high potential zone is depended on air flow pattern. Excessive air flow quantity generates turbulent environment inside the separation chamber, hence particles will be deviated from the plate that should move towards. Consequently, the optimum air flow speed will be that one providing sufficient contacting energy, and minimizing turbulence inside the separation chamber.

- Separation Voltage: The intensity of attracting force simultaneously boosts by each increase of electrical field potential. Thus, plates capture more amounts of materials, which results in higher yield percentage.
- Separation Zone Length: As previously described, the movement acceleration of charged particles towards the opposite plate is substantially depended on their charge - mass ratio. If the length of separation zone is too short, particles having low charge - mass ratio will not be provided with sufficient time to be attracted by associated electrode. This phenomenon may lead to impurities bypass to product stream. Conversely, excessively enlargement of separation chamber length would enhance particles' residence time which results in generation of turbulence and misplacement of particles to their non-corresponded stream. The acquired data demonstrate that 1200 mm length produces the best result.
- Humidity of Air Flow: Higher air humidity brings about raise of particles' surface moisture, hence minerals conductivity would increase. Therefore, the ability of particles in sustaining surface charge dramatically declines, which results in

charge - mass ratio reduction. This aspect makes major difficulties for proper separation. Analytical data demonstrates that there is a decreasing trend of yield percentage with increase of air flow humidity.

- **Position of Splitter:** That part of machine installed at the bottom of processing zone to separate particles' streams from each other. This experiment was carried out in three stages through which splitter initially mounted near to the positive electrode, and then gradually shifted towards the negative plate. At the first position, a wide gap is made between splitter and negative electrode that leads majority of particles to the clean coal stream and results in boost of yield. In addition, product ash percentage increases, as the probability of impurities misplacement into the mentioned stream increases. Diminishing the length of this interval, product yield and clean coal ash content dramatically decrease.
- **Flow Sheet Experiment:** This trial ran in two stages and completely involves in treating the clean coal stream in order to provide more purified product. At the first stage, raw materials are fed to the machine, processed, and finally separated into clean coal and reject streams. Subsequently, the product is retreated and generates much cleaner coal which contains less mineral matter comparing to first stage product. However, the amount of yield decreases due to extracting more middling particles / impurities from clean coal stream (Zhang et al., 2010).

This experiment proves that anthracite can be efficiency benefited by tribo-electrostatic separator if unit is set on the optimum parameters.

2.2.5.3.1 Double Drum Separator

Apart from the describe investigation, Eichas and Schonert has also evaluated the possibility of anthracite beneficiation through tribo-electrostatic mechanism by applying Double Drum Separator. Resembling previous discussed machine, the principle of separation relies on polarizing dielectric minerals and separating them based on differential surface charge sign. On the other hand, the procedure of particle charging and processing differs from conventional tribo-electrostatic separator.

Raw materials are fed into charging chamber coupled with a rotating brush (instead of plate) which agitates particles inside its housing and increases the probability of particle - particle collision. Having minerals rubbed over each other, they obtain positive or negative charge based on their work function differences. Since charging zone has been equipped with no plate, the process of polarization is only performed through particle - particle contact. The air stream is injected into brush housings and pushes down charged minerals towards the separation zone containing two non-conductive drums.

One pair of electrodes with opposite charge signs have been mounted in two different sides of each drum, which are separated by an insulator. Therefore, one electrode attracts particles towards the drum surface (capturing electrode), while the other of which exerts repulsive force on them. Providing more clarification, as particles enter electrical field, they are captured by opposite charge sign electrode and stick to the surface of roll. Revolving drum in clockwise direction, particles are shipped towards the back side of roll where the other electrode and brush have been installed at. Consequently, the adhered particles are detached from drum by repulsion force and brush, and finally deposited in corresponding boxes (Figure 2.23). Middling particles normally obtain low surface charge, thus are not attracted by drums. These sorts of minerals are removed from the machine by a frit designed at the end of separation zone (Eichas & Schonert, 1993).

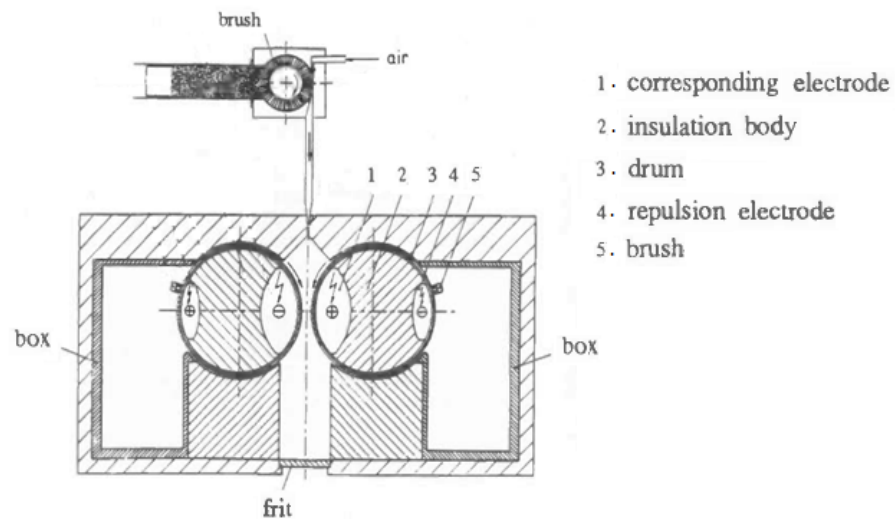


Figure 2.22 Structure of Double Drum Electrostatic Separator (Eichas & Schonert, 1993)

Mixture of quartz and anthracite was treated using this technology in which raw materials comprises 50 % of coal particles. Performance of unit has been evaluated by varying several factors including feed size fraction and electrical field intensity. During experiments, anthracite permanently receives positive surface charge, whereas quartz acquires negative charge since possessing higher work function than coal. The separation efficiency directly is depended on the amount of quartz and coal attracted by negative charge sign capturing electrode. As field intensity and feed size enhance, the amount of coal recovery increasingly improves; conversely the amount of quartz particle captured by the mentioned electrode follows a decreasing trend. Pointing to conclusion, the separation efficiency is promoted, due to with each percent of increase of combustible recovery the amount of ash recovery decreases (Eichas & Schonert, 1993).

2.2.5.3.2 Rotary Tribo-electrostatic Separator

Researchers at University of Kentucky have upgraded the existing tribo-electrostatic separators design, which has led to more efficient charging mechanism. In the new design, the stationary charging plate has been replaced with a rotary octagonal plate which is connected to a high voltage supplier. This plate revolves inside a cylindrical chamber connected to ground (Figure 2.24). In addition, to prevent creation of turbulent environment inside the separation chamber, the air velocity has been greatly decreased. The mechanism of particles charging is conducted by rotary charger, particle - particle contact, and particle-cylindrical chamber contact.

As raw material fed on the charging rotor, particles are agitates inside the interval existed between charger and cylindrical chamber. Hence, particles are provided with more chance to hit each other, and grounded chamber. Moreover, rotary charger revolves at a high speed which causes particles to be exerted great friction energy. Furthermore, the charged plate improves charge exchange between mineral and plate. In this charging mechanism, particles' surface charge density outstandingly enhances comparing to conventional charging method. Thus, the amount of middling / weakly polarized minerals arriving separation zone will be remarkably minimized (Bada et al., 2010).

Several coal samples have been purified from their following impurities by applying Rotary Tribo-electrostatic which has resulted in provision of such a satisfactory results (Tao, Sobhy, Li, & Honaker, 2010). However, no evidence / article have been found proving the capability of this technology in anthracite beneficiation.

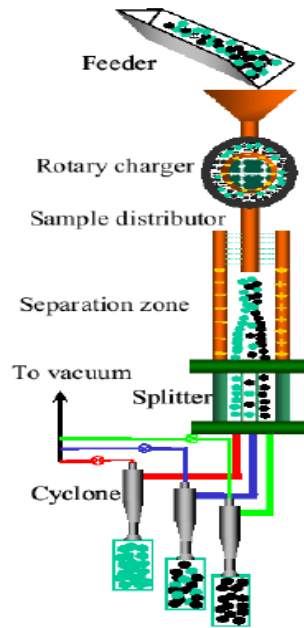


Figure 2.23 Process of coal cleaning by means of Rotary Tribo-electrostatic Separator (Tao & Al-Hwaiti, 2010)

2.2.6 Dual Energy X-ray Transmission Sorting Technology

Dual Energy X-Ray Transmission (DE-XRT) sorter is a state of the art device which has been recently introduced to mineral processing industry and employs as same technology as applied for baggage check at airports. This device is equipped with a chute / belt carrying particles towards an X-ray source, which emits radiation on particles in high and low energy levels. In addition, two sensors located beneath the belt, takes particle's images corresponded to the emitted energy level. Next, the captured images are transferred to a computer where they are processed by means of a pre-established criterion, which determines the target particles should be ejected or accepted (Dalmijn and De Jong 2003, Strydom 2010).

The process of separation entirely is conducted in four stages including:

1. Particle Presentation Mechanism: the treatment principle lays down capturing and analyzing clear pictures of each separate particle. Therefore, the excessive speed

of belt would increase the probability of particle-particle overlapping, which results in two particles to be detected as a one bulk element. Thereby, this mechanism should regulate moving rate of particles on the chute / belt somehow each particle is individually exposed to the x-ray beam.

2. **Detection System:** Two sensors have been mounted beneath the belt, opposite to radiation source, to take particle's image in two intensity levels of x-ray energy. The process of particle imaging is conducted in a "line by line" fashion, which provides high - resolution pictures of the target particle.
3. **Processing System.** The provided images are transmitted to the Programmable Logic Controller (PLC) to be analyzed, and then processed by employing a designed algorithm. This criterion, as mean of separation, indicates whether a given particle should be ejected from the belt or remained on the belt. Determining the position of particle which should be removed, the PLC actuates pneumatic air valves installed in the corresponding position.
4. **Ejection System.** A series of pneumatic air valves has been mounted at the end of belt, which quickly handle process of particles ejection. Since these valves operate in conjunction with PLC, the ejection mechanism would be capacitated to selectively remove individual particles (Strydom, 2010).

The mentioned stages are schematically shown in Figure 2.25.

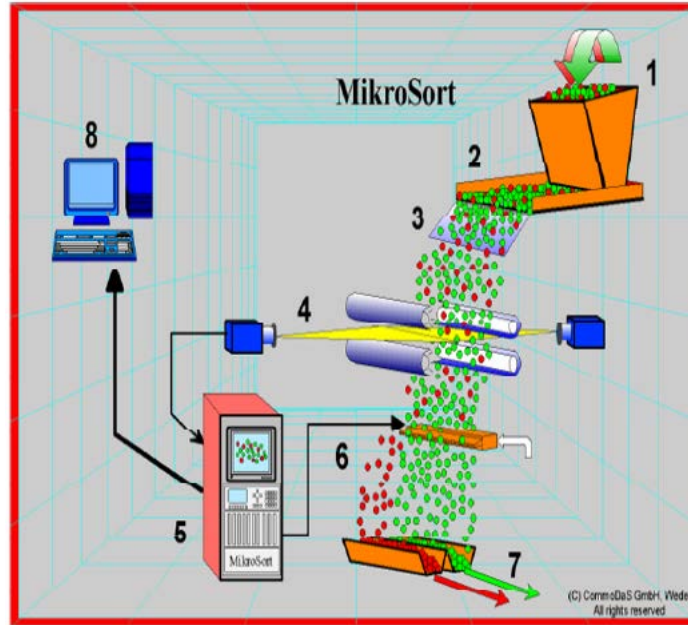


Figure 2.24 Operational principles of a belt type XRT based sorter (Strydom, 2010)

As x-ray is emitted to a particular particle, some portion of radiation is absorbed by particle. Therefore the detected x-ray would have less intensity/energy comparing to the original radiation. The degree of x-ray attenuation differs in accordance to density/ elemental composition of irradiated particle. This change of x-ray intensity is identified as ‘transmission damping’ which could be quantified by using Lambert’s law.

$$I_{\text{det}} = I_0 e^{-\mu(\lambda)\rho d} \quad (2.1)$$

As expressed on above equation, the intensity of penetrated radiation (I_{det}) is inversely proportional to density(ρ), thickness (d), and mass absorption co-efficient ($\mu(\lambda)$) of particle, which is exposed to x-ray beam.

Mass absorption co-efficient of a typical particle depends on mass absorption co-efficient and mass fraction of elements which are contained in that particle. Normally, the following equation is employed to estimate the mass absorption co-efficient of a particle comprising of ‘n’ elements.

$$\mu_{\text{eff}} = \sum_{i=1}^n f_i \mu_i \quad (2.2)$$

Where, μ_{eff} is total mass absorption co-efficient of particle, and f_i is percentage of a element 'i' in particle by weight (Tong 2009).

Referring to equation 2.1, the intensity of received x-ray would be exponentially correlated with thickness and density of particle subjected to emitted radiation. However, this technology mainly focuses on treating minerals by means of their differential density rather than thickness. Since raw feed consists of wide size range of materials, the effect of thickness in x-ray attenuation might dominate the effect of density in decreasing radiation intensity. Due to this fact, the detected intensity of x-ray passing through a thick particle might be less than the intensity of radiation penetrating through a dense particle. Hence, application of single energy level increases the probable error of treatment process. Thereby, to diminish the negative impact of particle thickness on separation efficiency, two x-ray beams are radiated which have different wavelengths.

With change of radiation energy, particle's mass absorption co-efficient will vary to some extent, proportional to the particle's atomic number. The degree of attenuation of high/low x-ray energies could be estimated by use of the following expression which has been driven from Lambert's law.

$$\frac{I_1}{I_2} = e^{-\Delta\mu\rho d} = (e^{-\Delta\mu\rho})^d = (C_m)^d \quad (2.3)$$

In which, $I_1 ; I_2 = \frac{I_{\text{det } 1;2}}{I_{01;2}} (\lambda_{1;2})$ are received intensity at two different level of x-ray energy and C_m is constant value functionally related to elemental composition of irradiated particle, and energy of emitted x-ray.

Thus, two particles with same size and various density could be simply separated, as if they obtain different values of ' C_m '. Finally, the thickness of target particle can be quantified by substituting the measured values of I_1 and I_2 into the above equation (Strydom 2010).

The fundamental of Dual Energy X-Ray Transmission Sorting has been established on applying transmission curves of several types of particles contained in raw feed. Different types of materials create specific transmission curves associating with their grades and size. A typical transmission curve is provided by plotting the amount of detected intensity of radiations versus a particular sort of material, which comprises particles having same elemental composition, but different size fractions. Various particles with several grades would generate a specific transmission curve, as illustrated in Figure 2.26 (Strydom 2010).

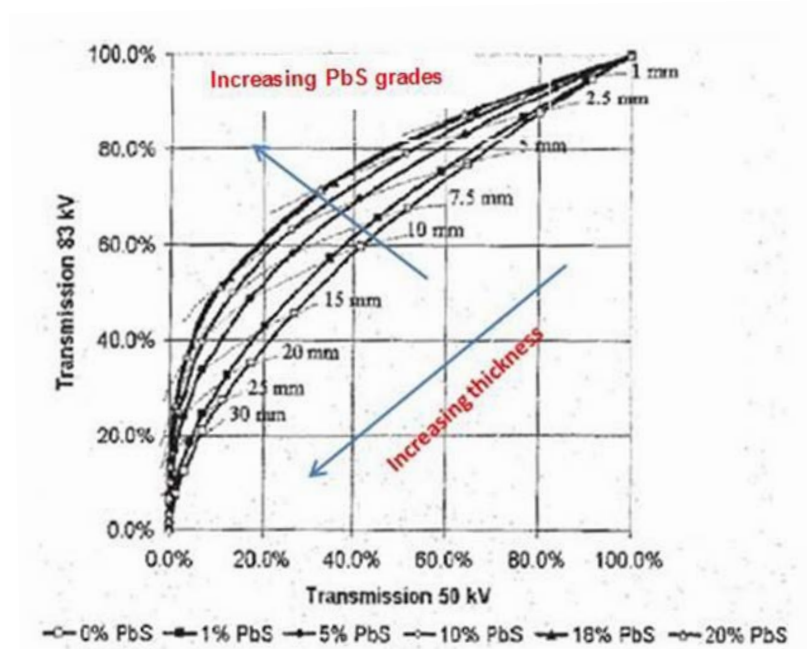


Figure 2.25 Transmission curve of mixtures with different PbS Grades at 83kV/50kV(Tong 2009)

The above plot clearly indicates that there would be great potential of treating minerals, if their transmission curves do not intersect.

The degree of brightness of images taken from a particle in two levels of radiation will provide invaluable data about intrinsic properties of that particle. Normally, on x-ray film, the high density particles seem darker comparing to low density particles. The existed correlation between transmission curves and degree of brightness of particles could be discovered by means of calibration curve. This curve is employed as treatment principle determining a given particle should either be ejected or accepted.

Briefly explaining the procedure of plotting this curve, high and low intensity x-rays are radiated on a bunch of samples of raw material which tends to be processed. Next, the captured images are sub-divided into individual pixels. Then, the brightness of each pixel is calculated by means of software, named as GIMP, which coupled with a brightness scale ranging from 0 (lowest degree of brightness / white) to 255 (highest level of brightness / blank). The values which ones that fall into this range are correspond to several levels of gray color. Having brightness of pixel compared with the brightness scale, the degree of brightness of that pixel is quantified. This trend continues to some extend which all pixels are analyzed (Figure 2.27) (Tong 2009).

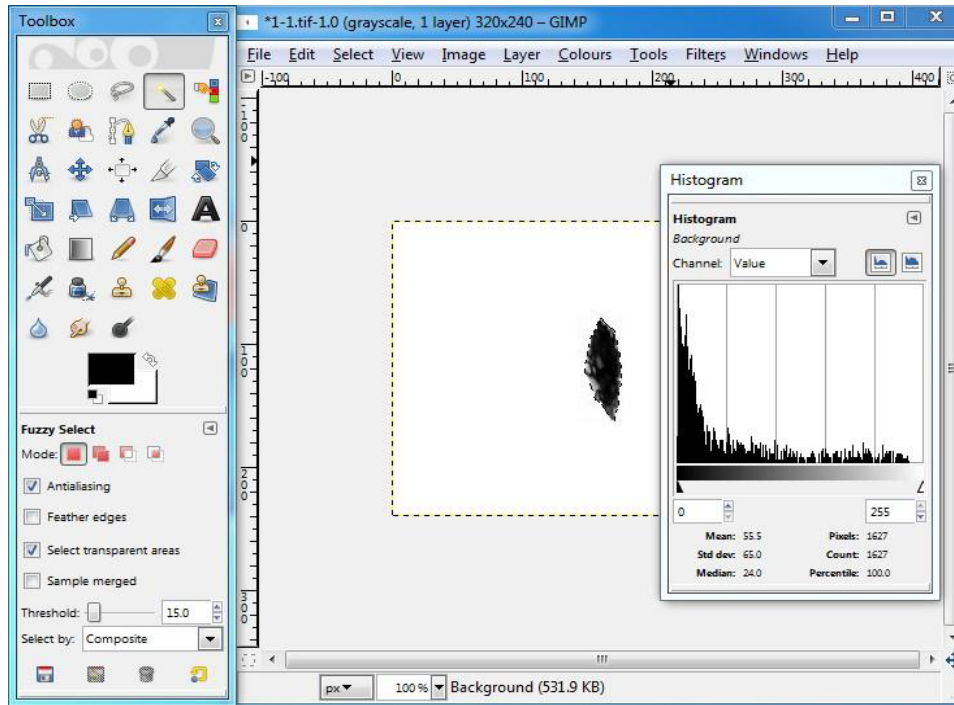


Figure 2.26 Screenshot of Brightness Value Extraction from the Image by GIMP (Tong 2009)

Thereafter, the total brightness of images generated by high and low intensity radiation is calculated by finding the average brightness of all pixels. This value is then converted to percentage by being divided on the highest level of brightness (255), so that the amount of x-ray transmission to be examined. Providing more explanation, the 100 percent of brightness demonstrates that the emitted x-ray has entirely penetrated through the irradiated particle without being attenuated (Tong 2009).

Subsequently, for each individual particle, average brightness of low intensity image is plotted against mean brightness high intensity image. Eventually, the calibration curve is formed by creating the linear regression of plotted spots. This curve designates the mean specific gravity of particles falling within the size range, which tends to be treated. Drawing the conclusion, this curve passes through transmission curves of particles having

different densities (Von Ketelhodt & Bergmann, 2010) (Tao & Al-Hwaiti, 2010). A typical calibration curve has been shown on the figure below.

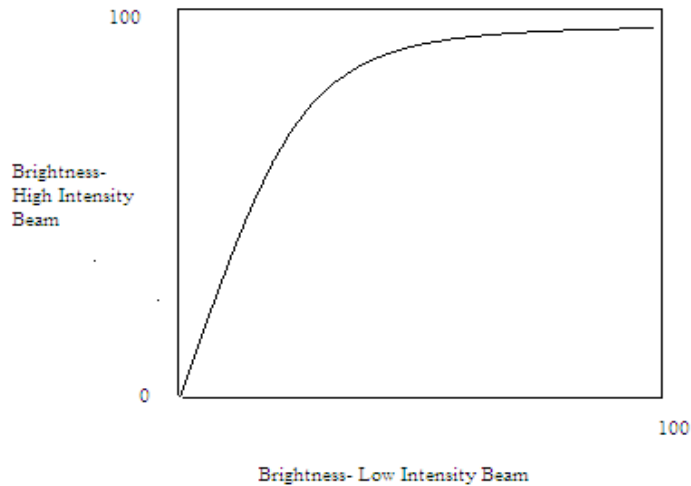


Figure 2.27 Typical Dual Energy X-Ray Transmission Sorting calibration curve (Strydom, 2010)

The separation criterion has been laid down the calibration curve generated from typical samples of raw feed. The entire area containing calibration curve is divided into two neighboring zones by means of calibration curve. The area located above the curve is identified as high density area, and designated by blue color. While, the other of which, plus the calibration curve area, are assigned as low density zone and illustrated by red color (Figure 2.29).

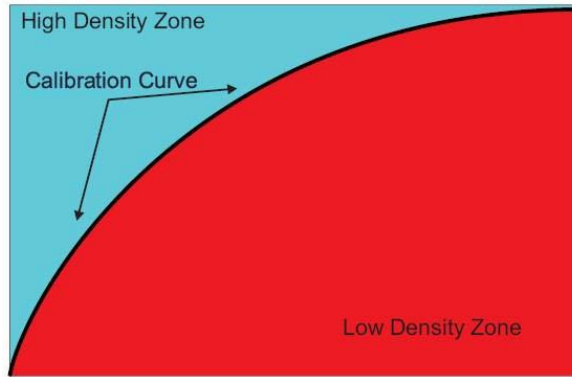


Figure 2.28 Determination of high and low density zones of XRT calibration curve (Tong 2009)

The processing criterion is established by means of representative samples, those ones which used for generating calibration curve. As previously discussed, GIMP software evaluates the degree of brightness of each individual pixel existing within whole picture of a given particle. Every single processed pixel is plotted on the calibration area as a function of degrees of brightness, and is designated as red or blue, depending on situating either on low or high density zone. Entire pixels of image are processed by applying the mentioned mechanism. The percentage of red and blue pixels aids to estimate the elemental composition of target particle (Tong, 2009). As schematically illustrated on Figure 2.30, low density particles (coal) almost entirely consist of red pixels, while the majority of pixels comprised in high density minerals (shale) are assigned as blue color (Von Ketelhodt & Bergmann, 2010). The separation principle is finally defined in accordance to percentage of blue/red pixels.

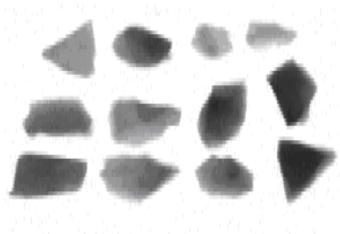
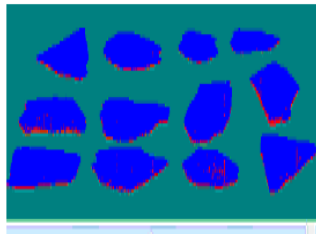
Sample	Sample Picture	X-Ray Image (Gray Scale)	Simulation Result
Coal Rich			
Shale Rich			

Figure 2.29 Simulation of coal and shale representative sample by XRT calibration curve (Strydom, 2010)

Having calibration curved formed, raw materials are fed in to machine to be treated. The process of beneficiation may be conducted either automatically or manually. More clarification, in the automatic method, initially the beneficiation criterion (setting) is established based on the percentage of blue / red pixels, as discussed above. Then, every single raw particle is analyzed. Next the percentage of red/blue pixels within that particle is quantified, and compared to separation criterion. Those particles which ones comprise number of blue / red pixels beyond the determined limit / separation criterion would be first identified by software. Thereafter, PLC adjusts the time of air valve activation, corresponded to the distance between target particle and air valve. As, particle meet the end of conveying belt, the air valve automatically pulses air and deflect the target particles towards the desired stream. Providing an instance, the principle of separation may be set on ejecting particles containing more than 30 % blue pixels. Increasing the ejection limit (for example, setting of 50 %) would result in accepting particles containing more percentage of blue pixels; hence the product ash content will be raised. As a result, the processing operator would exert no direct control on the process of preparation, after defining the separation criterion (Strydom 2010).

However, the second procedure employs a different type of separation criterion for ejecting particles. For each setting, a series of simulated classified pictures are developed. The percentage of red pixels of particles increases with change of settings. As illustrated on the Figure 2.31, for a given particle, the number of red pixels has been increased with change of setting. In this method, similar to automatic mechanism, every particles of raw feed is initially analyzed based on the established calibration curve. Then, all single pixels are assigned red / blue color. Subsequently, particles are shown on the screen of computer in form of colorful images. Afterwards, the processing operator clicks on the particles which contains the high amount of red pixels. Finally, the air valve injects the pressurized air at the convenient moment, and ejects the selected particle. Therefore, the processing operator completely directs the process of beneficiation. With increasing separation setting, higher ash content particles would have more chance to be ejected (as product) because of obtaining more percentage of red pixels. Hence, the product ash and yield would increase.

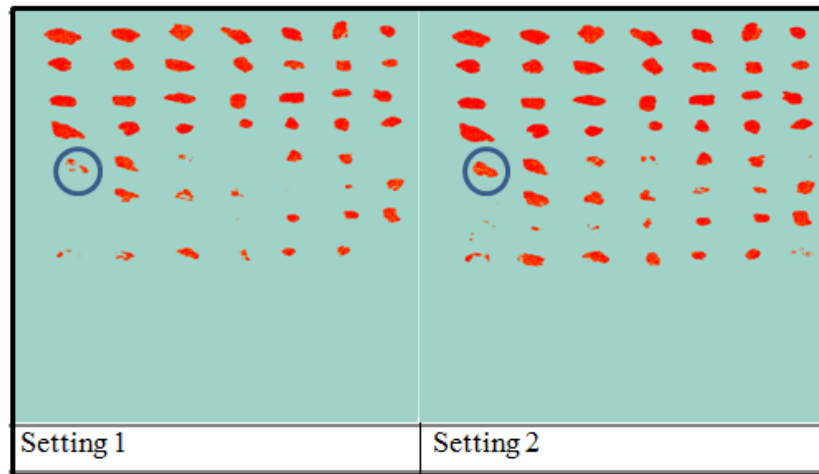


Figure 2.30 Separation settings used in XRT experiments in manual preparation method

2.3 Wet Based Anthracite Cleaning Technologies

2.3.1 Introduction

After 1920, trend of deployment of water based coal concentrators has more rapidly grown than dry separators due to the fact that they were able to satisfactorily meet necessities of new burning equipment. The major needs could be listed as: 1) the least amount of impurities in feed, and 2) the highest level of feed uniformity (Age, 1961). Mechanism of wet anthracite cleaning entirely lays down applying either particles gravity variations or differential degree of particles' surface hydrophobicity.

Considering operational principle of gravity based separators, bulk of technologies are categorized into two main groups as, some machines use upward pulsated water flow to initially float minerals, and then treat them based on settling velocity differences. While, the majority of those employ a fluid possessing specific gravity lying between coal and mineral matter densities by which light particles (coal) are floated whereas heavy ones sink (impurities). In mineral processing industry the mentioned fluid is termed as medium, which normally generated by appending high specific gravity minerals (such as Magnetite) to water or boiling some fraction of raw feed inside water (Autogenous Medium). All types of Wet Jigs fall into the first aforementioned category, whereas the second group includes Water Only Cyclone (WOC), Chance Cone, Teeter Bed Separator (TBS), Dense Medium Cyclone (DMC), Dynawhirpool Coal Cleaner, Conklin Process Separator, and Heavy Media Vessel (HMV).

As two other units belonging to gravity separators family, Humphreys Spiral and Wet Concentration Table, apply neither upward flow nor medium fluid, but use water flowing film for cleaning minerals. As raw materials fed into the Spiral in form of slurry, they are carried by water along the helical routes located from top to end of machine, thus exerted centrifugal force. Therefore, particles are gravitationally classified throughout traveling route based on their resistance against the subjected force (Alexis, 1980) . In Wet

Concentration Table, particles are exerted by gravitational force and pushing water film, hence they travel different distances on the deck based on their settling velocity, and clearly separated from each other.

As minerals put on higher degree of breakage, they are progressively more liberated which leads to the enhancement of beneficiation processes. In the contrary, particles finer than 150 micro-meter are not capable to simply settle down in the corresponding fluid, hence the effect of gravity differences on minerals separation substantially weakens and particles are transported by fluid wherever it moves. This phenomenon is identified as Brownian motion. Floatation, the alternative mechanism solving this issue, applies hydrophobic characteristics of minerals to purify valuable particles from mineral matters. Briefly describing the fundamental of operation, is established on four sequent stages including: 1) Air bubbles generation at near the end of floatation cell, 2) raw materials feed to the unit, 3) particle-bubble attachment, 4) adhered particles delivery to top of the cell through upward bubble movement (Albrecht, Coal Preparation Processes, 1980).

Among all wet based mineral processing machines, the above-mentioned technologies have been able to effectively beneficiate the anthracite coal. The following sections have been allocated for discussing individually operational principles of each unit, as well as providing analytical results achieved by that machine.

2.3.2 Gravity Separators

2.3.2.1 Teeter Bed Separator (TBS)

Fundamentally, the process of treatment involves in supplying continues upward flow which suspends a portion of heavy minerals of raw feed and generates autogenous floated medium (Honaker, Das, & Nombe, 2005). As rest of feed is subjected to the medium, coal particles elevate towards the overflow slot due to their inability to penetrate through

suspended bed (teeter bed), while tailings pass readily down the teeter bed and moves to their corresponding valve.

The framework of separation has been set on the variation of minerals' settling velocity inside water, which is directly proportional to their size and density. The water flow is perpendicularly pumped to the machine through a water tube installed at the end of unit, and uniformly distributed along the width of machine after passing through a perforated deck (teeter plate). Next, raw materials are tangentially introduced to the machine and commence descending along the vertical axis. Main factor of separation, the fluidized teeter bed, initiates formation when the velocities of settling particles and rising water set on the same value (Tao, Li, Wang, & Zhao, 2011). All particles located inside the bed are arranged beside each other within small distances, which results in creating narrow spaces / tiny holes. Ascending water, after passing through up the holes, attains increased velocity preventing low ash/small particles to settle down, hence leading them to the overflow slot. Conversely, coarse / high ash minerals possess higher falling velocity in compare with upward water rate, accordingly could simply overcome pushing up force, pass through down the teeter bed, and moves towards the tailing valve (Kohmuench J. N., Mankosa, Honaker, & Bratton, 2006).

The machine could provide most achievable separation efficiency if the average density of fluidized bed is set on the fixed value. This goal is readily attained by equipping the conventional Teeter Bed Separators with a precise probe and a PID controller. Primarily, probe measures the effective density of that part of teeter bed which is located above it. Thereafter, the probe sends a signal to PID which ranges from 4 to 20 mA corresponded to the effective density of floated bed. The PID compares the actual density of suspended bed with the desire theoretical density and regulates these two values by controlling the tailing removal rate. If the effective density exceeds the theoretical one, the PID opens the spigot valve to remove extra amount of materials. On the other hand, the controller device lessens the discharge velocity in those conditions when actual density needs to be

increased (Drummond, Nicol, & Swanson, 2002). The operational principles of this device has been shown on the Figure 2.32.

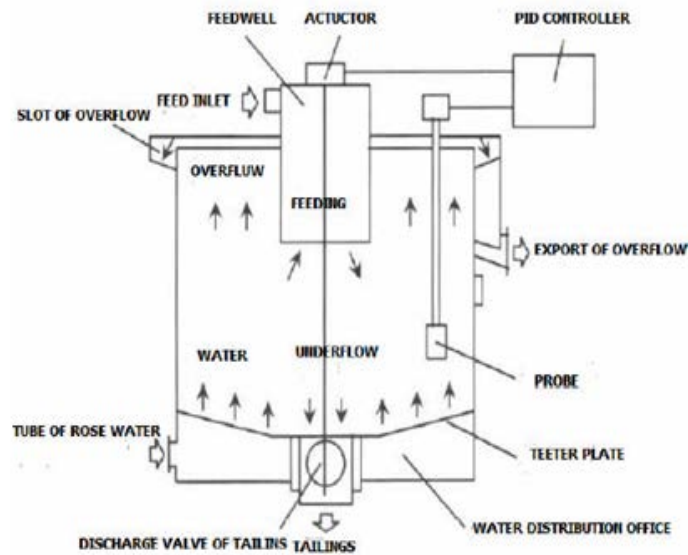


Figure 2.31 Operational fundamental of Teeter bed separator
(Tao et al., 2011)

One of the main issues enduring separation efficiency is associated with bypass of light-coarse particles to the wrong stream. In order to discover the reason causing this phenomenon, two factors should be considered: 1) Dependency of particle's settling velocity on its density and size, 2) Pushing force exerted light-coarse mineral inside the teeter bed. First of all, a low ash-coarse mineral may fall with a speed which exceeds the ascending velocity of water; hence the upward flow is not able to transport it to the overflow slot. Secondly, this particle individually is not dense enough to can pass through fluidized bed. However it is ultimately pushed down to the tailing valve through downward force which is generated due to high population of particles at top section of teeter bed. Regarding these factors, there is a high probability of coarse coal particles bypass to the tailing stream and losing product (Kohmuench J. , Mankosa, Yan, Wyslouzil, Christodoulou, & Luttrell, 2010).

Apart from density, the gravitational separation of particles is also proportion to feed size range which may cause misplacement of coarse-light minerals to tailing stream, as described before. In order to enhance the separation efficiency of TBS, several Investigations conducted by Reed et al on 1995 and Honaker on 1996 demonstrates that the optimum feed size should be fell into range varying from 1 mm x 150 μm (Honaker & Mondal, Dynamic modelling of fine particle separations in a hindered bed classifier, 1999).In addition, the design of machine has been modified which results in more efficient processes. The unit has been equipped with air holes injecting air bubbles into system which brings about improvement of coarse particles recovery (Figure 2.33).

Two Korean anthracite samples were treated using the modified version of TBS to study the applicability of this unit in recovering carbon from anthracite raw materials. The immediate objective of this test has been established on recovering the course-low ash materials / avoiding their misplacement, by examining several operational conditions. Feed samples are characterized to 'Feed 1' containing 41 % mineral matter and 'Feed 2' with 51 % ash content. During trials, dependency of separation efficiency to three parameters including upward water flow rate, set point, and air bubble, has been systematically assessed.

In order to evaluate the effect of two first mentioned parameters on recovery of coarse coal particles, one parameter is gradually changed with keeping the other one constant. In these cases, no air bubble injected to the machine. However, the effect of air bubble is examined when rising water is pumped up at a fixed velocity, and set points vary between two values. Clarifying the acting parameters, the set points represent the height of bed from top of sensor (probe), as set on 20, 30 and 50 values, which are corresponded to 62, 74, and 88 cm of bed height, respectively. The teeter water flow rate ranges from 3.8 to 9.5 L/min and air bubbles are subjected into machine in two set points of 20 and 30. Having cleaned raw materials in each test, the product is screened out on 70 mesh sieve size and divided into coarse (+210 μm) and fine ($- 210 \mu\text{m}$) fractions. Thereafter, the

yield of each size fraction is calculated using the solid percentage of corresponding size comprised in the feed. Eventually, the success of machine in floating coarse coal particles is simply evaluated through comparing the yield of coarse size fractions provided in tests.

As set point grows, the yields of coarse size portion of 'Feed 2' enhance. This clearly indicates that rise of bed height improves the possibility of recovering coarse particles. On the other hand, for 'Feed 1', the corresponding values follow a fluctuating trend by increasing set point. The yield of coarse particles boosts as the set point grows to 25 and subsequently declines with more increase of set point to 30. Coming with the conclusion, the characteristics of samples directly determines the efficiency of coarse particles recovering process.

The correlation between upward flow rate and amount of coarse particles subjected to overflow has been evaluated running tests in constant bed height of 74 cm and four flow rates including 3.84, 5.76, 7.68 and 9.60 L/min. Analyzing products of both samples, the yield of coarse minerals is progressively enhanced with increase of velocity of ascending water. Obviously, the improvement of recovery would results in growing product ash content.

The last parameter applied in this experiment, air bubble, is injected to machine at bed heights of 62 and 74 cm with teeter water flow having constant ascending velocity of 5.68 L/min. The provided results demonstrate that rise of bed height causes increase of ash content and yield of coarse size fraction (Cho & Kim, 2002).

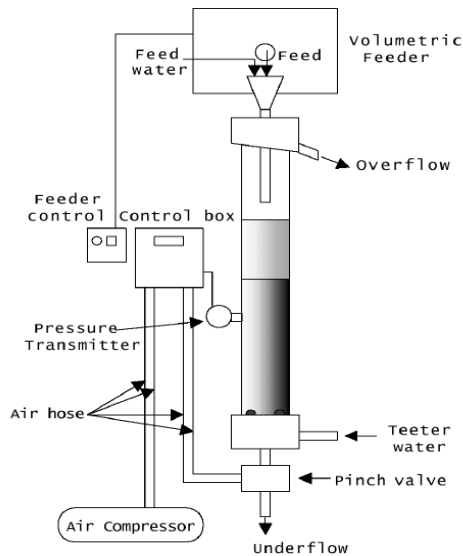


Figure 2.32 Modified teeter bed separator (Cho & Kim, 2002)

2.3.2.2 Wet Jig

As previously explained, wet / water based jig employs four general stages of jigging to treat particles along the separation zone located over a perforated deck. The entire jigging process is conducted via upward water stream created inside a U-shaped tube and particles differential falling velocity. With introduction of new machines, the mechanism of jigging and providing water flow were progressively changed. In early units, the screen was manually lifted up and thrown down which resulted in continuous water pulsation and suction inside the separation zone. Hence, the consolidation trickling was carried out during suction mechanism, whereas the other three stages initiated after pulsation. The other types of jig are equipped with a pulsator which pumps up the water in steady intervals. Likewise, some types of this unit are coupled with a plunger which pushes down the water on the left side of U-shaped tube and raises it up inside the opposite part (Ashmead, 1920; Price & Bertholf, 1949).

The conventional wet jigs normally consumed excessive amount of manpower, as all separation stages and discharge of treated materials were carried out by means of hand (Eckerd and Spencer 1971). Overcoming these limitations, several versions of this device were gradually developed that substituted mechanical energy to manual energy for cleaning and removing separated layers. Specifically citing, Reading, Lehigh Valley, Elmore, Wilmot-simplex, Delaware, and the James jigs have sequentially been introduced to the anthracite preparation industry. The Wilmot-simplex jig resembles the operational principle of conventional jigs by this difference that the screen is moved mechanically. The rest of aforementioned units are coupled with a fixed perforated deck, and a plunger moving along vertical axis, which supplies upward and downward water flow. The denser particles forms the lower layer due to attaining faster settling velocity, whereas lighter ones are accumulate on upper layer (Eckerd and Spencer 1971).

The mechanized member of this family identified as Baum or pneumatic jig equipped with an automatic valve which pulses compressed air on the surface of water and creates upward flow (Ashmead 1920). This part also is responsible to produce downward flow via ejecting injected air. Two main factors including period of air pulsation and air exhaust directly affect the efficiency of jiggling process. The number of pulsation exerted on the surface of water over a specific time is proportion to number of air valve cycles. Thus, stroke amplitude and acceleration of water after pulsation stroke are depended on time and rate of air injection. Therefore, the air pulsation time should be adjusted so that the bed can completely be extended, the upward flow decelerates, and water obtains the proper velocity. Similarly, period and intensity of air ejection mechanism needs to be accurately regulated with the intention that particles are provided with enough time to can be appropriately classified (Figure 2.34) (Price & Bertholf, 1949).

The ideal result would be achieved if the time gap between air pulsation and air exhaust is completely adjusted to particles' settling velocity. This interval is call injection-ejection interval. Providing more explanation, the best up stroke is that one being capable to lift and expand particles inside the separation zone during pulsation time. However, a

perfect down stroke is one which commences after hindered settling, thus expedites consolidation trickling process. Based on the size range of feed particles, time-velocity curve is plotted that well anticipates the motion of particles inside the separation zone throughout several air valve cycles. This curve generates regression between separation efficiency and injection-ejection interval by which plant manager would be able to precisely automate the air valve cycle (Price & Bertholf, 1949).

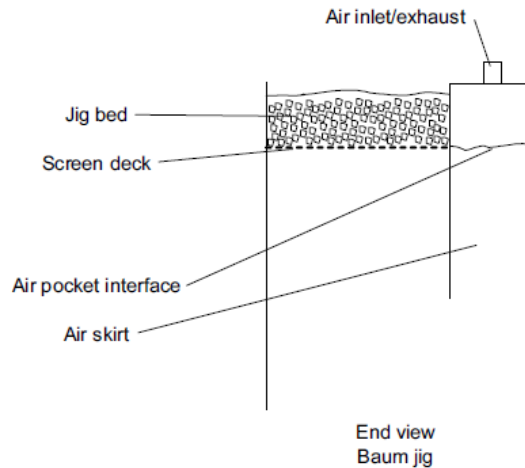


Figure 2.33 Baum Jig (Dieudonné, Jonkers, & Loveday, 2006)

2.3.2.3 Wet Concentration Table

The Wet Concentration Table operationally simulates the air based version of table concentrators, although the perforated deck has been substituted by riffled plane surface. Structurally, the unit consists of a rectangular deck which is mounted with a smooth upward slip in direction of long axis, inclines downwards along the short axis, and asymmetrically shakes along its tall axis. In addition, a series of the surface longitudinal riffles arranged from upper side of table to lower side which decelerate minerals transversal movement, hence particles are provided with more time to be gravitationally classified (Figure 2.35) (Tiernon, 1980).

The fundamentals of separation completely depended on the differential settling velocity of particles along the width of table. Considering the velocity profile of flowing films, the velocity of water exponentially increases from surface of deck to free plane of water. Since large particles are more likely to be exposed to higher velocity zones than smaller one, they tend to move more distance along the tilting deck. Hence, two same density particles with various sizes, the larger of which falls at the slower rate than the finer one. On the other hand, comparing settling rate of two particles having same size and different densities, the heavier one meet the table surface sooner than the lighter particle. Consequently, the particles are stratified within the longitudinal riffles according to the trend illustrated on the following picture (Weiss, 1985)

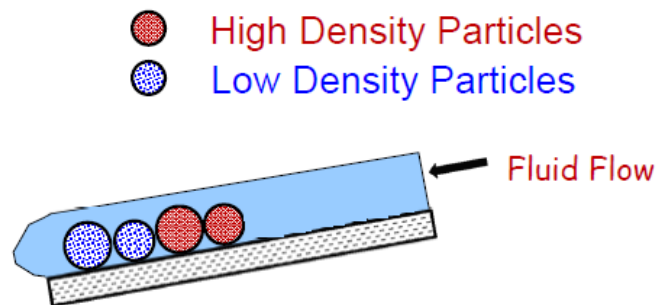


Figure 2.34 Arrangement of particles with different size and density under effect of flowing film (Weiss, 1985)

As particles introduced to the deck in form of slurry, they are transported towards the end of long axis through pushing force generated via table's motion. Afterward, wash water is subjected to table perpendicular to direction of particles movement, flown along the short axis of deck, and attempts to carry particles along the path parallel to direction of flow. Referring principle of separation, denser minerals generally have high settling velocity and quickly reach the plane of deck. As a result, these minerals are exposed to pushing force for longer period of time, which brings about they travel more longitudinal distance on the surface of table.

Conversely, the lighter ones can be moved by water film more transversal distances before falling down to the deck, hence they are influenced by subjected force in shorter period and less transported along the length of table. The heavy minerals normally fall inside the riffles located near the upper side of table by which are led towards the end of long axis. While, the lighter ones roll over riffles and go down the width of deck. The traveling route of different minerals has been shown on figure 2.35. As a result, light minerals (coal) could be efficiently separated from heavy ones (impurities) (Tiernon, 1980). Figure 2.36 clearly demonstrates that how various particles are led to different zones one the table corresponding to their density and size.

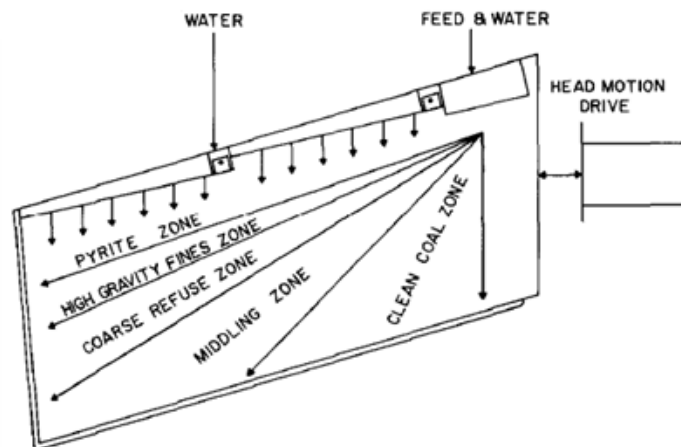


Figure 2.35 Separation zones on wet concentration table (Tiernon, 1980)

Wet concentration tables initially applied for beneficiation of metal based minerals and short after introduced to coal preparation industry. The Hudson Coal Co. has investigated the capability of unit in treating anthracite coal through conducting a series of cleaning trials. The Analytical data indicates that the machine could reach the highest efficiency as long as is fed up to 3 to 4 tons of materials per hour. A typical sample was beneficiated through this machine which has top size of 1.2 mm and contained more and less 28 % of

mineral matters. This unit managed to declines the ash percentage as less as 15 % with meeting approximately 53 % and 86 % of separation efficiency and combustible recovery, respectively. The provided data clearly proves the efficiency of Wet concentration tables in processing anthracite coal (Weiss, 1985).

2.3.2.4 Humphreys Spiral

The first unit of Humphreys Spiral was invented on 1940, and rapidly deployed into the mineral processing plants by reasons of being capable to treat various types of minerals and having low operational cost. The early application of Humphreys Spiral in coal preparation industry dates back to 1980's, since then this machine employed generally for treating particles ranging between 3 to 0.1 mm. Generally, this unit is considered as an efficient mid-processing stage between floatation and dense medium separation, since is able to treat a specific size range of minerals, which are too fine to be properly cleaned in heavy media separators and too coarse for being treated by floatation cells (Kohmuench J. N., 2000).

Raw materials are fed to top of the machine in form of pulp containing 15 to 45 % of solid by weight, and separated along a helical channel extended from top to end of unit. As slurry moves down the semicircular path, centrifugal force pushes it up towards the outer wall of trough until this force becomes equivalent to downward gravity force. In this condition majority of water accumulates near the outer rim, which causes the level of water in this part to elevate and water height in inward rim to be decreased. Thus, the thickness of water changes according to decreasing trend from outer wall of curved trough to the opposite wall (Lotz, 1960).

As stream keeps flowing down the helical rout, it is subjected to friction force, which negatively impacts its flowing velocity. The intensity of this force becomes maximum on the surface of through and greatly weakens on the center of stream. Regarding this phenomenon, the lower parts of fluid would obtain lower velocity than the upper levels,

hence lower parts are subjected to less magnitude of centrifugal force. As a result, the gravity force predominate the centrifugal force bringing about lower level moves towards the inner rim (Lotz, 1960).

In order to keep equivalent condition constant, the upper layers should shift upward along the spiral channel. Therefore, upper and lower level are repeatedly substituted with each other causing a revolving motion generated inside the stream, by which the denser minerals (middling and tailing) are transported towards the thinner layers, while the lighter particles (clean coal) shifted to the thicker ones. The described principle has been illustrated on (Figure 2.37 (a)) (Alexis, 1980; Lotz, 1960). Eventually, reject minerals are removed from the unit through splitters installed in each spiral trough, closer to inner wall. However, two other products travel along the whole helical path and are discharged out via corresponded ports mounted at the end of machine (Figure 2.37 (b)).

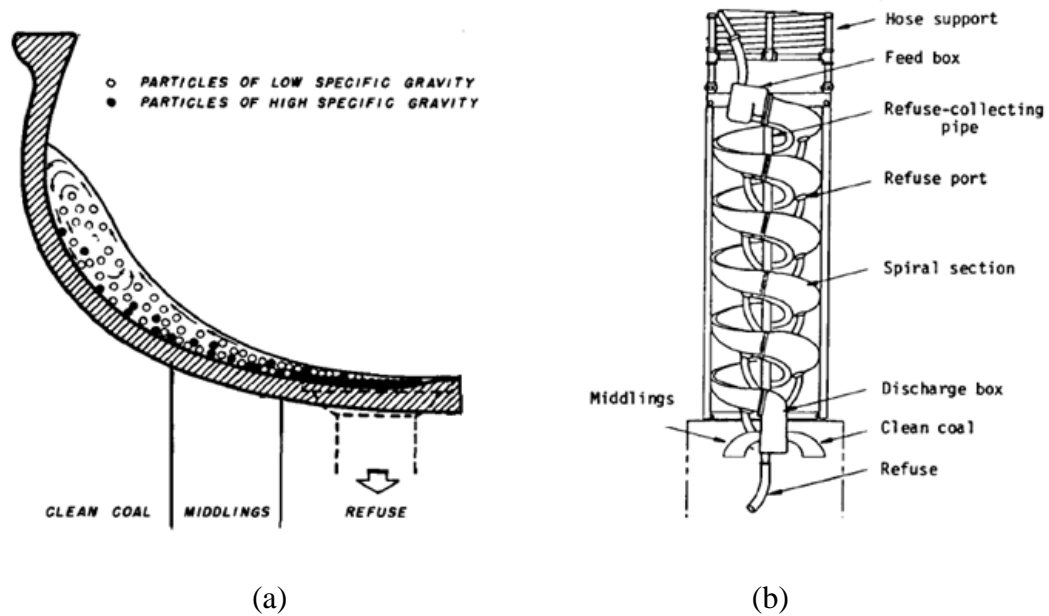


Figure 2.36 Humphreys spiral separator: cross section of rim (a) and full body of structure (b) (Alexis, 1980; Lotz, 1960)

The refuse ports (splitters), installed on inner wall of curved routs, can control the amount of product and reject ash. As the conduit of splitter excessively opens, not only more impurities are taken out from the slurry, but also a fraction of coal particles are misplaced to reject stream. At the contrary, decrease of conduit width would result in increasing the amount of ash recovery in both clean coal and tailing stream (Dennen & Wilson, 1948).

The Hudson Coal Co, on 1947, evaluated the possibility of anthracite silt cleaning by this wet based separators through implementing detailed experiments in an industrial scale plant. The feed of spiral was originally derived out the underflow stream of thickener, which before being subjected to spiral, was classified based on size in two stages: First, the underflow of thickener is introduced to 3/16 inch aperture size screen where particles remained on the surface of screen are taken out from the slurry. Next, that portion of materials which has passed through the holes, are fed to a cylindrical-conical shape tank where particles finer than 200 mesh are led to over flow and removed from the tank. The rest of particles sink and accumulate at the bottom of conical section. These particles, afterwards, are directly pumped to the spiral. Hence, the feed of machine is limited to particles ranging from 3/16 inch to 200 mesh size (Dennen & Wilson, 1948).

Referring fundamentals of operation, anthracite particles are pushed towards the outer rim of curved trough due to possessing lower specific gravity than mineral matters whose densities are higher. During a period of five months, a variation of anthracite coal samples were processed, which their ash content's range spread over 19 % to 41.5 %. The amount of impurities in reject product varies from 64.5 % to 86 %, and the produced clean coals' ash percentage ranged between 10.8 and 21. The average combustible recovery achieved by unit was approximately 65 %. Hence, the cleaned anthracite silt could perfectly be consumed in boiler furnaces which had been designed to burn a fuel containing 13% to 22 % ash content (Dennen & Wilson, 1948).

Unfortunately, the separation efficiency of single stage spiral has proved to be so sensitive to amount of particles led to middling stream. This product totally comprises

two sorts of particles: Bypassed minerals including both coal and reject. And, weakly liberated particles containing significant amounts of coal and impurities, which cause the specific gravity of that particle lies between densities of mineral matter and pure coal. In single stage circuit, middling product is mixed to any of clean coal or reject stream which resulted in following issues. If these minerals are added to the concentrated coal, the product ash would considerably increase. On the other hand, removal of this stream with impurities negatively impacts combustible recovery and product yield due to loose of some portion of pure coal.

To provide an effective solution dealing with the mentioned problems, a complimentary spiral has been appended to the separation circuit, which re-processes either middling or product of the primary unit, depending on the arrangement of spirals. As illustrated on Figure 2.38 (a), the middling stream of primary spiral is fed to secondary unit in which the misplaced coal and weakly liberated particles are provided with more chance to be recovered. This configuration is termed as rougher-scavenger which increases the cut density of overall separation. Thus, the combustible recovery enhances, while the quality of final product significantly suffers. As another inefficiency associated with this arrangement, the primary spiral's product stream is completely disregarded which may include some amount of misplaced mineral matters, bringing about raise of clean coal's ash content (Arnold, Klima, & Bethell, 2007).

To keep the quality of clean coal on the satisfactory level, the rougher-cleaner configuration has been developed which involves in combining primary product and middling streams, and subsequently introducing the mixture to the secondary unit for more treatment. As a result, mineral matters are increasingly extracted from final product which results in cut density reduction, and separation efficiency enhancement (Figure 2.38 (b)) (Arnold, Klima, & Bethell, 2007). The middling stream provided from the secondary spiral is directed back to the primary unit. Coming to the conclusion, this arrangement has been proved to have efficiency 1.22 time of the previous configuration (Luttrell, Kohmuench, Stanley, & Trump, 1998).

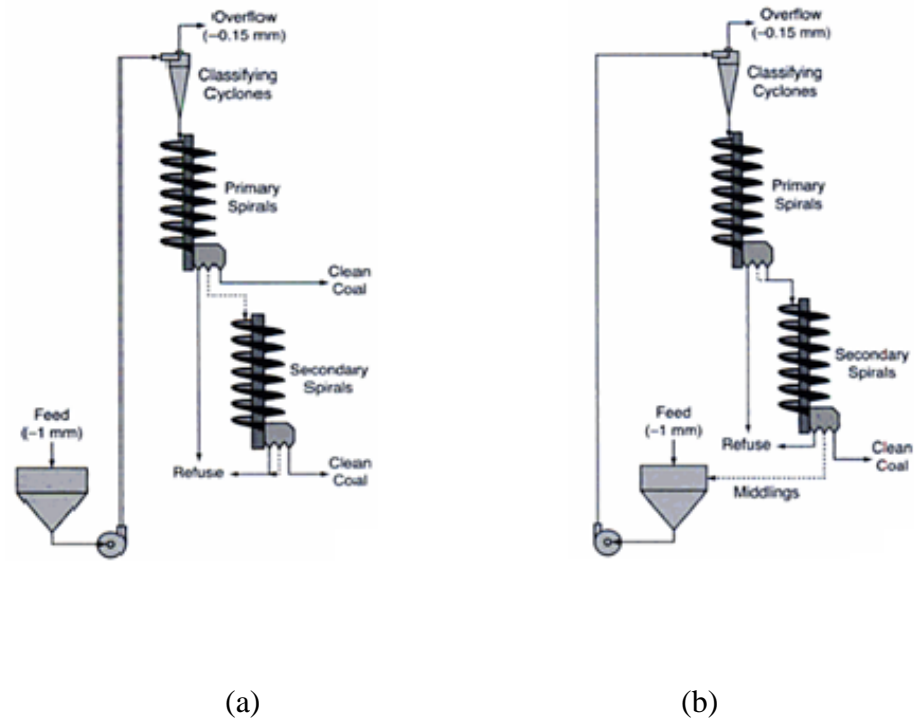


Figure 2.37 Two stage circuit including: rougher-scavenger (a) and rougher-cleaner (b) (Arnold, Klima, & Bethell, 2007)

The higher efficiency of rougher – cleaner arrangement has directed attention of manufacturers to develop a single stage spiral, identified as compound spiral, which implements both processes of roughing and cleaning in a same unit. The total helical route includes upper four turns conducting primary treatment process, and three lower turns re-preparing middling and product streams, as shown in Figure 2.39. The principle of operation entirely stimulates two-stage-spiral rougher - cleaner circuit.

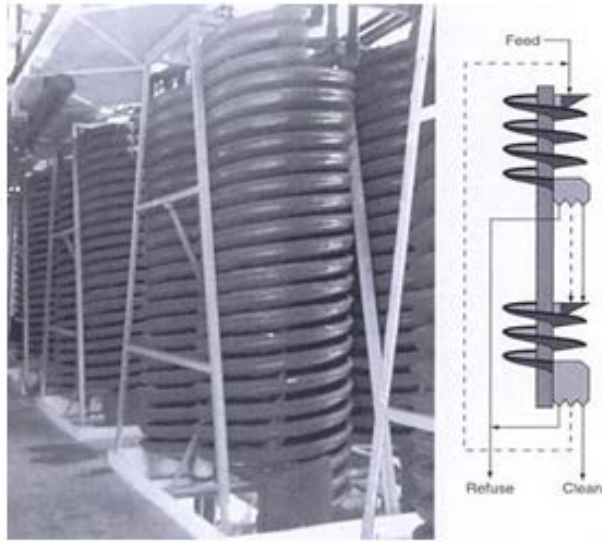


Figure 2.38 Compound cleaner spiral (Arnold, Klima, & Bethell, 2007)

To study the efficiency of compound spiral in beneficiating anthracite coal, two sets of anthracite samples from eastern Pennsylvania have been treated using this unit. The samples are classified into two categories including 'sample 1' taken from thickener feed, and 'sample 2' taken from thickener underflow, which the first sample comprised much coarser particles than the other one.

During the experiments conducted on 'Sample 1', several pulp flow rates have been applied that each of which contain different solid concentration by weight. For a specific slurry rate, product yield and ash percentage increase with decrease of solid content. The trend could be justified by the fact that particles would not hinder each other and could move towards the outer wall when the proportion of water to solids in pulp increases. At the constant solid concentration, decreasing the pulp flow rate would bring about increase of product ash, due to weaker centrifugal force is exerted on minerals. Thereby, less amount of coal particles are shifted to outer rim.

The above explained approach has also been used for evaluating the applicability of unit in processing 'Sample 2'. As mentioned before, this sample is collected from underflow

stream of thickener; therefore it normally contains too much fine minerals. Having beneficiated sample in different conditions, the analytical results demonstrate that the process of ash removal was not really acceptable. Because, feed comprises the excessive amount of - 0.025 mm particles which tend to move to outer wall, notwithstanding their differential density (Benusa & Klima, 2009).

2.3.2.5 Water Only Cyclone (WOC)

The idea of development of this machine has been drawn from classifying cyclone, by this difference that the conical section tilts 75 degree angle from vertical axis. Similar to classifying cyclone, the majority of particles tend to move towards the bottom of machine, however the structural change of conical part causes accumulated particles to be pushed up into the cylindrical part. As the high-density particles shift faster to the walls, they are subjected by elevating force and suspended around the end of cylindrical part, which results in generating an autogenous medium. The denser particles (mineral matter) pass through the medium and move to underflow, whereas the lighter minerals (coal) are led to overflow, due to lack of capability in penetrating through the suspended bed (Figure 2.40).

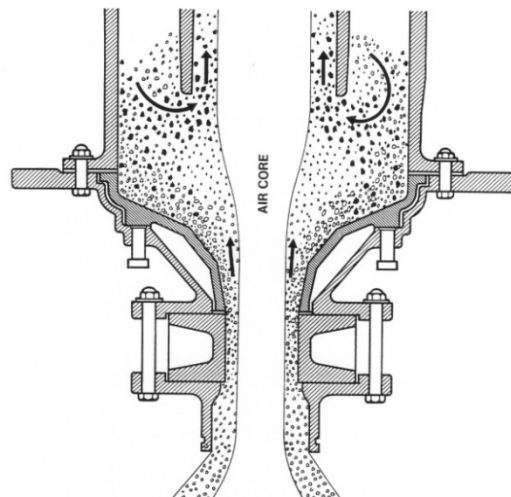


Figure 2.39 Particles distribution inside the water only cyclone (Albrecht, 1982)

The machine has been coupled with two passages as vortex finder and Apex, which direct purified coal and impurities to over flow and under flow streams, respectively.

There are several influential variables controlling the separation efficiency of process, as explaining the most important ones: 1) the length of vortex finder should be increases to optimum limit to facilitate medium formation, and minimize the probability of misplacement of high ash particles to the overflow, 2) excessive feed solid content would result in increase of cut density and declines of separation efficiency, 3) the optimum feed pressure found to be 15 psig or higher. More increase of feed pressure enhances separation efficiency, 4) extension of diameter of feed and overflow orifices would increase the flow rate of particles in on hand which causes decrease of particles retention time, thereby the cut density increases, 5) the rate of refuse discharge increases by broadening the diameter of underflow orifice. As a result, the cut density declines, which negatively impact the separation efficiency (Weiss, 1985).

The performance of water only cyclone in processing anthracite coal was investigated, by simulating three stages configuration including: 1) Re-circulating pair, over flow: the over flow of rougher unit is retreated in the second cyclone, 2) Re-circulating pair, under flow: the underflow of the first WOC is flowed to the second unit to be scavenged, 3) Re-circulating triple, overflow and underflow: consists of three WOC units in which both underflow and over flow streams of primary cyclone are introduced to two individual units for cleaning and scavenging.

Five samples from tailings of anthracite coal preparation plant were collected, subsequently screened out to three size fractions ranging 48 x 28, 28 x 100, and 100 x 200 mesh sizes, and finally treated in five single stage water only cyclone circuits. Thereafter, the partition data of these size fractions were generated. The procedure of simulating involves in using the partition data of each size range to evaluate the efficiency of whole circuit. The provided data demonstrates that the amount of ash

reduction maximizes in configurations which the overflow of primary unit is reprocessed in secondary cyclone such as re-circulating pair, overflow and the re-circulating triple, overflow and underflow arrangements. In addition, at a specific product ash percentage, the most product yield would be achieved by circuit which consists of rougher, cleaner, and scavenger units (Klima, Chander, & Subbarayan, 1995).

2.3.2.6 Heavy Media Separation

2.3.2.6.1 Introduction

The fundamental of treatment has been established on applying laboratory washability data on an industrial scale (Mitchell D. R., 1950). Briefly describing the process of separation, two types of minerals with different density are subjected to a heavy medium having intermediate specific gravity between them, which causes the lighter particles are floated while the heavier of which sink. The medium typically comprises heavy solids such as sand/magnetite suspended in water in several volumetric proportions, which result in increase of specific gravity of water to the desired separation density.

Compared to Baum jigs, normally, these machines have higher operational cost. However, they are preferred over jigs, due to being able to reduce the amount of coal loose throughout the separation process. Considering this fact, there are some specific cases in which the application of Heavy Media Separator surely provides more satisfactory results, as listed:

- Too much particles coarser than 6 inch in feed
- Anthracite cleaning which feed top size exceeds over $4\frac{3}{8}$ inch
- Treating coal materials that are potentially hardly cleaned (Lotz, 1960)

Since the early development of Heavy Media Separators, several types of these machines have been gradually introduced into mineral processing industry, which each of those have unique properties and principles of operation. These units are classified into two

general categories, based on the procedure of introducing medium to system. The first group, 'Static Separators' , structurally consists of a tank which the medium is either provided inside the system through mixing water with heavy minerals (chance cone), or linearly subjected into machine after being prepared in particular sumps (Conklin Process Separator). The fundamental of separation lays down the difference of particles' vertical settling velocity under influence of gravity force. This group of separators is typically characterized as 'Heavy Media Vessels'.

The other group is termed as 'Dynamic Separators', in which the medium is tangentially injected to the system and circulated along the length of machine. As a result, particles are separated in accordance to their centrifugal velocity which is directly proportional to differential density of particle and medium. In instance, Dense Medium Cyclone (DMC), and Dynawhirlpool Coal Cleaner fall into this class.

The operational principles of above-named machines have been comprehensively studied in two separate sections in which the first one discusses units belonging to the primary category(Static Separators), while the following section considers machines classified into second category(Dynamic Separators) (Srinivasa, 1981).

2.3.2.6.2 Static Separators

Heavy Media Vessels have proved to be significant members of Dense Medium Separators family, as they are capable of treating lump particles on an efficient manner. Several types of these machines have been developed which each one is distinguished from the others based on body shape, procedure of introducing raw feed, method of preparing medium, and mechanism of discharging products. Regardless the mentioned differences, all sorts of machines apply the same separation principle in which minerals with different density are separated by means of heavy medium, and move along the opposite vertical trajectories towards their corresponding discharges (Weiss, 1985).

In a typical classification, vessels are identified as tank and drum types. The tank-shaped vessels are more subdivided into shallow, intermediate, and deep pools separators. Each of four named categories consists of several types of machines applying various principles of preparation and employing unique mechanism of particles removal. A great deal of these technologies has been used in coal cleaning industry, which are well worth discussing. However, study of all of which would lie outside the scope of this thesis. For that reason, those machine have been described in detail, which ones that are specifically applied for anthracite beneficiation. Listing the selected units corresponding to their category:

- Chance cone: Represents Deep Bath Tank Vessels
- Conkling Process Separator: As typifies Shallow Bath Tank Vessel group
- Teska: Drum type vessel

Chance cone, a cylindrical-conical shape separator, purifies coal particle from accompanying impurities employing a medium which is generated by suspending sand particles inside the water. The water is pumped into unit through nozzles horizontally installed at the periphery of conical part and are arranged towards the center of bath. Having water injected to the system, it suspends sand particles and forms a teeter. As particles are fed to the system, the lighter minerals (coal) move towards the overflow discharge and the denser ones (tailings) sink to the end of conical part.

Thereafter, each product is subjected to a sets of screens equipped with spraying water so that sand particles sticking to minerals are washed out. The removed sand particles, in the form of pulp, are transported to a sump and gradually settle at the bottom of unit. As a result, the upper levels of sump comprise clear water, while the lower level is almost entirely occupied by sand particles. Subsequently, the water, after passing over the lips of sump, is pumped back to the nozzles. And, the accumulated sand particles are shifted towards a box located at the top side of machine, where they initially are deposited and finally subjected to the unit. The process of recycling water and sand assists density of medium to be stabilized.

In addition, the machine has been coupled with an agitator installed at the top of the unit and deeply extended into conical part. This part has been designed to perform two duties as, stirring the mixture of sand and water which results in the sand particles are kept fluidized inside the water. As well as, the agitator disperses treated minerals which have been accumulated in dead zones located at the center of cone (Lotz, 1960). The principle of separation has been clearly shown on Figure 2.41.

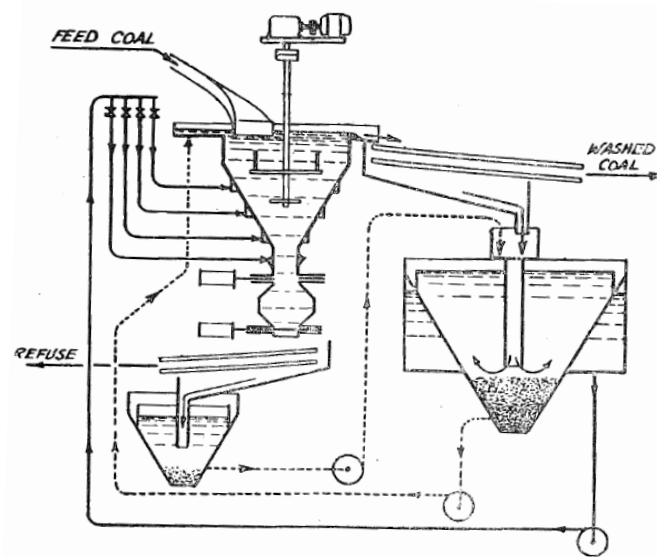


Figure 2.40 Chance Cone separation machine
(Mitchell D. R., 1950)

Conklin Process Separator, the other unit categorized in this group, initially employed in anthracite coal cleaning industry by Hudson Coal Co. As illustrated on Figure 2.42, this machine consists of a rectangular bath working as separation zone which both vertical sides have been tilted towards the center of machine. The separation medium generally is prepared by blending - 200 mesh size magnetite particles with water, in which for every volumetric unit of magnetite, there are 4.4 units of volume of water inside the medium.

At the left side of machine, a paddlewheel has been mounted near the feed chute generating longitudinal flow at the top level of medium, which causes the floated particles (coal) to be shifted along the length of unit towards the opposite side. At this part, an inclined revolving comb conveyor has been mounted over a drainage screen in such a way that the entire surface of screen is covered properly. The conveyor continuously collects clean coal minerals and simultaneously subjects them to the screen, which brings about the medium is recovered and recycled back to the system. Thereafter, coal particles are exposed to a water jet so that remained magnetite particles to be washed.

At the bottom of the tank, a screw conveyor has been installed to lead sunken minerals (tailings) to an elevator located at one side of machine. This part lifts particles up and discharges them over a screen coupled with wash water, which is responsible to remove minerals adhering to the coal. During this process, the original / correct medium is contaminated with wasted minerals, and excessive amount of water which cause the primary properties of medium to be entirely changed. As a result, the medium (diluted) would not be more suitable to be reused in treating process. To convert the diluted medium to the corrected one, a series of purifying and thickening processes are conducted on the medium, by means of classifying cyclone and thickener. Eventually, the regulated medium is directed back to the machine (Mitchell D. R., 1950).

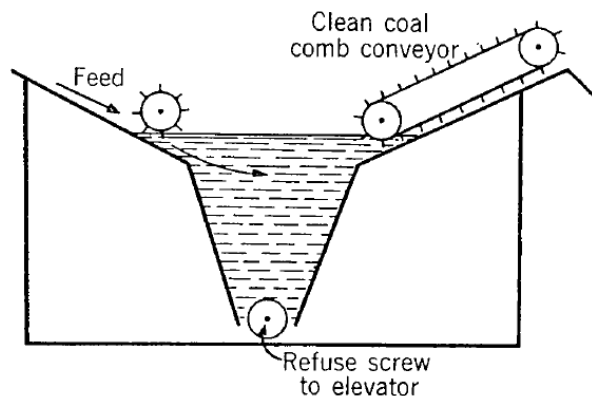


Figure 2.41 Conklin Process Separator (Eckerd and Spencer 1971)

Teska, a drum type vessel, resembles as the same operational principle as applied for pre-mentioned machine (Conklin Process Separator), in which clean coal and refuse particles are carried in different trajectories, perpendicular to each other. Raw materials are transversally introduced to the bath through an inclined chute which is located over a fan shaped valve pumping medium into the system. Consequently, on the top level of medium, a linear flow is provided along the width of machine. This stream exerts a pushing force on the floated particles (coal), and carries them towards the left side weir (Weiss, 1985). The machine would be coupled with a rotating paddle, in special cases that the upper size of particles exceeds beyond 2 inch. This mechanism greatly simplifies the process of discharge of coarse floated minerals (Leonard, 1979).

Separation bath, from the end, meets a cylinder consisting of perforated chambers. This wheel has been located parallel to the length of machine and revolves in clockwise direction, around the separation zone (pool). As high density minerals sink inside the bath, they continuously accumulate into the chambers and are lifted up with rotation of the wheel. As collected minerals reach top of the machine, they are discharged on a steep chute which leads them towards the refuse launder (Leonard, 1979; Weiss, 1985).

The machine could provide the most separation efficiency if density of heavy medium is kept constant, throughout the preparation process. To obtain this purpose, that portion of medium (around 20%) which passes through down the perforated wheel, should be directed back to the system. Therefore, several nozzles have been instated at the periphery of cylinder, which channel this fraction of medium to its corresponding sump for recycling (Leonard, 1979). This unit has been schematically illustrated on the Figure 2.43.

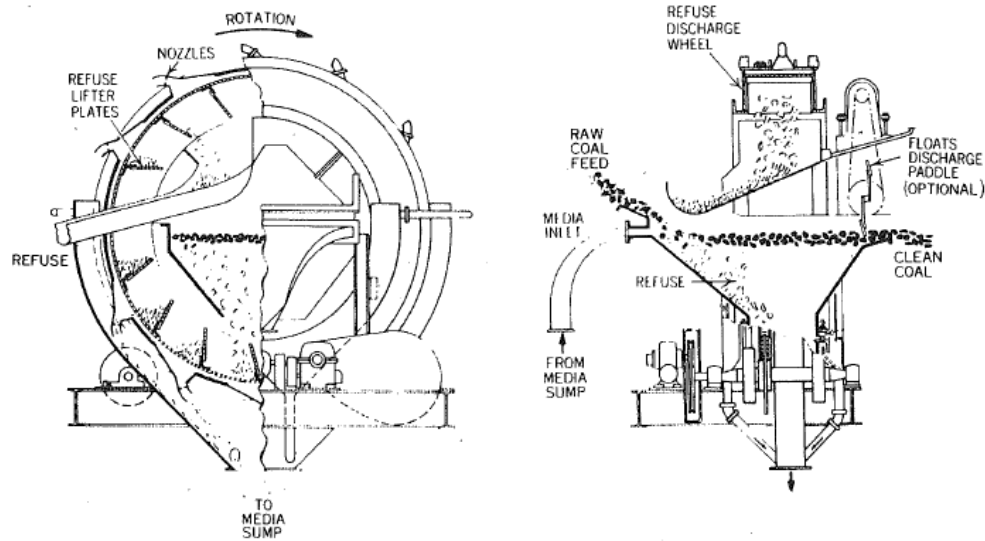


Figure 2.42 Teska vessel (Leonard, 1979)

2.3.2.6.3 Dynamic Separators

The feed of mineral processing plants generally comprises particles with variety of sizes which a number of particles are too fine to could be properly cleaned in vessels, and some of those are excessively large that flotation columns would be capable to handle their treatment. These sorts of particles are identified as intermediate size range. The high amount of intermediate particles in feed has highlighted the necessity to such efficient gravity based separators which be able to efficiently treat this particles size range (Weiss, 1985).

To reach this goal, several machines have been introduced to mineral processing industry, which all exert centrifugal force on particles to implement separation of light minerals from heavy ones. The settling velocity /gravitational acceleration of particles under influence of centrifugal force, is proportional to centrifugal acceleration and differential density of particles and medium, that could be formulated as:

$$V = d^2 \frac{(\rho - \rho')}{18 \mu} \frac{v^2}{r} \quad (2.4)$$

In which, ' v ' is tangential velocity of particle at movement radius of ' r '. ' ρ ' is density of a given particle located inside a medium having density of ' ρ' ' and viscosity of ' μ '. And, ' d ' is considered as particle's size (Bimpong, 2008).

Hence, various minerals obtain different gravitational acceleration which may be either negative (if particle's density is less than medium density) or positive (Those cases which particle has greater density than medium). As a result, dense particles obtain positive acceleration and move towards the outer wall of machine, while light minerals acquire negative acceleration and are attracted to the center of unit. This phenomenon is generally identified as the principle of separation of 'dynamic separators'.

Three major machines are categorized into this class, which operate based on the provided formula. They are listed as: Water Only Cyclone (WOC), Dense Medium Cyclone, Dynawhirpool Coal Cleaner (Weiss, 1985). As previously discussed, the Water Only Cyclone applies an autogenous medium for particles treatment. While, the other two machines, classified as Centrifugal specific gravity separators, which employ a dense fluid comprising heavy minerals suspended in water. As clearly conceived, units of this class, similar to Heavy Media Vessels, apply dense medium for particle-particle separation. However, the effective force is centrifugal rather than gravitational.

As Water Only Cyclone has been already described in a separate section, the following sentences have been only allocated for discussing operational fundamentals of the rest of aforementioned machines.

Dynawhirlpool Coal Cleaner structurally is a cylindrical body tilting around 25 degree angle from horizon line, which consists of two tangential openings and two auxiliary orifices located on both upper and lower ends of unit (Figure 2.44). The medium is tangentially introduced to the system from the bottom tangential opening, and centrifugally flows along the length of unit. This motion not only generates an air core extending from top auxiliary orifice (feed inlet) towards the lower one (underflow discharge), but also is converted to two centrifugal currents having different moving directions (Weiss, 1985).

One of these currents is created close to outer wall and moves upward to the upper tangential opening (overflow). Whereas, the other of which circulates around the air core, downward to underflow discharge. Referring to equation 1, as raw minerals are subjected into system, the heavier minerals are shifted towards the outer wall and transported by upward current to the overflow discharge. However, the lighter ones are attracted towards the air core and pushed down to the underflow discharge by means of downward centrifugal current (Eckerd and Spencer 1971).

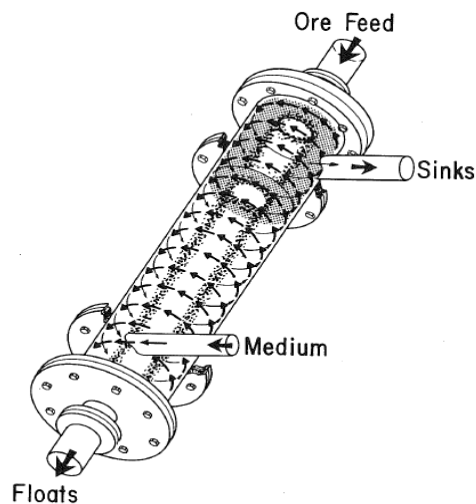


Figure 2.43 Dynawhirlpool coal cleaner (Weiss, 1985)

Principally, dense medium cyclone follows as same procedure of separation as applied in Dynawhirpool coal cleaner. However, these units have different structure and also apply distinct mechanisms of feed introduction, and product removal. Dense medium cyclone consists of a cylindrical part connected to a conical section which has been inclined between 14 and 25 degree angle from centerline of machine (Weiss, 1985). In mineral processing plants, this unit usually is installed at 10 degree angle from horizontal axis (Honaker, Akram, & Groppo, Recovery and utilization of bottom ash magnetics for coal cleaning medium, 2009). Several openings have been mounted on both inside and outside parts of machine, which perform specific duties. These openings are termed as:

- Feed inlet: introduce medium and feed to the machine
- Overflow orifice: discharge coal particles
- Vortex finder: Extended into cylindrical section of cyclone and leads floated particles to the overflow orifice
- Apex: has been designed to remove sink materials from the system (Figure 2.45)

As illustrated in Figure 2.46, the mixture of feed materials and heavy medium are pumped into machine under a tangential motion, and travel helically along the length of machine. Similar to Dynawhirpool, an air core is generated between vortex finder and Apex and the medium is divided into two distinguished flows, which have different moving direction. Impurities pass through the medium and move towards the wall, and then are shifted to the Apex with downward current. Whereas, coal particles those ones which are not able to penetrate through medium, are transported to the vortex finder by upward central flow.

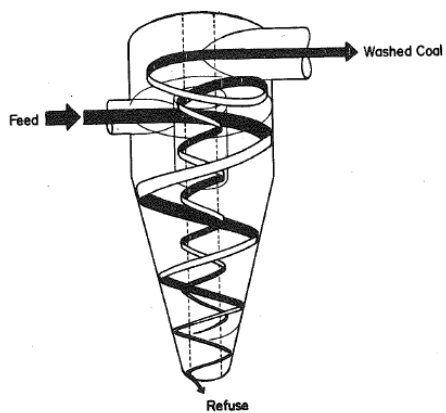


Figure 2.44 Dense Medium Cyclone (Mitchell D. R., 1950)

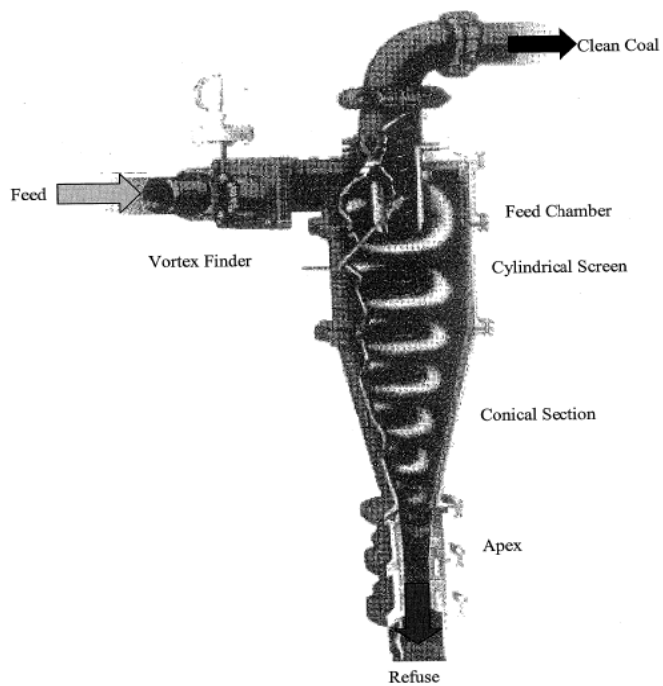


Figure 2.45 Several parts of Dense Medium Cyclone (Bimpong, 2008)

The separation efficiency is greatly correlated with two substantial characteristics of medium, which identified as Viscosity and Stability. The operational condition, especially cut density, considerably changes with decrease or increase of these factors, which may results in either better or worse separation process. To determine the effects of viscosity on separation efficiency, a general formula (equation 2) has been developed, which reveals the relation of E_p to particles size (d), medium viscosity (μ), and constant value of 'k'.

$$E_p = \frac{k\mu}{d} \quad (2.5)$$

The above equation clearly demonstrates that the separation efficiency declines with decrease of feed materials size and increase of medium viscosity.

Apart from raw materials, magnetite particles are also exerted centrifugal force which causes the majority of magnetite particles to be accumulated near wall rather than centerline. As a result, the medium streams coming out from over flow and underflow, would differ in amount of density. Medium stability is defined as the differential density of overflow and underflow mediums. As this difference decreases, the medium would become more stable, which brings about the more efficient separation process. The accepted amount of this difference has been found to be equal and less than 0.4 (Bimpong, 2008).

Laskowski et al, have comprehensively investigated the effect of size of magnetite particles on viscosity and stability. During the experiment, three magnetite samples have been used which had several sizes ranging from fine to coarse (Table 2.2).

Table 2.2 Mean size of magnetite samples used for evaluating effect of magnetite size on medium stability and viscosity (He & Laskowski, 1993)

Sample	$d_{63.2}$ (μm)
Mag # 2	18.0
Mag # 3	33.0
Mag # 4	4.3

Referring to Figure 2.46, with the raise of medium density, the density differential of all mediums initially increases by a maximum value, and then commences to decline. Interpreting this decreasing trend, adding more amounts of magnetite particles in medium would result in increase of viscosity, which improves distribution of magnetite particles in entire areas of cyclone. However, the density differential of coarser magnetite sample would never fall below 0.8, which means this medium is poorly stable.

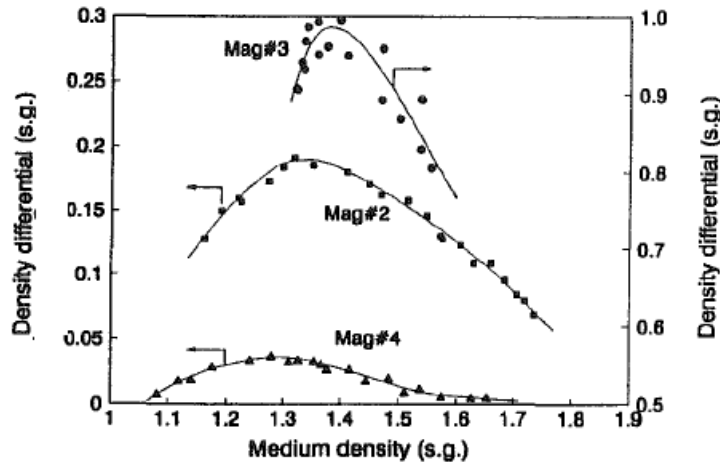


Figure 2.46 The effect of magnetite particle size on density differential of dense medium separation technologies (He & Laskowski, 1993)

The other part of trials has been allocated to determine the effect of medium viscosity on separation efficiency. E_p value will decrease by increase of density of mediums which ones comprise fine and intermediate magnetite particles (Mag # 2 and Mag # 4). This ascending trend of E_p is resulted due to increase of the viscosity of medium with adding more amounts of magnetite particles. However, the raise of medium density by using coarse sample (Mag # 3), provides much better results. As previously discussed, this medium is unstable on lower densities. With increase of the quantity of magnetite particles, this medium would convert to more stable one, which results in enhancement of separation efficiency (Figure 2.47).

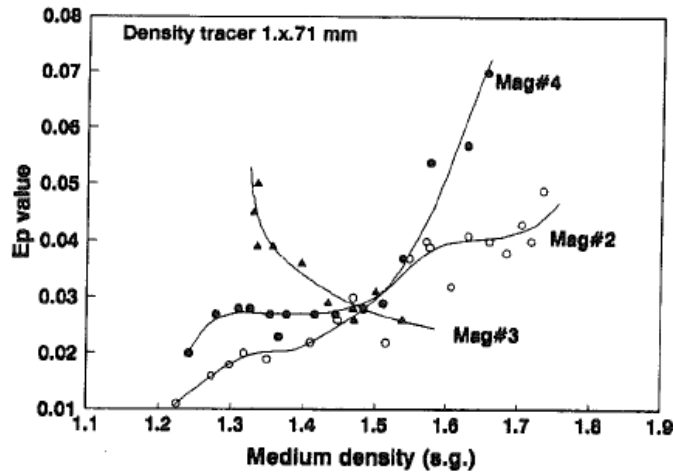


Figure 2.47 Effect of magnetite particle size on E_p of dense medium separation technologies (He & Laskowski, 1993)

Based on this finding, it could be deduced that the increase of viscosity would improve the stability of medium which consists of coarse particles, hence causes more efficient separation process. However, in case of existence of fine and intermediate magnetite particles in water, the increase of medium density directly rise the amount of viscosity which negatively impacts the separation efficiency.

In experimental section, the performance of Dense Medium Cyclone in treating anthracite coal has been studied in detail. Moreover, the separation efficiency of each cleaning trial has been analyzed considering the effect of aforementioned factors.

2.3.3 Froth Flotation

The fundamental of froth flotation is established on separating particles in accordance to their degree of surface hydrophobicity. The process of treatment is entirely conducted by means of air bubbles in an environment which comprises three phases of liquid, solid, and gas. Raw materials are fed into the flotation cell in form of slurry and commence to descend along the length of machine. Air bubbles are generated at the bottom of flotation cell and start ascending towards the froth zone located at top of machine (Dube, 2012).

Bubbles, throughout their travel route, collide with minerals having various amounts of hydrophobicity. The hydrophobic minerals are selectively adhere to the surface of bubble and transported towards the froth, with the raise of bubble. While, the hydrophilic particles detach bubble; and move downward to the end of cell, where they are discharged from (Dube, 2012). The operational principle of flotation cell has been schematically shown in Figure 2.49.

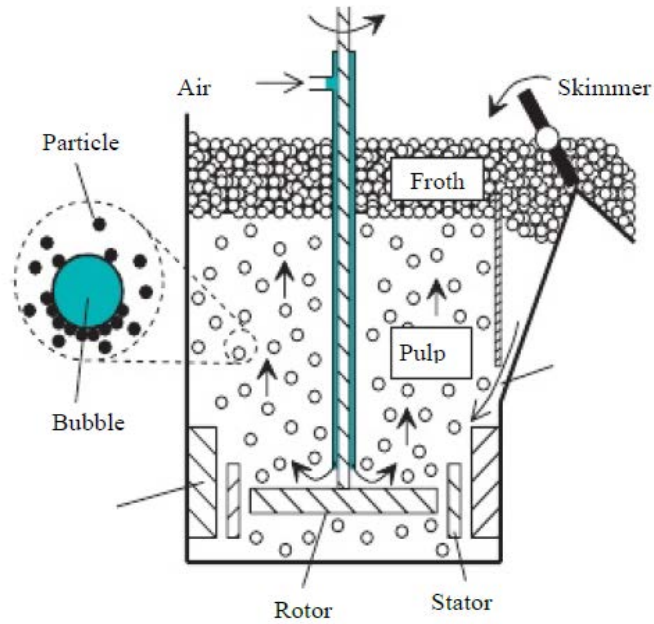


Figure 2.48 Typical separation process of flotation cell (Dube, 2012)

The prime froth flotation machine was devised on early 19th, and its application has gradually been deployed in mineral processing industry, since then. In the U.S, the first processing plant equipped with flotation machines, was constructed on 1911 and the initial application of this technology in coal treatment industry dates back to 1930 (Dube, 2012).

The particle-bubble attachment is one of the most significant processes of froth flotation, which results in establishment of three phase (liquid-gas-solid) contact (Figure 2.50). Thermodynamic of this process could be determined via Young's equation:

$$\gamma_{SG} = \gamma_{SL} + \gamma_{LG} \cos \theta \quad (2.6)$$

In which, (θ) is contact angle, and γ_{sv} , γ_{sl} and γ_{lv} are the tensions of solid-gas, solid-liquid and liquid-gas interfaces, respectively (Fuerstenau & Raghavan, 1976).

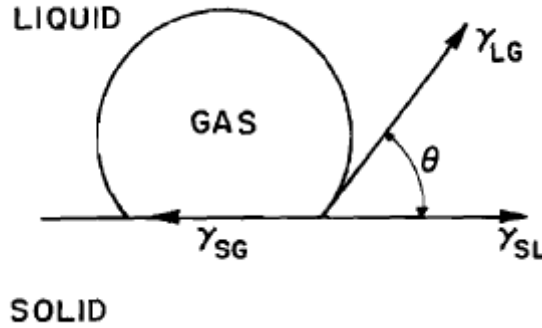


Figure 2.49 Schematic representation of the equilibrium contact between an air bubble and a solid immersed in a liquid. The contact angle is the angle between the liquid/gas and the liquid/ solid interfaces, measured through the liquid (Fuerstenau & Raghavan, 1976)

In addition, the substitution of a unit area of solid- liquid interface with solid-gas would cause the free energy to be varied. The amount of this change could be expressed by Dupre's Equation:

$$\Delta G = \gamma_{SG} - (\gamma_{SL} + \gamma_{LG}) \quad (2.7)$$

Considering the above formula, the air bubble replaces water on the surface of solid, if the absolute magnitude of ΔG is negative. Providing more clarification, the bubble particle adhesion would be thermodynamically probable, as long as the interfacial tension of solid-gas is less than the summation of interfacial tensions of solid- liquid and liquid-gas. Thereby, the greater decrease of level of free energy would increasingly enhance the possibility of particle-bubble attachment (Fuerstenau & Raghavan, 1976).

Substituting Young's equation into Dupre's formula provides a new equation which discovers correlation of free energy change with contact angle and tension of liquid-gas interface.

$$\Delta G = \gamma_{LG} (\cos \theta - 1) \quad (2.8)$$

The degree of particle's hydrophobicity is a function of contact angle (Koca, Bektas, & Koca, 2010). Referring above equation, the maximum decrease of free energy would occur whenever the bubble adheres to the surface of an ideal hydrophobic solid which have contact angle of 180 °.

The floatation rate is considered as one of the key aspects of floatation process which directly control the amount of coal recovery. This factor could be calculated using the following formula:

$$\frac{dN}{dt} = -kN \quad (2.9)$$

Where, 'N' represents the amount of floatable particles existing in separation zone, and k is constant value which is depended on superficial aeration rate 'V_g', bubble radius 'R₂', and the probability of particles collection 'P'. This probability is more sub-divided into three basic probabilities, as expressed on following equation:

$$P = P_a P_c (1 - P_d) \quad (2.10)$$

In which P_a, P_c, and P_d are probabilities of adhesion, collision, and detachment, respectively (Mao & Yoon, 1997).

The size of a given particle directly determines its probability of collision and detachment. As raw feed consists of ultra-fine particles the probability of collision

dramatically declines which brings about decrease of flotation rate. On the other side of coin, the coarse particles have high degree of probability to detach the bubble surface. As a result, the probability of detachment could estimate the top size limit of materials being able to be recovered in flotation process. Likewise, with boost surface hydrophobicity, probability of attachment increases, while the probability of detachment reduces (Mao & Yoon, 1997).

Coming to the conclusion, both physical and chemical properties of a given mineral directly determine its capability to be collected by air bubble.

CHAPTER 3

EXPERIMENTAL

3.1 Introduction

As previously described, the potential to upgrade difficult - to - clean Korean anthracite was investigated using tests on three dry cleaning technologies and a water - based density unit. All samples were provided by KIGAM (Korean Institute of Geoscience and Mineral Resources). The first two phases of experiments focused on using an air table and dense medium cyclone for cleaning two types of samples originally obtained from different coal seams. The remaining phases involved the use of a rotary tribo-electric separator, and dual energy X-ray transmission sorter to conduct beneficiation tests on another type of Korean coal totally having different characteristics.

Therefore, the size and cleanability properties of samples treated via named technologies completely differed. Regarding the type of employed machine, the experimental approaches have been precisely described in the following sections.

3.2 Experimental Procedure of air table and dense medium cyclone

3.2.1 Particle Size and Washability Analysis

KIGAM delivered two coal samples collected in 208 liters barrels, which namely categorized as coarse (8 x 4 mm) and fine (5 x 1 mm). Upon receiving samples, a representative sample was collected and subjected to particle size analysis using wet sieving. The material in each fraction were weighed and analyzed for ash content. The particle size and ash distributions of the two samples are provided in Tables 3.1 and 3.2.

The size analysis conducted on coarse sample demonstrates that the largest portion of the materials had a particle size between 4 mm and 1.19 mm which is smaller than the described sample identification. This is likely due to the friability of the coal and the

impact of the handling from Korea to the U.S. A significant amount of material was smaller than 0.21 mm which is also due to the friability of the coal and extensive handling.

The majority of impurities accumulated in the ultrafine fraction which likely reflects the presence and liberation of clay particles (Table 3.1). The 5.6 x 4 mm fraction had the lowest ash content which was a positive given the separation processes being evaluated. The overall average ash content of 52.31% was largely impacted by the 4 x 1.19 mm with an ash content of 46.27 %.

Table 3.1 Particle size and ash distribution of nominally coarse (8 x 4 mm) Korean anthracite coal sample

Particle Size (mm)	Weight (%)	Ash (%)
5.6	3.99	65.05
5.6 x 4	13.33	28.65
4 x 1.19	50.43	46.27
1.19 x 0.6	10.68	72.14
0.6 x 0.21	4.75	71.69
-0.21	16.82	86.06
Total	100.00	52.31

The friability of the coal was even more apparent for the fine (nominal 5 x 1 mm) sample. As shown in table 3.2, about 44 % of the particles were finer than 0.15 mm. On the positive side, the remaining material was well distributed, mostly between 5 mm and 0.3 mm.

As opposed to the coarser sample, the ash-based material was well distributed among all size fractions with the lowest content values in the finest size fractions. The reversal in the trend could be due to preferential breakage of coal into the finer fractions. As shown

in Table 3.2, the overall ash content of 41.88 % is largely due to the mass of material in the - 0.15 mm fraction which had an ash content of 41.88 %.

Table 3.2 Particle size and ash distribution of nominally fine (5 x 1 mm) Korean anthracite coal sample

Particle Size (mm)	Weight (%)	Ash (%)
+ 5	0.55	57.54
5 x 2.38	12.90	50.67
2.38 x 1.19	14.88	47.31
1.19 x 0.6	11.19	42.84
0.6 x 0.3	7.95	39.87
0.3 x 0.21	4.52	38.25
0.21 x 0.15	3.83	36.70
-0.15	44.17	38.24
Total	100.00	41.88

Two of the processes evaluated in this study rely on particle density differences. Due to this fact, a clear understanding about the density distribution in the Korean coals was essential to theoretically assess the product quality and combustible recovery potential at a particular separation density.

The cleanability values of both samples were evaluated by exploiting a prevalent analysis termed float - and - sink / washability. This test precisely determines the density distribution of coarse and fine representative samples at various densities. The procedure of preparing media involved dissolving different amounts of lithium metatungstate in water, corresponding to the desired density. The washability tests were conducted to obtain five density fractions, beginning at 1.6 and successively increased in increments of 0.1.

Given that the finest material in each sample, i.e., - 0.6 mm for the coarse sample and - 0.21 mm for the fine sample, is not treatable by the density - based separation process in this study, the fraction was removed prior to the washability analysis. Each sample was screened using circular sieves and the overflow subjected to washability analysis.

Initially, the entire representative sample was immersed into the container holding medium with specific gravity of 1.6. The floated particles were collected as the fraction of material which has a specific gravity density lower than 1.6. The portion of the sample that sank in the 1.6 medium was subjected to the next medium (1.7). This procedure was repeated to the final step of the washability test, in which particles floated and sunk in specific gravity of 2.0.

Materials recovered in each density fraction were washed by hot water to eliminate the lithium metatungstate remaining on the surface of the particles. The cleaned samples were dewatered by mean of filters and subsequently dried. The process of analysis of representative sample was finalized by measuring weight and assaying for mineral matter content.

The washability data for coarse and fine samples have been respectively provided in Tables 3.3 and 3.4. The data clearly shows a significant difference between the coarse and fine samples with the fine material unexpectedly having a significantly more difficult cleaning potential. The density of both coal samples is greater than 1.6 gm/ml which is higher than bituminous coal but typical of anthracite.

Table 3.3 Density-by-density weight and ash distribution data of the obtained coarse (+ 0.6 mm) Korean anthracite coal sample

Specific Gravity	Incremental		Cumulative		
	Weight (%)	Ash (%)	Weight (%)	Ash (%)	Combustible Recovery (%)
1.60 Float	3.40	3.65	3.40	3.65	6.23
1.60 x 1.70	23.94	7.68	27.34	7.18	48.26
1.70 x 1.80	10.72	17.00	38.06	9.95	65.18
1.80 x 1.90	8.34	30.17	46.40	13.58	76.26
1.90 x 2.00	6.40	42.84	52.80	17.13	83.22
2.00 Sink	47.20	81.30	100.00	47.42	100.00
Total	100.00	47.42			

Table 3.4 Density-by-density weight and ash distribution data of the obtained fine (+ 0.212 mm) Korean anthracite coal sample

Specific Gravity	Incremental		Cumulative		
	Weight (%)	Ash (%)	Weight (%)	Ash (%)	Combustible Recovery (%)
1.60 Float	0.00	0.00	0.00	0.00	0.00
1.60 x 1.70	0.50	5.66	0.50	5.66	0.87
1.70 x 1.80	2.85	10.52	3.35	9.79	5.60
1.80 x 1.90	12.19	18.76	15.54	16.83	23.94
1.90 x 2.00	26.75	27.80	42.29	23.77	59.70
2.00 Sink	57.71	62.30	100.00	46.00	100.00
Total	100.00	46.00			

For the coarser sample, the analytical data indicates that a considerable portion of the total mass has a relative density less than 1.8 has an ash content of around 10 %. The material heavier than 2.0 S.G. is significant in weight and has an ash content of 81.30 %.

As such, removing the 2.0 sink material significantly upgrades the quality of the clean coal product.

The relative cleanability of the coal can be assessed by plotting the percentage of near-gravity material that is within ± 0.1 S.G. units of the target cut point. As shown in Figure 3.1, the amount of near-gravity material in the 1.8 to 1.9 range is between 15% and 20%. This density range represents the optimum cut points for achieving effective upgrading of the coal while maximizing yield. Dense medium processes should be very effective for achieving the desired separation.

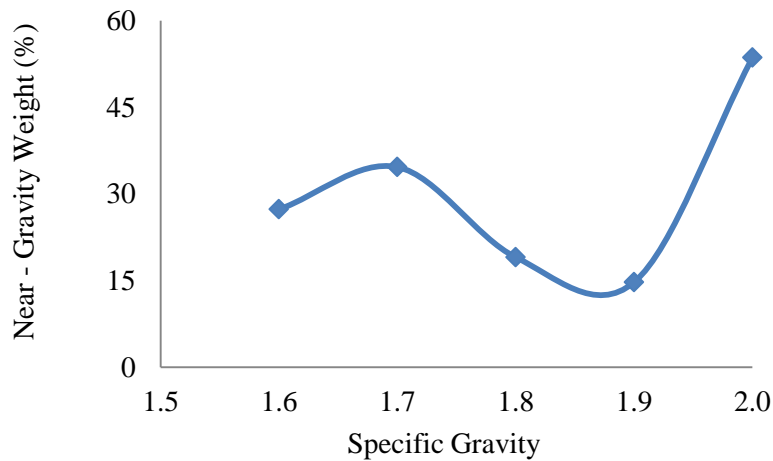


Figure 3.1 Near gravity curve for coarse size fraction of Korean Anthracite coal sample

To more evaluate the cleanability of subjected coal sample, theoretical combustible recovery curve and cumulative float curve have been plotted by use of washability data. These curves show that a 10 % product ash is achievable from the 47 % ash feed while recovery nearly 40 % of the feed weight and 65 % of the combustible material (Figure 3.2).

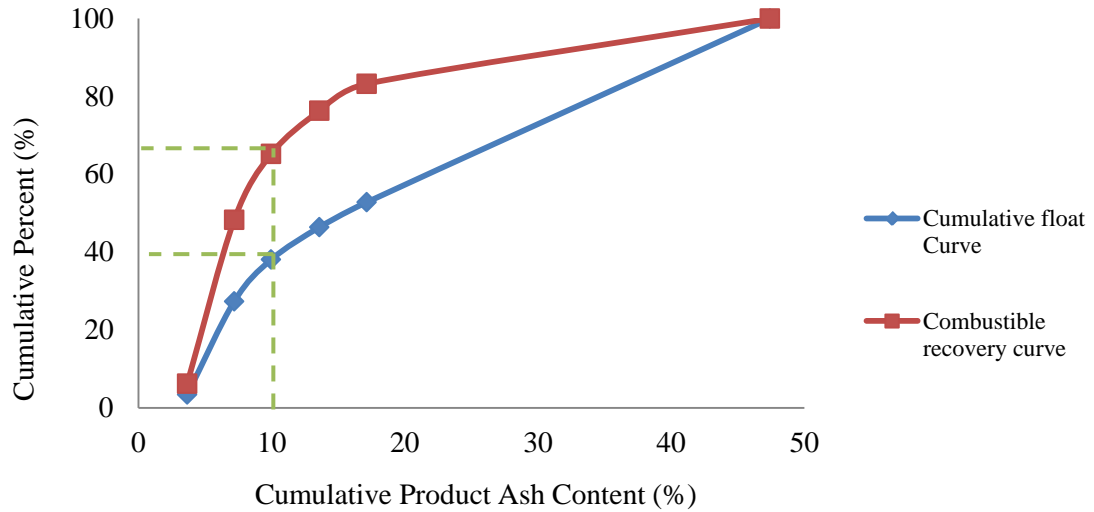


Figure 3.2 Cumulative float yield and combustible recovery curves for coarse size fraction of Korean Anthracite coal sample

The fine Korean coal sample had very unusual washability characteristics that made it very difficult to clean by density techniques. As shown in Figure 3.3, the percentage of near-gravity material is reasonable for density-based separations at S.G. values of 1.8 or lower. However, the majority of the fine coal has a relative density above 1.8 thereby indicating very limited potential for upgrading. Figure 3.4 shows that a cut point of 2.0 S.G. will result in a product ash content of 46.0 %. However, the amount of near-gravity at this cut point is well above 50 %. As such, a separation at a 2.0 S.G. would be formidable.

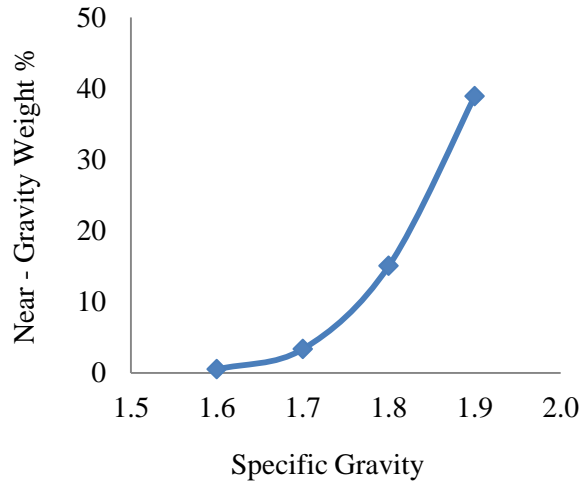


Figure 3.3 Amount of near-gravity curve material as a function of medium specific gravity for the fine Korean Anthracite coal sample

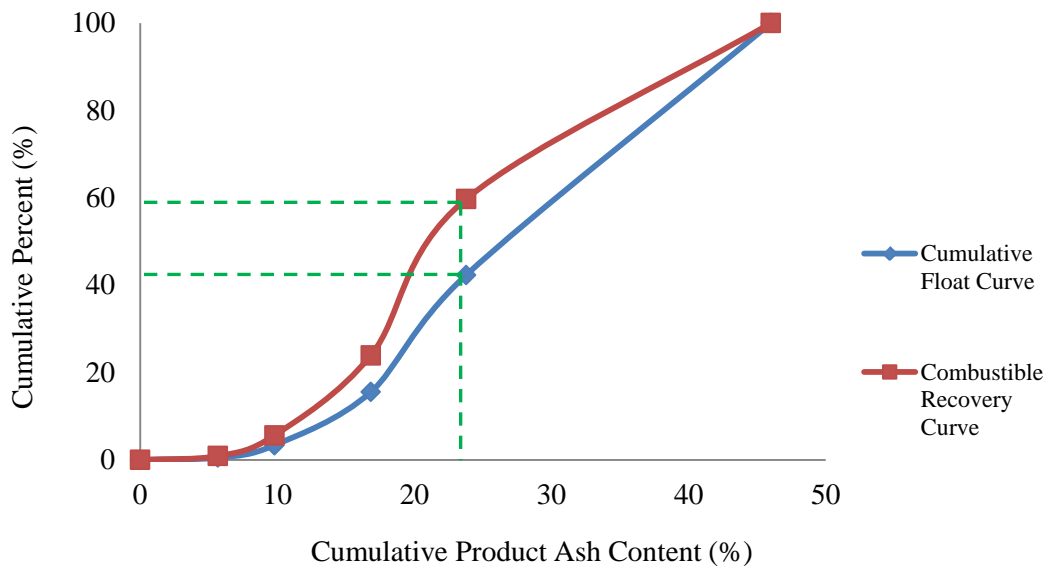


Figure 3.4 Cumulative float yield and combustible recovery curves for the fine size fraction of Korean Anthracite coal sample.

3.2.2 Experimental Approach, Dense Medium Cyclone

The only water-based coal preparation technology evaluated in this investigation was achieved by means of a laboratory-scale dense medium cyclone manufactured by Krebs and mounted with 20 degree angle from horizontal axis. Based on the washability data of the coarse sample, tests were performed at four medium density values including 1.70, 1.75, 1.85, and 1.90. However, the cleaning characteristics of the fine coal revealed a difficult separation even using a medium density of 2.0.

The geometric and operating characteristics of the dense medium cyclone were:

- Outer Diameter: approximately 15 cm
- Vortex Diameter: 63 mm
- Apex Diameter: 45 mm
- Inlet Pressure: 2.5 to 10 psi. For the coarse sample, the inlet pressure was maintained at 4 psi throughout the tests conducted on 1.7, 1.75, and 1.85 medium densities. However, the pressure was increased to 6 psi for the 1.9 S.G. test, so that the dense medium could be properly circulated.

Excluding inlet pressure, the other mentioned parameters were held constant during trials.

The medium utilized for coal cleaning was formed via blending magnetite particles with water in a sump located beneath the cyclone. The magnetite was categorized as the ultrafine class with 91 % of cumulative mass having a particle size below 45 μ m. Regarding the size of magnetite particles, the potential of generation of a viscous medium seemed to be probably high, if the density of medium increased by 2.0 gm/ml.

Briefly describing the procedure of running experiments, a measured amount of magnetite was added to water with the aim of generating a medium having a predetermined density (e.g.1.7 gm/ml). Afterwards, the density differential was measured to assess the relative stability of the medium at the inlet pressure set of 5 psi. At this

pressure, the quantified density differences between overflow and underflow was beyond the accepted range of 0.4, due to magnitude of the centrifugal force acting on the magnetite particles. Thus, the inlet pressure was reduced to 4 psi, which resulted in enhancement of the medium stability, as the density differential reduced to 0.3. Thereafter, the coal particles were introduced to the sump to a concentration providing a volumetric ratio of coal-to-medium inside the sump of about 5:1.

Subsequently, a portion of the coal and medium mixture was pumped into the cyclone through the feed inlet, while the other fraction returned back to the sump through a feed bypass stream. The overflow and underflow products were returned to the sump where they remixed and recycled back to the cyclone in a closed circuit. The above-described procedure has been schematically illustrated on the Figure 3.5.

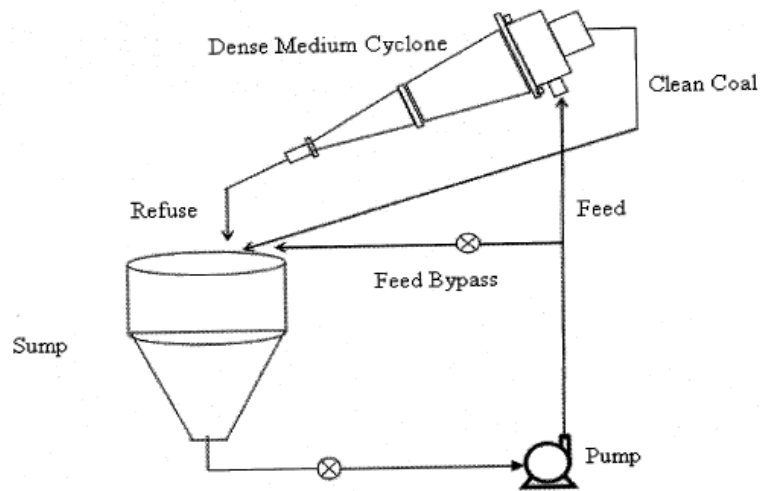


Figure 3.5 Closed-loop dense medium cyclone circuit

The laboratory Dense Medium Cyclone unit and its operating circuit have been shown on Figures 3.6 and 3.7.

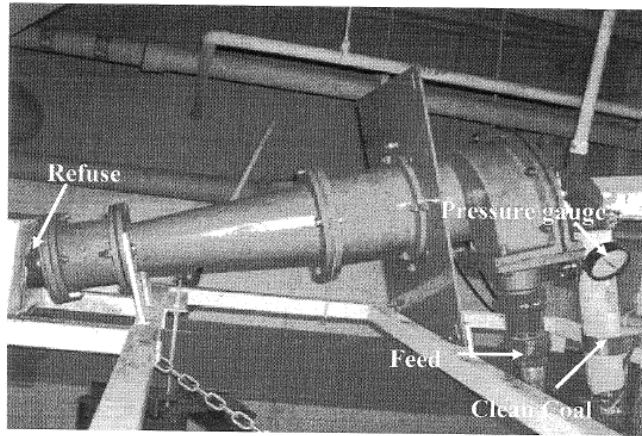


Figure 3.6 Fifteen centimeter diameter Krebs dense medium cyclone

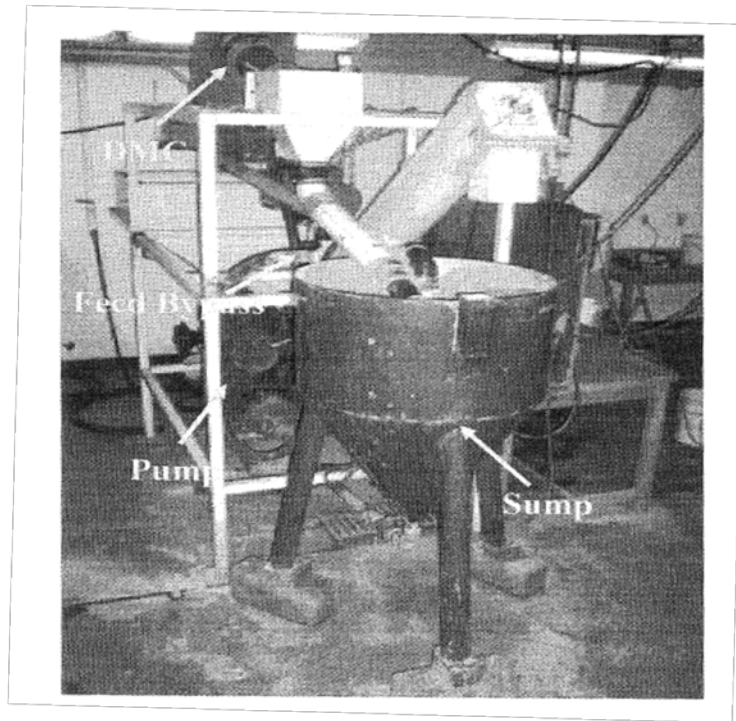


Figure 3.7 Dense medium cyclone circuit

The process was allowed to run almost 10 minutes with the purpose of providing materials with sufficient chance to well mix, as well as establishing the steady operational condition. At a particular density, separation efficiency, product quality, as well as the amounts of mass and coal recovery were quantified by analyzing feed, clean coal, and

tailing samples. To obtain the aforesaid analytical data, the feed representative sample was taken from the bypass valve. Subsequently, samples of underflow and overflow were collected.

After wet screening the samples to remove the magnetite particles, the samples were split into two representative lots and analyzed to gain required data for assessing the coal cleaning performance. Specifically, Ep value and cut density (as two of the most substantial parameters reflecting the separation efficiency) were measured by conducting washability analysis on the clean coal and reject samples. In addition, since the coal had a relative high hard groove index, the material was easily broken while circulating inside the system. Due to this fact, feed samples were also subjected to float-and-sink analysis to gain cleanability data of individual feeds utilized in each density fraction (Figure 3.8).

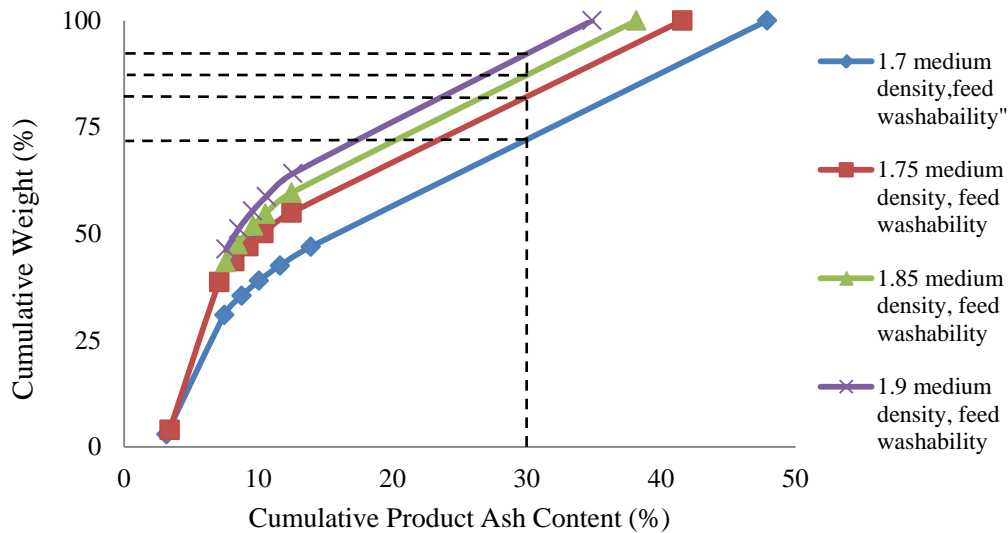


Figure 3.8 Changes in the feed cleanability characteristics resulting from particle size degradation during feed recirculation in the dense medium circuit

As the data demonstrates, feed washability characteristics improved with an increase in medium density, which results in providing higher product yield at the same product ash content. The trend reflects the order of the experiments, which involved conducting the 1.70 feed medium tests first followed by sequentially higher feed medium density values. Liberation caused by the particle size degradation resulted in the enhanced washability characteristics. Finally, the quantity of cumulative recovered feed mass, and coal were estimated by the two-product equation and the ash analysis data from the feed, product and tailing samples.

3.2.3 Experimental Approach, Air table

The dry based Korean coal beneficiation experiments were initiated employing a modified air table separator manufactured by CIMBRIA HEID. The laboratory machine structurally simulates currently-used industrial-scale air tables. However, the unit's operational properties vary to some extent due to the re-designed. Two major modifications were carried out on the original machine. The primary change was the substitution of the 6 mm screen bed with a 1 mm aperture size screen. The more significant alteration was the addition of flap gates with artificial lips leading to continuous removal of particles from the table deck. This adjustment enhanced the process of particle bed formation, expedited the material discharge rate, and converted semi-batch process to a continuous operation. Figures 3.9 and 3.10 show the original machine and its modified version.

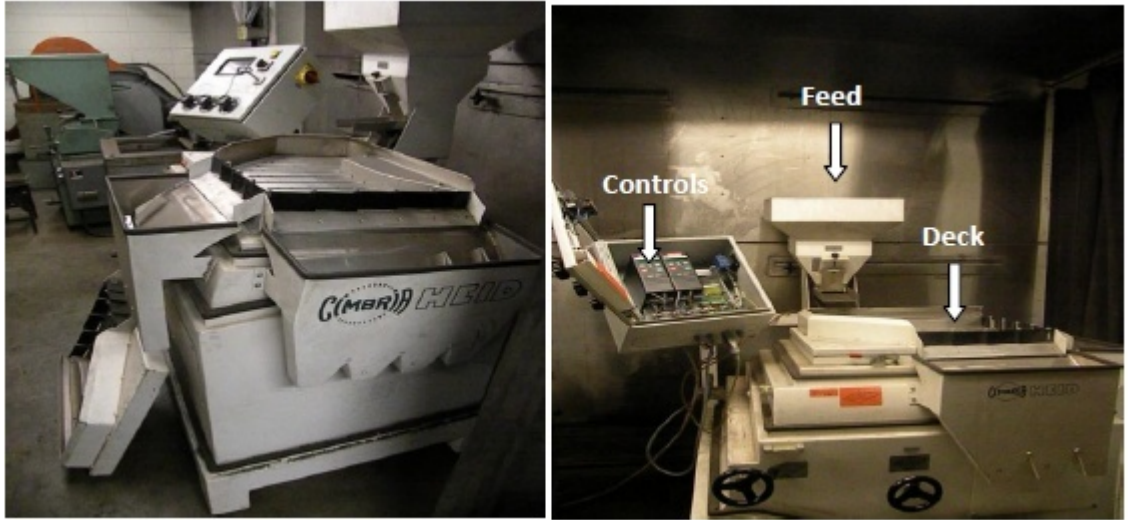


Figure 3.9 Laboratory-scale air table separator with vibratory feeder and various other components

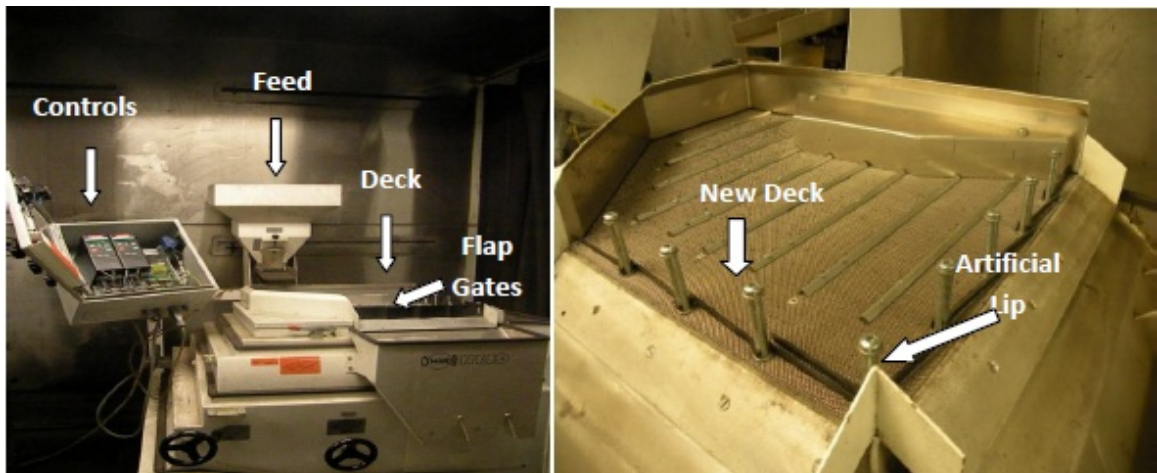


Figure 3.10 Modified air table with 1 mm aperture screen deck and discharge gates

To determine the potential of modified air table to clean Korean anthracite coal, a set of experiments were performed on both coarse and fine samples. Initially, the trials were designed based on a general statistical procedure, known as the Box-Behnken method. The process of design involved randomized tests studying various operational parameters (including feed rate, air flow rate, longitudinal angle, transverse angle, and table

frequency), and their associated values (assigned as low, medium , and high). The parameters and their respective value ranges studied for the treatment of coarse coal fraction are shown in Table 3.5. A total of 46 experiments were designed to be carried out on coarse sample.

Table 3.5 Operating parameters and their respective value ranges evaluated in the statistically-designed test program conducted on the air table for the treatment of the 8 x 4 mm Korean coal sample

Parameter	Level		
	Low	Medium	High
Feed Rate (kg/sec)	0.055	0.069	0.083
Fan Frequency (Hz)	30	40	50
Table Frequency (Hz)	30	35	40
Longitudinal Angle (°)	1	1.5	2
Transverse Angle (°)	5	6.5	8

For the fine coal sample, the feed rate was kept constant at 200 kg/hr and only four test parameters were varied during the experimental program (Table 3.6). The total number of designed trials decreased to 26 for the fine coal sample. The test-by-test details for the experimental programs conducted on the coarse and fine coal samples are provided in Appendices Tables A.1 and A.2.

Table 3.6 Operating parameters and their respective value ranges evaluated in the statistically-designed test program conducted on the air table for the treatment of the 5 x 1 mm Korean coal sample.

Parameter	Level		
	Low	Medium	High
Fan Frequency (Hz)	30	40	50
Table Frequency (Hz)	30	35	40
Longitudinal Angle (°)	1	1.5	2
Transverse Angle (°)	5	6.5	8

For each individual experiment, the raw materials were fed onto the table's deck after adjusting the operational parameter values, e.g. feed rate, longitudinal angle, etc. Initially, the vibration frequency of the feeder chute was set on a specific value which introduced materials on the deck at a flow rate equivalent to the predetermined feed rate value. Subsequently, the table's deck was tilted in accordance to the desired longitudinal and transverse angles, which was followed by regulating table's vibration frequency and air flow rate. Finally, the raw feed flowed onto the table's screen and the test provided adequate time to form an uniform particle bed. As the particle bed reached stable conditions, representative samples were simultaneously taken from collecting zones (named as A, B, C, D, and E) located along the two sides of the table (Figure 3.11). To measure the variability of the feed characteristics, a sample was collected from the feed chute.

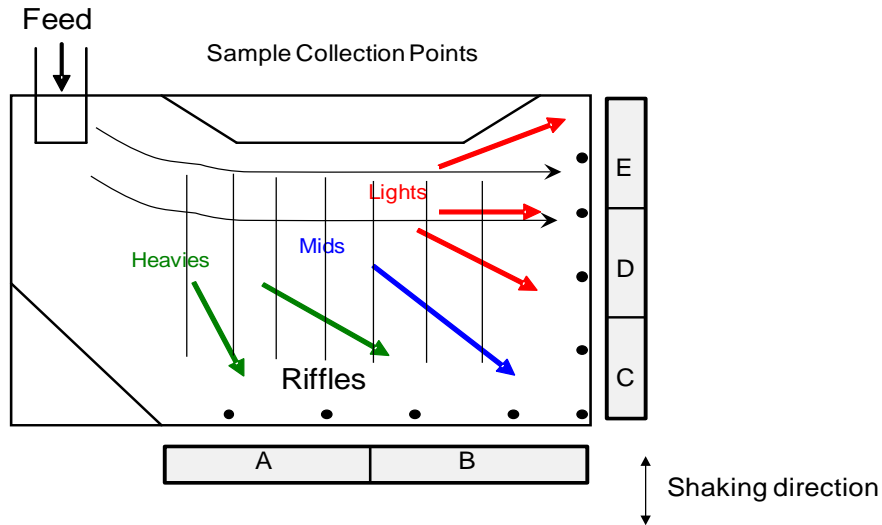


Figure 3.11 Sample collection points, A, B, C, D and E located along the edge of air table

The five product samples plus the feed from each test they were weighted to determine the amount of feed mass recovery. Then, a representative sample of each was assayed for the ash content.

The particle movement on the table was a fraction of particle density and thus the ash content. At several experimental conditions, the lighter-lower ash content particles tended to move longitudinally towards the right end of deck, as they were not subjected to transversal pushing force. On the other hand, movement of the denser minerals comprising higher amount of mineral matter was influenced by the transverse movement of the table which caused discharge to the opposite side. The reason is the location of the heavier particles near the table surface and the impact of the riffles, which decelerate these particles' longitudinal movement rate. Therefore, samples taken from A and B collecting zones were identified as tailings, whereas the samples from C, D, and E were combined as the clean coal product.

Coal and mass recovery values along with the product ash content for each test were entered into a statistical software package. The package assisted in developing empirical expressions describing the response variables as a function of the operating parameters. The significance of suggested model and its dependency to each parameters and parameter interactions were assessed applying a statistical technique, named as Analysis of Variance. The empirical models were used to identify the set of operating parameter values that provided maximum mass recovery while achieving the target product ash content.

3.3 Experimental Procedure of Rotary Tribo-electric Separator (RTS) and Dual Energy X-ray Transmission Sorting Technology (DE-XRT)

3.3.1 Particle Size and Washability Analysis

The Korean anthracite coal samples utilized for these experiments were delivered in Four 208 liter barrels. After splitting to obtain representative samples, particle size-by-size, weight, and ash content analysis were conducted.

The data provided on the table 3.7 shows that the top size of the coal was around 63.5 mm. the coal was relatively coarse with very little material having a particle size smaller than 5 mm. The total feed ash was almost 60 % which was not equally distributed. With the exception of last three fine size fractions, the rest of size ranges approximately contain equal amount of impurities and reflective of the overall feed. Moreover, the ultrafine size fraction comprised the lowest percentage of mineral matters, which could be directly attributed to high hard grove index of the sample.

Table 3.7 Particle size and ash distribution for coal sample treated by Rotary Tribo-electric Separator (RTS) and Dual Energy X-ray Transmission Sorting Technology (DE-XRT)

Particle Size (mm)	Incremental		Cumulative		
	Weight (%)	Ash (%)	Weight (%)	Ash (%)	Combustible Recovery (%)
63.50	0.00	0.00	0.00	0.00	0.00
63.5 x 31.75	11.69	65.14	11.69	65.14	10.78
31.75 x 19	30.12	64.00	41.81	64.32	39.45
19 x 12.7	33.27	64.56	75.08	64.43	70.64
12.7 x 5	19.03	60.46	94.11	63.62	90.54
5 x 1	1.58	55.80	95.69	63.49	92.38
1 x 0.15	1.46	39.05	97.15	63.13	94.74
-0.15	2.85	30.17	100.00	62.19	100.00
total	100.00	62.19			

Generally, the efficiency of X-ray Transmission Sorter (XRT) in treating minerals would be progressively enhanced, as the size of particles increases above 10 mm. On the other hand, the Tribo-electric Separator (RTS) has been proven to be capable of performing the best cleaning process, if the top size of raw feed do not exceed beyond the 1 mm. Due to the discussed facts, the third stage of experiments concentrated on employing XRT to beneficiate particles presented in three sizes, listed as 63.5 x 31.75 mm, 31.75 x 19 mm, and 63.5 x 19 mm. The experiments on the RTS device involved the treatment of two of the finest particle size fractions.

The cleanability of aforesaid size ranges were individually assessed through conducting float-and-sink analysis using mediums with specific gravities of 1.65, 1.80, 2.00, and 2.20. It is noted that the washability characteristics of the RTS feed were determined after

removing the - 0.15 mm size particles. The data from the particle size-by-size washability tests are provided in Tables 3.8 through 3.11.

Table 3.8 Washability data for the 63.5 x 31.75 mm size fraction used to assess the Dual Energy X-ray Transmission Sorting (DE-XRT) process

Specific Gravity	Incremental		Cumulative		
	Weight (%)	Ash (%)	Weight (%)	Ash (%)	Combustible Recovery (%)
1.65 Float	0.00	0.00	0.00	0.00	0.00
1.65 x 1.80	8.65	12.43	8.65	12.43	23.69
1.80 x 2.00	16.61	28.15	25.26	22.76	60.98
2.00 x 2.20	17.28	53.52	42.54	35.26	86.08
2.20 sink	57.46	92.25	100.00	68.01	100.00
Total	100	68.01			

Table 3.9 Washability data for the 31.75 x 19 mm size fraction used to assess the Dual X-ray Transmission Sorting (DE-XRT) process

Specific Gravity	Incremental		Cumulative		
	Weight (%)	Ash (%)	Weight (%)	Ash (%)	Combustible Recovery (%)
1.65 Float	0.00	0.00	0.00	0.00	0.00
1.65 x 1.80	6.98	10.97	6.98	10.97	20.73
1.80 x 2.00	12.66	23.09	19.64	18.78	53.24
2.00 x 2.20	12.88	41.90	32.52	27.94	78.22
2.20 sink	67.48	90.33	100.00	70.04	100.00
Total	100.00	70.04			

Table 3.10 Washability data for the 63.5 x 19 mm size fraction used to assess the Dual Energy X-ray Transmission Sorting (DE-XRT) process

Specific Gravity	Incremental		Cumulative		
	Weight (%)	Ash (%)	Weight (%)	Ash (%)	Combustible Recovery (%)
1.65 Float	0.00	0.00	0.00	0.00	0.00
1.65 x 1.80	7.45	11.44	7.45	11.44	21.60
1.80 x 2.00	13.77	24.80	21.21	20.11	55.51
2.00 x 2.20	14.11	45.88	35.32	30.40	80.52
2.20 sink	64.68	90.81	100.00	69.47	100.00
Total	100.00	69.47			

Table 3.11 Washability data for the 1 x 0.15 mm size fraction used to assess the Rotary Tribo-electric Separator (RTS) process

Specific Gravity	Incremental		Cumulative		
	Weight (%)	Ash (%)	Weight (%)	Ash (%)	Combustible Recovery (%)
1.65 Float	3.41	4.12	3.41	4.12	5.37
1.65 x 1.80	31.14	6.31	34.55	6.09	53.23
1.80 x 2.00	24.97	16.02	59.52	10.26	87.63
2.00 x 2.20	3.56	41.86	63.08	12.04	91.03
2.20 sink	36.92	85.19	100.00	39.05	100.00
Total	100.00	39.05			

Considering the coarse fraction washability results, a great portion of feed consists of materials which are denser than 2.2, and approximately contain 90 % impurities. Therefore, the total ash would lessen from 69 % to 30 % by excluding particles in the last density fraction. Likewise, during this process, over 30 % of cumulative mass and 78 % of combustible materials could be recovered.

Moreover, a clean coal with 12 % ash content can potentially be generated from the fine fraction if cut density is around 2.2. To exploit more comprehensive data of cleanability of each size fraction, the common washability curves have been plotted, as shown in Figures 3.12 through 3.14.

Comparison of the washability curves shows that the curves are nearly equal, which means combustible recovery, quality of upgraded product, and the amount of concentrated mass is essentially independent of raw feed size. In addition, the cleanability properties of the fine coal show the potential of reducing cumulative ash percentage by almost 30 % while recovering 87 % of total energy, and 60 % of cumulative feed weight.

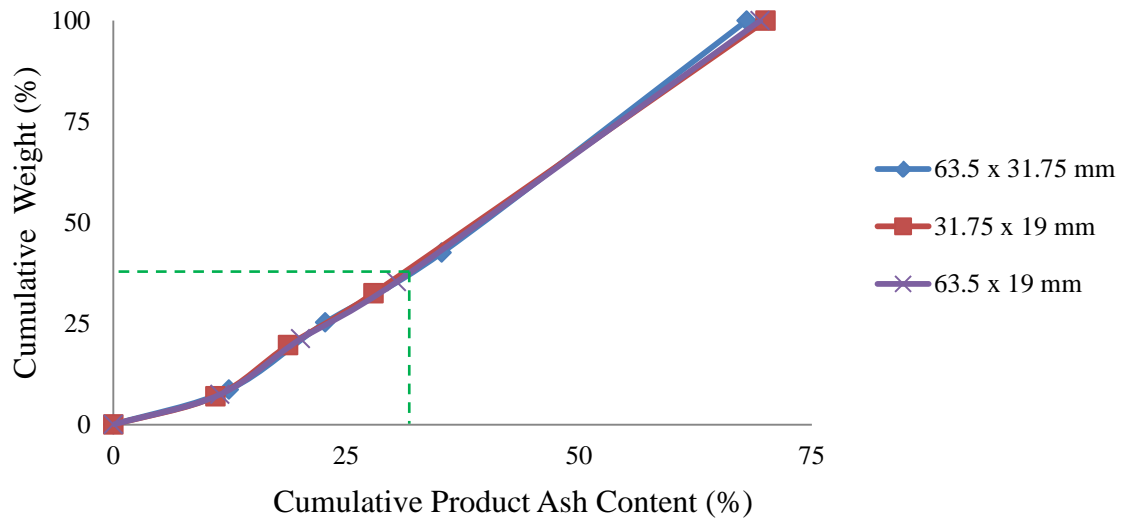


Figure 3.12 Cumulative float curves obtained from the coarse size fractions of the coal sample used for the tests involving the Dual Energy X-ray Transmission Sorting Technology (DE-XRT)

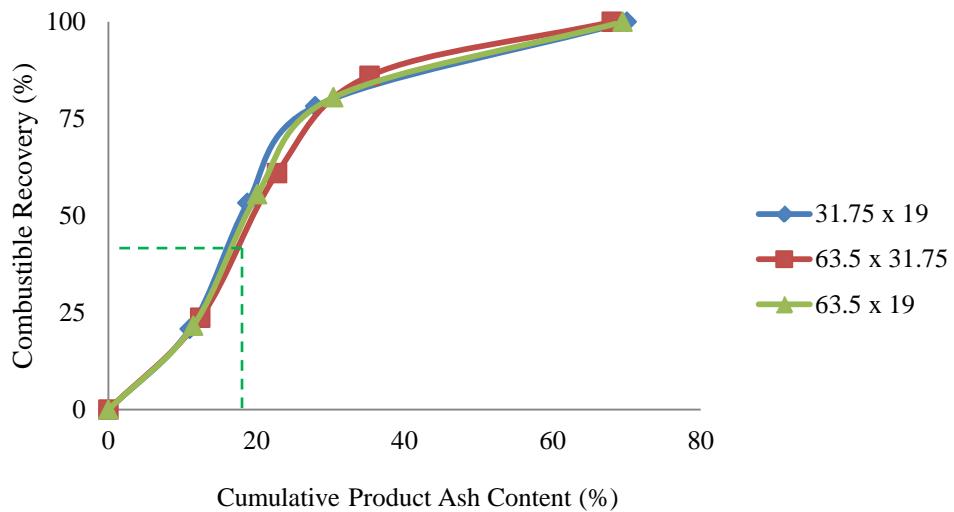


Figure 3.13 Recovery curve obtained from the coarse size fractions of the coal sample used for the tests involving the Dual energy X-ray Transmission Sorting Technology (XRT)

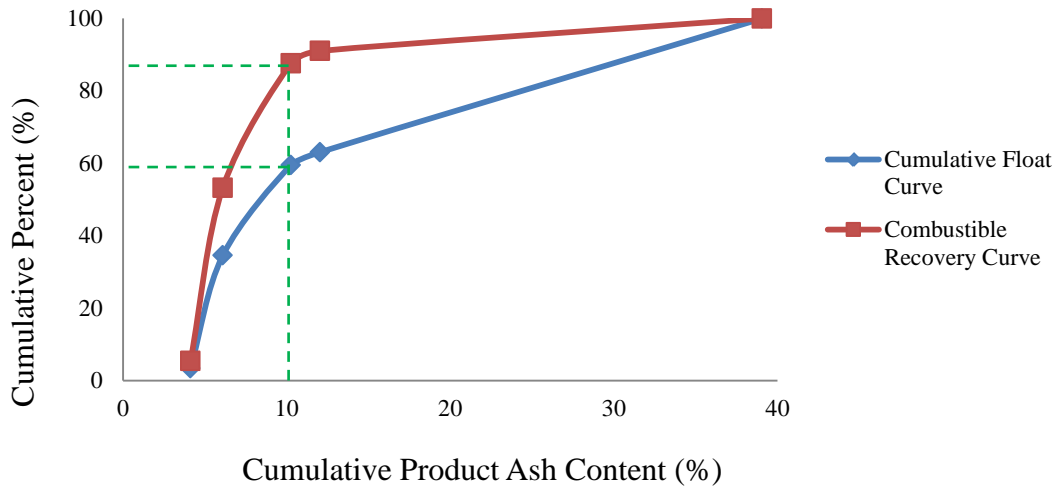


Figure 3.14 Cumulative float curve and recovery curve from washability analysis of the fine size fraction (1 x 0.15 mm) of coal sample used in the tests involving the Rotary Tribo-electric Separator (RTS)

3.3.2 Experimental Approach, Rotary Tribo-electric Separator (RTS)

To assess the potential of upgrading fine size fraction of Korean coal, a parametric investigation was conducted using the RTS technology. The test program was established using a Box-Behnken statistical design which allowed an evaluation of the operating parameters. The parameters included feed rate, charger voltage, charger rotation speed, and airflow velocity. The parameters and their value ranges are provided in Table 3.12. A total of 29 tests were performed in a randomized order. The details of each test are provided in appendices Table C.

Table 3.12 Operating parameters and their respective value ranges evaluated in the statistically-designed test program conducted on the Rotary Tribo-electric Separator (RTS) for the treatment of fine size fraction of Korean Anthracite coal sample

Parameter	Level		
	Low	Medium	High
Feed Rate (kg/sec)	0.00063	0.0016	0.0025
Charger Rotation Speed (rpm)	1000	3000	5000
Charger Voltage (V)	-3000	0	3000
Air Flow Velocity (m/s)	1.00	1.75	2.00

At a single set of experiment, initially, the operational parameters were set on the pre-determined values. Subsequently, 100 grams of raw material was introduced to the unit through vibratory feeder and chute. During the process, clean coal, middling, and tailing products were accumulated in the containers assigned as left, center, and right. Since the middling particles obtains almost zero charge density, they are exerted no electrical force. Hence, these particles are expected to report to the central container. The other particles report to the right or left container depending on their electrical sign and polarity.

The low ash-positively charged minerals are directed to the left container if the left electrode has negative charge (Figure 3.15). After all the feed was treated through a single pass, the achieved products were identified as left, center, and right corresponding to the container. Thereafter, each collected product was weighed and subsequently analyzed for ash content.

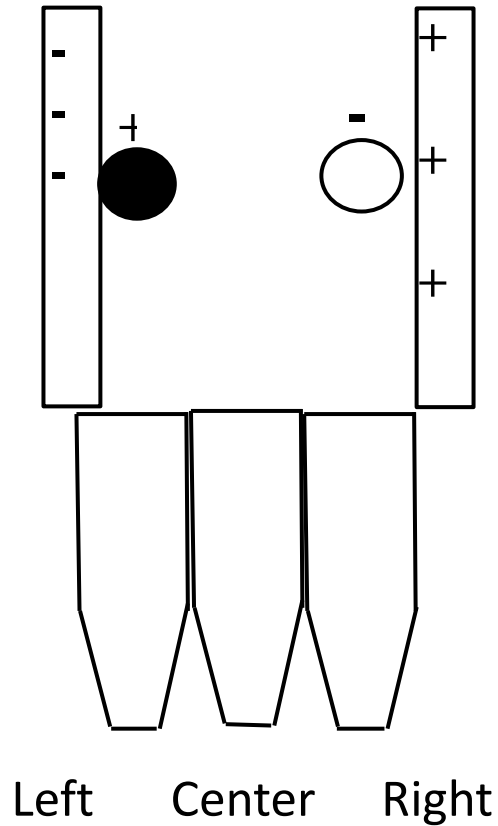


Figure 3.15 Schematic of the separation zone in the Rotary Triboelectric Separator showing the charged electrode plates and the direction of charged particles

Before conducting trials, the ultimate goal had been established on statistically investigating the effect of each operational parameter on preparation process by developing analytical models. To could reach this purpose, the ash content of products should have set on an increasing trend from clean coal to tailing. However, in majority of experiments, the middling product contained the most amount of impurity comparing to two other products. This fact indicates that particles had been poorly separated from each other. As a result, there was no possibility to develop such analytical models, which demonstrate dependency of product ash/yield to operational parameters. The low separation efficiency could be attributed to existence of conductive particles in raw feed.

The negative impact of particles' conductivity on cleaning performance has been broadly discussed in the Chapter 4: Result and Discussion.

3.3.3 Experimental Approach, X-ray Transmission Sorting (XRT)

The last phase of processing experiments involved applying XRT technology to treat three coarse size fractions (63.5 x 31.75 mm, 31.75 x 19 mm, and 63.5 x 19 mm) separately. The mechanism of preparation was established on using manual preparation procedure. As explained in Chapter 2, in this method every particles of raw feed is initially analyzed by using calibration curve and all single pixels are assigned red / blue color. Subsequently, particles are shown on the screen of computer in form of colorful images and the unit operator clicks on the particles which contains the high amount of red pixels. Finally, the air valve injects the pressurized air at the convenient moment, and ejects the selected particle. Therefore, the processing operator completely controls the process of treatment.

The processing strategy involved a rougher stage followed by a cleaner stage. The feed coal was fed into the rougher in which low ash particles were ejected as initial product while the high ash materials were accepted as tailings. The ejected portion was then re-treated in a cleaner stage, while the accepted particles were set aside as final reject. In the cleaning stage, the separation criterion was set on accepting low ash particles and ejecting high ash materials since the high ash particles represented a minority of the feed to the cleaner stage. A schematic representing the process followed for the XRT tests is provided in Figure 3.16.

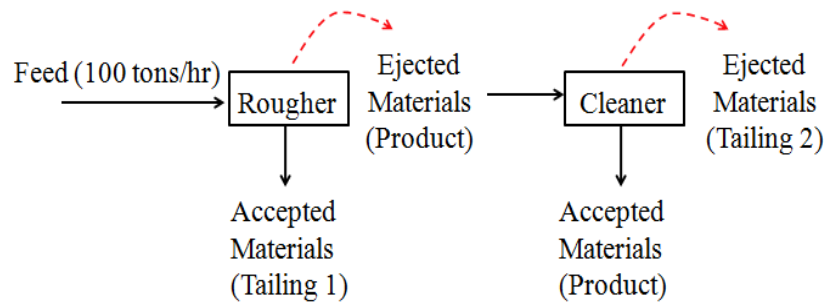


Figure 3.16 Methodology used in the XRT sorting test program

The experimental program involved the performance of three tests in which the particles ejection settings were varied as shown in Figure 3.17. The settings were based on a pre-section of particles that were to be ejected by the air jets to an outer container based on a XRT scan of the particles. Particles appearing as low density, low ash particles were selected for Test No.1. For Test No.2, slighter higher ash particles were included in the ejection stream. Even higher ash particles were included in the ejection stream for Test No.3. As a result, more middling particles are recovered with increasing separation setting, due to increasingly selecting particles which have more and more percentage of blue pixels.

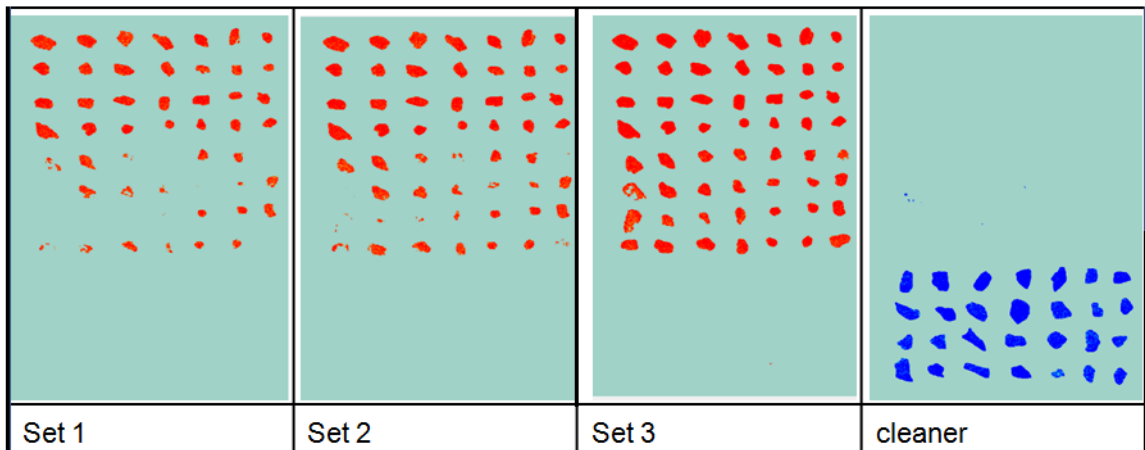


Figure 3.17 Different DE-XRT settings used for cleaning coarse size fraction of Korean Anthracite coal sample

The experimental work was conducted at the Tomra Sorting Test Facility located in Wedel, Germany. To calibrate the XRT device for the Korean coal, 5 kg of representative samples from the 63.5 x 31.75 mm and 31.75 x 19 mm size fractions were subjected to washability analysis using medium specific gravity values of 1.8 and 2.2. At the Tomra test facility, each density fraction was subjected to an XRT scan which generated images similar to those in Figure 3.17. These images formed the basis for the pre-selection process.

Once the pre-selection process was complete, the material was loaded into a feed bin containing a conveyor belt. The speed of the conveyor belt was adjusted to achieve a rate of approximately 100 tph. At the discharge of the conveyor belt an XRT unit identified each particle and directed air jets to eject the pre-selection particles to an outer bin (Figure 3.18). The final clean coal products and tailing samples generated from the three tests were carefully packaged to avoid particle size degradation during the shipment back to the University of Kentucky. Upon receiving the returned samples, a representative sample from each bulk sample was analyzed for ash content. The remaining bulk sample of each clean coal and tailing sample was subjected to washability analysis used medium specific gravity values of 1.8, 1.9, 2.0, 2.1, and 2.2.

Materials floated in each density fraction were screen out on sieve trays having 19 mm and 31.75 mm aperture size. Thereafter, materials remained on each screen was weighed, and analyzed for assaying ash content. Then, for three mentioned size fractions, separately, the amount of mass distribution in each density fraction with percentage of impurities, were determined.

Applying data obtained from the previous stage, the cleaning performance were estimated in terms of partition curve parameters (such as E_p , and cut density), organic efficiency, combustible recovery, and clean coal properties (e.g. cumulative concentrated mass and product quality).

CHAPTER 4

RESULT AND DISCUSSION

4.1 Introduction

Throughout this chapter, Korean coal beneficiation results will be presented and analytically discussed in an effort to evaluate the cleaning performance of separating devices described in chapters 2 and 3. The separation performances achieved by the different technologies will be presented and discussed in separate sections since the characteristics of the Korean feed coal used in each study were significantly different.

The separation achieved using an air table was evaluated and optimized by conducting a test program that was based on a statistical experimental design. The impacts of process variable values were assessed following a test program developed using Design Expert software. The test results were used to develop empirical relationships that describe product quality, combustible recovery and mass yield as a function of the process parameter values. Optimized conditions were identified that provide the ultimate separation performance.

Likewise, the separation performances achieved by Dense Medium Cyclone and XRT sorting technology were evaluated by means of all abovementioned factors, partition curve, and organic efficiency. However, the analytical data of the rotary tribo-electric separator indicated that no separation was achieved for the Korean coal. Potential explanations leading to the weak separation performance has been provided in the third section.

Organic efficiency is defined as the ratio of the achieved (practical) mass recovery and theoretical mass recovery (determined from feed washability data) at a given product grade. This factor clearly reflects the impact of process inefficiencies

associated with near-gravity material and those associated with bypass. The minimum accepted value for organic efficiency is 0.95 depends on the feed cleanliness.

The separation efficiency values obtained from Dense Medium Cyclone, and XRT units were comprehensively assessed in terms of partition curve parameters, namely E_p , cut density, and product/reject bypass. In an ideal preparation process, the estimated E_p and bypass would be exactly zero and the estimated cut density would become equivalent to medium density / theoretical density. Any differences between the obtained results and ideal values reveal some degree of separation inefficiency, which could be attributed to several factors such as product/reject misplacement (Figure 4.1).

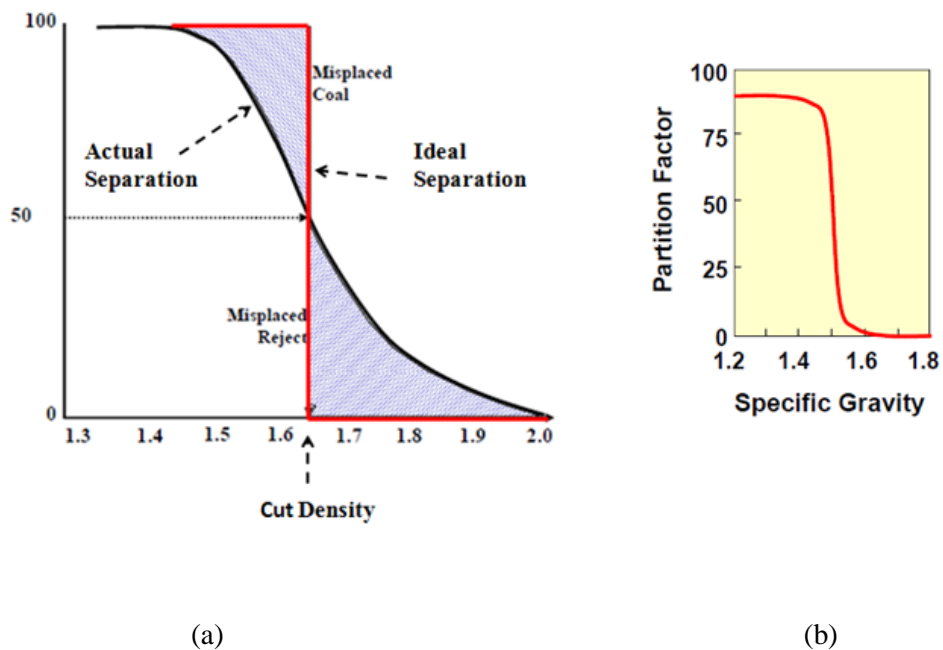


Figure 4.1 Separation efficiency factors as revealed by partition curves: (a) comparison of ideal separation and actual separation and (b) partition curve showing low density bypass to the high density stream.

4.2 Dense Medium Cyclone

4.2.1 Introduction

The separation performance of dense medium cyclones is dependent on several factors. During experiments, all operational parameters were kept constant excluding inlet pressure, and medium viscosity and stability. Thus, the cleaning performance of the dense medium cyclone was only impacted by the varying parameters. In this section, experimental results achieved in each medium density fraction, will be interpreted based on these factors. The procedure of data analysis will be conducted in two distinct phases. The initial phase studies the trend of product quality, coal recovery, organic efficiency, and product yield. Afterward, the parameter impacts will be studied in regards to their impact on the partition curve parameters.

4.2.2 Phase 1

As previously described in Chapter 3, the Korean anthracite coal has relatively difficult cleanability characteristics. Dense medium cyclones are likely the ultimate upgrading option due to the relatively high separation efficiencies. As shown in Table 4.1, a product ash content as low as 6.14 % was achieved but the combustible recovery was only 34 %. Increasing the medium specific gravity from 1.70 to 1.85 provided a minimal elevation in product ash content to 9.38 %. However, mass yield substantially improved to 49 % and 72 % of the combustible material recovered. Organic efficiency reached an acceptable level of 96 %. The achieved data were compared to theoretical washability curve to provide much clear vision of cleaning performance of dense medium cyclone (Figure 4.2).

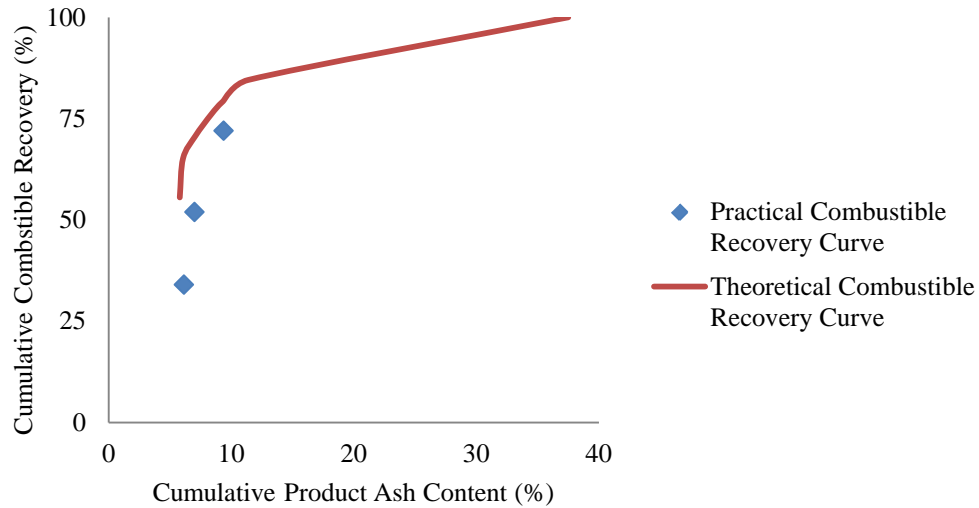


Figure 4.2 Theoretical combustible recovery curve vs. practical combustible recovery curve for dense medium cyclone test.

The medium specific gravity was increased further to 1.9 which provided the expected result of increasing the product ash content. However, the negative impact on combustible recovery was unexpected and likely due to experimental error. The analytical data achieved on 1.70, 1.75, 1.85 and 1.90 specific gravities have been listed on the Table 4.1.

Table 4.1 Dense medium cyclone analytical data achieved on 1.70, 1.75, 1.85 and 1.90 specific gravities

Response Variables	Medium Specific Gravity			
	1.70	1.75	1.85	1.90
Feed Ash (%)	47.42	42.26	37.50	34.86
Product Ash (%)	6.14	7.02	9.38	10.61
Tailings Ash (%)	57.02	59.33	64.67	46.31
Mass Yield (%)	18.87	32.63	49.14	32.07
Combustible Recovery (%)	33.99	51.94	72.01	44.01
Organic Efficiency (%)	86	83.69	96.36	56.27

4.2.3 Phase 2

The product and tailing samples collected from the tests involving medium specific gravity values of 1.70, 1.75, and 1.85 were subjected to washability analysis. The results were used to construct the partition curves shown in Figure 4.3.

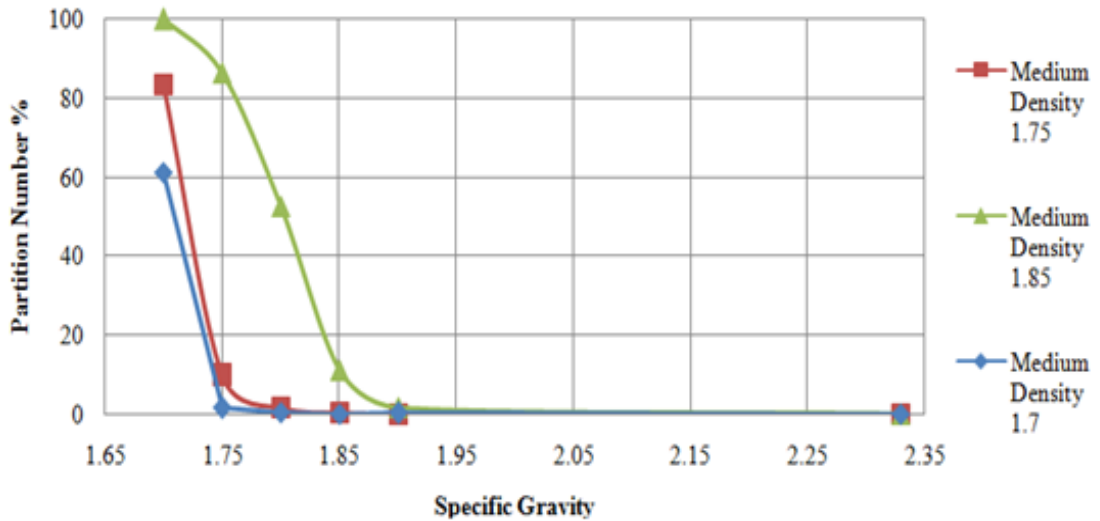


Figure 4.3 Partition curves obtained from dense medium cyclone performances when using medium specific gravity value

The partition curves are typical of separation performances achieved under specific gravity cut points near the lowest particle specific gravity in the feed coal. The medium specific gravity values of 1.70 and 1.75 appear to be bypassing high quality low density coal to the reject. However, it is reflective of the medium specific gravity values selected for the washability data and the lowest specific gravity particles in the feed coal. As typical with dense medium processes, no true bypass is apparent from the partition curve data.

A summary of the efficiency and performance data from the partition curves is provided in Table 4.2. The E_p values indicate a typical level of efficiency for each medium specific gravity. As such, the low organic efficiency values in Table 4.1 for specific

gravities of 1.70 and 1.75 was due to the lower recovery of 1.65 float material. The specific gravity offset, which is defined by the difference between the specific gravity cut point and the medium gravity, was near zero for the three tests. This is due to the excellent stability of the medium.

Table 4.2 Separation performance summary achieved by a dense medium cyclone treating 6 x 1 mm Korean coal

Medium Density (t/m ³)	Cut Density (ρ_{50})	Product to Reject Bypass (%)	Ep
1.70	1.73	38.97	0.02
1.75	1.73	16.74	0.02
1.85	1.83	1.37	0.03

The proposed project had also established on performing dense medium cyclone cleaning trials on another type of Korean anthracite coal, termed as fine sample. Before conducting experiments, cleanability characteristics of fine sample were utilized, to identify medium densities which could recover the highest amount of coal with desired product ash content. As conceived from associated washability curve, the mentioned goals could potentially be achieved, as if cleaning tests were performed on 1.9 and 2 medium densities. As previously discussed, 1.9 medium density was not sufficiently stable to could recover great portion of floatable materials. Due to this fact, this type of coal could not potentially be treated by means of Dense Medium Cyclone. Therefore, cleaning trials was never implemented on fine sample.

4.3 Air Table

The probable error (Ep) values obtained by Air table are so sensitive to size of particles. Normally, narrow particle size range will result in better separation efficiency (lower Ep value). However, high values of Ep would be achieved if the size range of particles becomes wide. In addition, Air table is not able to effectively treat near gravity particles.

Therefore, the provided relative density would be high, between 1.8 and 2.0. In this section, the cleaning performance of air table on coarse and fine samples will be evaluated. Initially, the obtained results will be comprehensively analyzed and then the effect of operational parameters on forgoing results will be studied. For coarse sample, totally, 46 trials were conducted and provided products were analyzed to estimate the amount of product ash, combustible recovery, and product yield. The analytical results have been listed on table presented on appendices table B.1. The data shows that a clean coal with 18 % ash could be obtained, with respectively recovering 7% and 11% of feed mass and combustible materials. The provided data demonstrates that the high percentage of feed mass and coal could be concentrated with producing a clean coal containing high amount of impurities. On the other hand, a low ash content clean coal would be obtained with low amount of combustible recovery and product yield.

The process of data analysis persuaded with generating empirical models which define response parameters (product ash, product yield, and combustible recovery) as functions of operational variables. The process of analysis was initiated by employing a quadratic model to describe each response based on individual and interactional parameters. Then, significance of each response and its dependency to variables were assessed applying a general statistical method, named as analysis of variance. Along this method, associated p-values were used to identify significant parameters. The associated p-values ("Prob>|F|") are interpreted as the probability of realizing a coefficient as large as that observed, when the true coefficient equals zero. In other words, small values of p (less than 0.05) indicate significant coefficients in the model.

Having a response analyzed, some individual and interactional variables were found to be insignificant, which means they exert no impact on the response. To amend the provided model, a backward elimination process was performed. This process involved in consequently deleting insignificant interactional parameters which have the highest p-values. Finally, the remained parameters formed the modified model, as depicted on Tables 4.3, 4.4, and 4.5.

Table 4.3 Analysis of variance of product yield for coarse sample cleaned by Air Table

Source	Sum of Squares	df	Mean Square	F Value	p-value Prob> F	
Model	20217.80	9	2246.42	13.05	< 0.0001	Significant
A-Feed Rate	263.01	1	263.01	1.53	0.2244	
B-Air Freq	7628.71	1	7628.71	44.33	< 0.0001	
C-Table Freq	339.30	1	339.30	1.97	0.1688	
D-Long. Angle	98.26	1	98.26	0.57	0.4548	
E-Transverse. Angle	4263.11	1	4263.11	24.77	< 0.0001	
BE	731.70	1	731.70	4.25	0.0465	
A ²	1874.45	1	1874.45	10.89	0.0022	
B ²	2537.06	1	2537.06	14.74	0.0005	
E ²	1546.43	1	1546.43	8.99	0.0049	

Table 4.4 Analysis of variance of combustible recovery for coarse sample cleaned by Air Table

Source	Sum of Squares	df	Mean Square	F Value	p-value Prob> F	
Model	19753.800	9	2194.870	9.701	2.50E-07	significant
A-Feed Rate	295.067	1	295.067	1.304	0.261	
B-Air Freq	6764.240	1	6764.240	29.90	3.60E-06	
C-Table Freq	193.419	1	193.419	0.855	0.36134	
D-Long. Angle	273.737	1	273.737	1.210	0.27866	
E-Transverse Angle	3982.870	1	3982.870	17.60	0.00017	
BE	417.794	1	417.794	1.847	0.18264	
A ²	2804.450	1	2804.450	12.400	0.00119	
B ²	2442.610	1	2442.610	10.800	0.00227	
E ²	1341.240	1	1341.240	5.928	0.01999	

Table 4.5 Analysis of variance of product ash for coarse sample cleaned by Air Table

Source	Sum of Squares	df	Mean Square	F Value	p-value Prob>F	
Model	1223.880	8	152.985	7.427	7.50E-06	significant
A-Feed Rate	6.452	1	6.452	0.313	0.57909	
B-Air Freq	473.280	1	473.280	22.98	2.70E-05	
C-Table Freq	31.360	1	31.360	1.522	0.22502	
D-Long. Angle	0.672	1	0.6724	0.033	0.85761	
E-Transverse Angle	288.830	1	288.830	14.020	0.00061	
BE	11.156	1	11.1556	0.542	0.46642	
B ²	285.882	1	285.882	13.880	0.00065	
E ²	186.189	1	186.189	9.039	0.00473	

The variance analyses of generated models suggest that the effects of air frequency and transverse angle are highly significant on all three responses. These facts demonstrates that product yield, combustible recovery, and product ash values increase with increase of Transverse angle, due to the high upward slope towards the reject discharge end. Thus, the solid flow rate towards the product discharge rises, as it becomes increasingly difficult for particles to overcome the effect of gravity and report to the reject end. During trials, it was also observed that with increasing fan frequency the heavy density coal particles were lifted by upward air flow and move towards product end. The higher air flow coupled with the increase in the transverse angle helps in a homogeneous fluidized bed formation thus maximizing combustible recovery, product yield and clean coal ash (Figures 4.4, 4.5, and 4.6). As there are high amounts of near gravity particles inside the feed material, the separation was so difficult. Hence, the higher fractions of stratified material move towards product end. So, the separation density increases and quality of clean coal reduces.

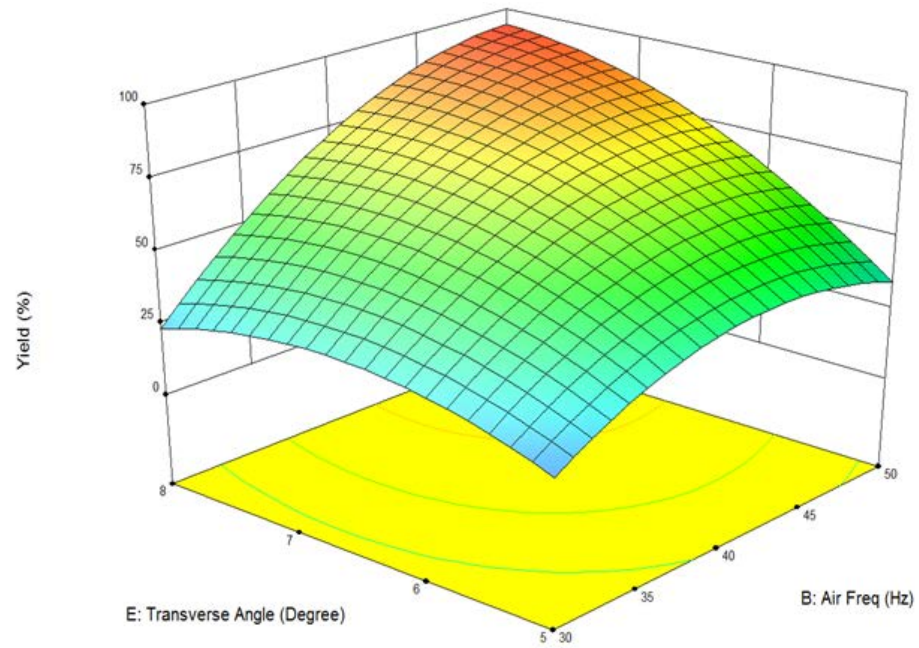


Figure 4.4 Effect of fan frequency (air flow rate) and transverse angle on product yield achieved from coarse sample by using Air Table

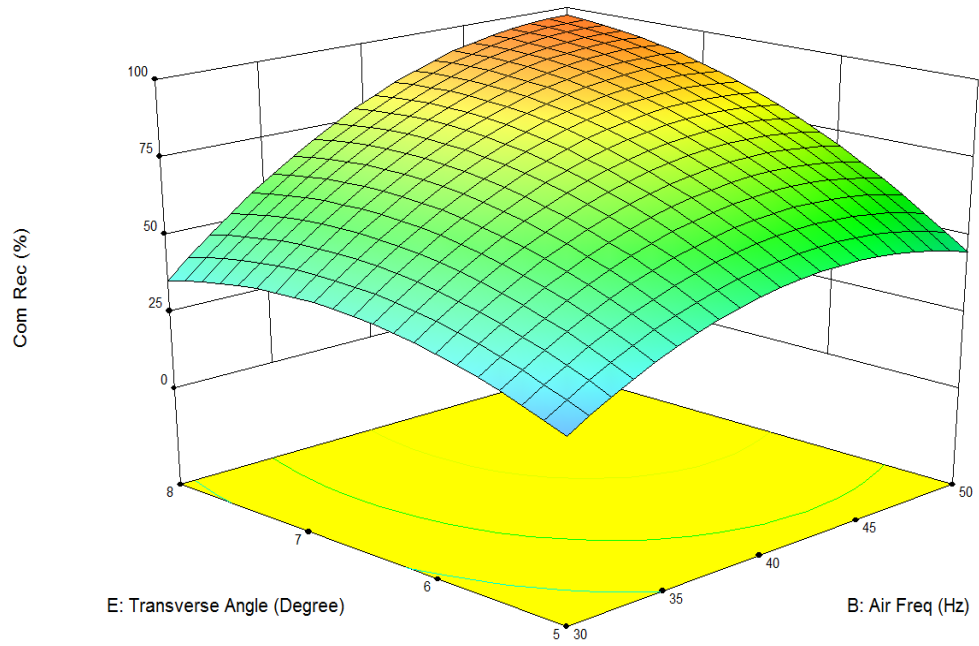


Figure 4.5 Effect of blower frequency (air flow rate) and transverse angle on achieved combustible recovery from coarse sample by using Air Table.

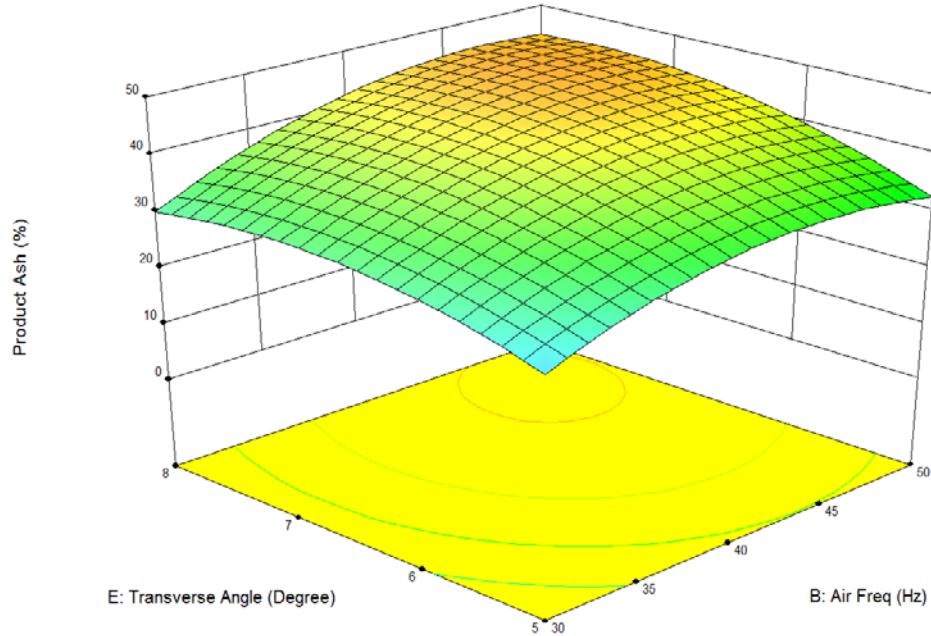


Figure 4.6 Effect of blower frequency (air flow rate) and transverse angle on product ash content of clean coal of coarse sample cleaned by Air Table.

Subsequently, the relationship between each response and remained parameters were defined in terms of mathematical equations. In this type of modeling, each parameter is provided with proper coefficients. Thereby, these models would be able to numerically demonstrate effect of increase / decrease of a given parameter on a response variable. Converting the modified models to numerical models, the expressions 4.1, 4.2 and 4.3 were provided.

$$\text{Product Yield (\%)} = 71.25 - 4.05 A + 21.84 B - 4.61 C + 2.48 D + 16.32 E + 13.53 BE + 13.77 A^2 - 16.02 B^2 - 12.51 E^2 \quad (4.1)$$

$$\text{Combustible Recovery (\%)} = 78.18 - 4.29 A + 20.56 B - 3.48 C + 4.14 D + 15.78 E + 10.22 BE + 16.85 A^2 - 15.72 B^2 - 11.65 E^2 \quad (4.2)$$

$$\text{Product Ash Content (\%)} = 42.70 + 0.63 A + 5.44 B - 1.40 C + 0.21 D + 4.25 E + 1.67 BE - 5.29 B^2 - 4.27 E^2 \quad (4.3)$$

Where, A = Feed Rate (Kg/hr), B = Blower Frequency (Hz), C = Table Frequency (Hz), D = Longitudinal Angle ($^{\circ}$), and E = Transverse Angle ($^{\circ}$)

In order to identify operational conditions leading the best obtainable results, the entire achieved data were subjected to pre-determined optimization study. The procedure of optimizing involved in minimizing the product ash content in a range of combustible recoveries and product yields. Thereby, the least product ash contents were determined, against several product yields and combustible recoveries (Honaker & Patil, Parametric evaluation of a dense-medium process using an enhanced gravity separator, 2002). As observed on Tables 4.6, 4.7 and 4.8, operational parameters were changed to some extent, so that a clean coal with 18.06 % impurities to be produced.

Table 4.6 Optimum operational parameters and their effect on Product Yield of coarse sample cleaned by Air Table

Test	Feed Rate (Kg/hr)	Fan Frequency (Hz)	Table Frequency (Hz)	Longitudinal Angle ($^{\circ}$)	Transverse Angle ($^{\circ}$)	Product Yield (%)
1	275.16	30.03	38.86	1.06	5.02	7.42
2	293.37	30.22	39.06	1.09	5.01	10.64
3	295.50	30.44	39.53	1.08	5	10.80

Table 4.7 Optimum operational parameters and their effect on Product Ash content of coarse sample cleaned by Air Table

Test	Feed Rate (Kg/hr)	Fan Frequency (Hz)	Table Frequency (Hz)	Longitudinal Angle ($^{\circ}$)	Transverse Angle ($^{\circ}$)	Product Ash (%)
1	275.16	30.03	38.86	1.06	5.02	18.06
2	293.37	30.22	39.06	1.09	5.01	18.06
3	295.50	30.44	39.53	1.08	5	18.06

Table 4.8 Optimum operational parameters and their effect on Combustible Recovery of coarse sample cleaned by Air Table

Test	Feed Rate (Kg/hr)	Fan Frequency (Hz)	Table Frequency (Hz)	Longitudinal Angle (°)	Transverse Angle (°)	Combustible Recovery (%)
1	275.16	30.03	38.86	1.06	5.02	13.66
2	293.37	30.22	39.06	1.09	5.01	17.95
3	295.50	30.44	39.53	1.08	5	17.80

As explained on experimental section, design expert software totally designed 27 trials for treating fine sample by means of Air Table. The cleaning performance of this unit on fine sample was evaluated under the same procedure as used for analyzing coarse sample. Initially, the obtained results were analyzed to identify the best product quality, as well as the most amounts of recovered feed mass and coal. Then, empirical models were generated to assess the effect of operational parameters on three response variables (product yield, combustible recovery, and product ash). The achieved results have been listed on table B.2, as presented on appendices. These data demonstrate that the lowest achievable product ash content would be almost 34.41%. In addition, producing a clean coal with this quality would result in recovering 21% and 24 % of feed mass and combustible materials, respectively. In majority of experiments, high percentage of total mass and combustible materials was recovered while generating a high ash content product. This fact clearly proves this type of sample was not well beneficiated, due to a great deal of materials were reported to product discharge end, without being efficiently separated. As a result, there would be no possibility to obtain a low ash clean coal with high amount of product yield and combustible recovery.

The associated response parameters were defined based on a quadratic model and their correlation to operational parameters was evaluated by means of analysis of variance method. The empirical models were modified through backward eliminating insignificant interactional parameters. The amended models highlighted operational parameters, those ones which had effect on a response variable (Tables 4.7, 4.8, and 4.9).

Table 4.9 Analysis of variance of product ash for fine sample cleaned by Air Table

Source	Sum of Squares	df	Mean Square	F Value	p-value Prob> F	
Model	16230.6	9	1803.39	20.85	< 0.0001	significant
A-Air Frequency	7743.95	1	7743.95	89.55	< 0.0001	
B-Table Frequency	1256.24	1	1256.24	14.53	0.0014	
C-Long. Angle	0.37	1	0.37	4.29E-03	0.9485	
D-Trans. Angle	3132.78	1	3132.78	36.23	< 0.0001	
AB	399.4	1	399.4	4.62	0.0463	
CD	561.69	1	561.69	6.5	0.0208	
A ²	1753.26	1	1753.26	20.28	0.0003	
C ²	456.27	1	456.27	5.28	0.0346	
D ²	2141.09	1	2141.09	24.76	0.0001	

Table 4.10 Analysis of variance of combustible recovery for fine sample cleaned by Air Table

Source	Sum of Squares	df	Mean Square	F Value	p-value Prob> F	
Model	16981.3	9	1886.81	20.7849	1.8E-07	significant
A-Air Frequency	7907.9	1	7907.9	87.1123	4.2E-08	
B-Table Frequency	1128.11	1	1128.11	12.4271	0.0026	
C-Long. Angle	7.50501	1	7.50501	0.08267	0.77718	
D-Trans Angle	3618.87	1	3618.87	39.8649	7.8E-06	
AB	519.612	1	519.612	5.72397	0.02856	
CD	593.166	1	593.166	6.53423	0.02045	
A ²	1897.07	1	1897.07	20.8978	0.00027	
C ²	548.808	1	548.808	6.04559	0.02496	
D ²	2065.48	1	2065.48	22.753	0.00018	

Table 4.11 Analysis of variance of product ash for fine sample cleaned by Air Table

Source	Sum of Squares	df	Mean Square	F Value	p-value Prob> F	
Model	100.67	7	14.38	14.58	< 0.0001	significant
A-Air Frequency	62.11	1	62.11	62.98	< 0.0001	
B-Table Frequency	14.02	1	14.02	14.22	0.0013	
C-Long. Angle	1.99	1	1.99	2.02	0.1714	
D-Trans Angle	7.05	1	7.05	7.15	0.015	
AB	1.9	1	1.9	1.93	0.1807	
A ²	9.42	1	9.42	9.56	0.006	
D ²	6.83	1	6.83	6.93	0.0164	

The variance analyses of provided models indicate that air frequency, transverse angle, and table frequency significantly affect all three responses. As previously explained, with each increase in transverse angle, particles would have lower chance to elevate along the transversal side of table. Thus, the higher portion of feed material longitudinally travels towards the product discharge end. In addition, as air flow rate increases, the high ash content particles are lifted up the bed surface. Hence, these sorts of particles would be exerted no pushing force, and finally reported to product stream. Moreover, with decreasing table shaking frequency, denser particles would be exerted weaker transversal force. Thereby, high ash-high density particles would not be effectually directed to the reject discharge end. The combination of low table frequency, sharp transverse angle, and high air flow rate would result in decrease of clean coal quality with enhancement of product yield and combustible recovery. The interactional effects of table frequency and blower frequency on three responses have been illustrated on Figures 4.7, 4.8, and 4.9.

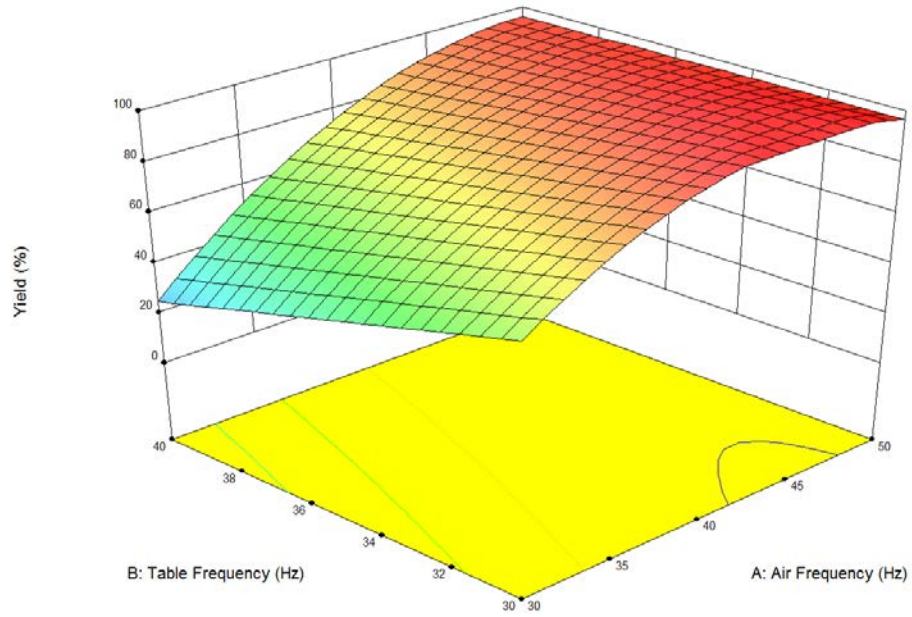


Figure 4.7 Effect of blower frequency (air flow rate) and table frequency on product yield achieved from fine sample using Air Table

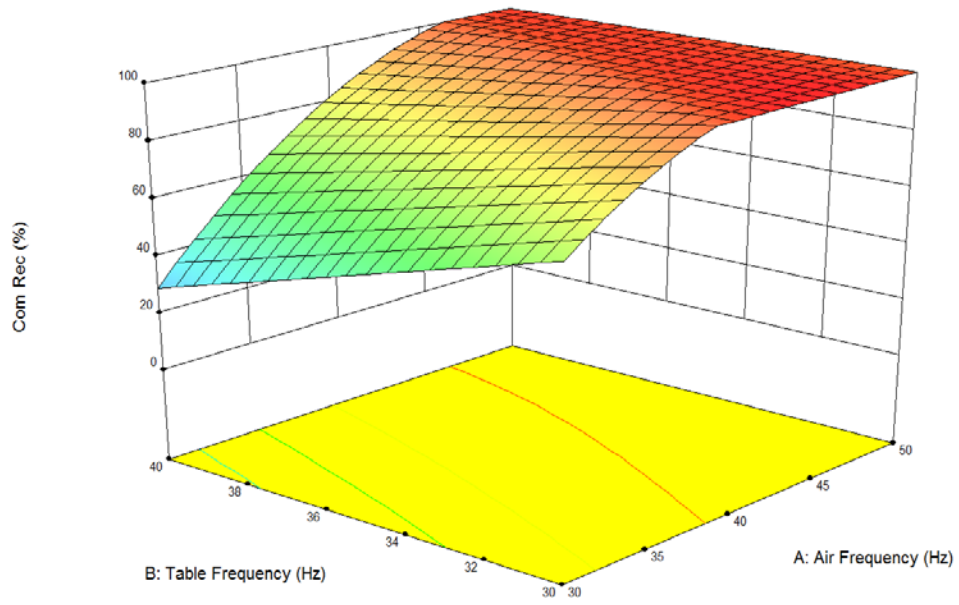


Figure 4.8 Effect of blower frequency (air flow rate) and table frequency on combustible recovery achieved from fine sample using Air Table

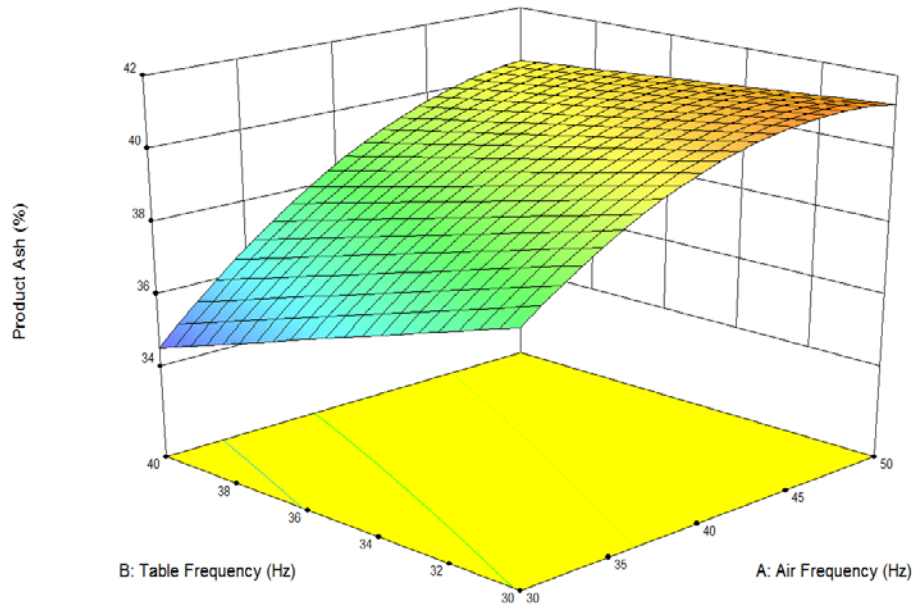


Figure 4.9 Effect of blower frequency (air flow rate) and table frequency on product ash content of clean coal achieved from fine sample using Air table.

The next stage of analyzing fine sample's results involved in developing numerical models for each response, based on the effective parameters (individual and interactional). These mathematical equations help in predicting the numerical value of each response by allocating different values to each operational parameter. The associated numerical expressions have been provided in equations 4.4, 4.5, and 4.6.

$$\text{Product Yield (\%)} = 88.2 + 25.4 A - 10.23 B - 0.18 C + 16.16 D + 9.99 AB - 11.85 CD - 17.09 A^2 - 8.72 C^2 - 18.89 D^2 \quad (4.4)$$

$$\text{Combustible Recovery (\%)} = 93.95 + 25.67 A - 9.7 B + 0.79 C + 17.37 D + 11.4 AB - 12.18 CD - 17.78 A^2 - 9.56 C^2 - 18.55 D^2 \quad (4.5)$$

$$\text{Product Ash (\%)} = 39.78 + 2.28 A - 1.08 B - 0.41 C + 0.77 D + 0.69 AB - 1.21 A^2 - 1.03 D^2 \quad (4.6)$$

Where, A = Blower Frequency (Hz), B = Table Frequency (Hz), C = Longitudinal Angle ($^{\circ}$), and D = Transverse Angle ($^{\circ}$)

Finally, the achieved data were optimized to determine optimum operational conditions resulting in the lowest product ash content. Level of operational parameters leading to optimal results, has been presented on Table 4.10.

Table 4.12 Optimum operational parameters and analytical results of fine sample cleaned by Air Table

Test	Fan Frequency (Hz)	Table Frequency (Hz)	Longitudinal Angle ($^{\circ}$)	Transverse Angle ($^{\circ}$)	Product Yield (%)	Combustible Recovery (%)	Product Ash (%)
1	37.22	40	1.34	8	67.00	74.03	37.65
2	37.22	40	1.34	8	67.07	74.08	37.65
3	37.24	40	1.33	8	67.22	74.23	37.66

4.4 Rotary Tribo-electric Separator

To assess the cleaning performance of RTS on fine size fraction of Korean anthracite coal, the ash content of three obtained products were analyzed. As mentioned before, in great number of trials, the ash content of acquired products was relied on an abnormal fluctuating trend, in which ash content of middling materials exceeded over tailings. Likewise, in some cases, particles were deflected towards the wrong electrode, thus were collected to wrong container. More clarification, the high ash content particles were collected in a container corresponded to the right electrode, when this electrode had been negatively charged. Referring the principles of separation, the low ash content particles should have obtained positive charge, and been reported to right container. For each trial, the ash content of generated products, and the sign of electrodes, have been listed on table D, presented in appendices.

The mentioned issues clearly demonstrate that raw materials were inefficiently separated from each other. As a result, there was no possibility to achieve actual values for three response variables (product ash, combustible recovery, and product yield). Due to this fact, we were unable to create analytical models, those ones which correlate response variables to operational parameters.

Considering the operational fundamentals of RTS, this unit would perform the most efficient beneficiation process, as raw feed contains isolator particles. In case of cleaning fine fraction of Korean anthracite coal, low separation efficiency is associated with excessive amount of conductive particles presenting in raw feed. The high degree of conductivity negatively impacts the process of charging, and decreases the capability of particles in sustaining their surface charge. To clearly realize the correlation between low separation efficiency and particles' conductivity, two probabilities needs to be considered, which cause a polarized particle loses its surface charge.

- 1) Conductive particle - grounded cylinder contact: referring the mechanisms of particle charging (as explained on literature review chapter), a conductive particles may be initially polarized by one of the three mentioned mechanisms. Consequently, this polarized particle may hit the grounded cylinder, and to be discharged.
- 2) Isolator particle - conductive particle - grounded cylinder contact: In his case, an isolator particles may primary obtains surface charge, and then hit a conductive particle, which has already connected to grounded cylinder. Thus, an electrical circuit would be generated between isolator particle and grounded cylinder which causes the polarized particle to lose its surface charge.

As discharged particles enter separation zone, they would be attracted by neither positive nor negative electrode, hence their trajectories may be only changed in accordance to the amount of air turbulence in the separation chamber. Therefore, these sorts of particles may likely not be deflected from center line of separation zone, and hence be collected in the center container, if the minimized turbulent condition exists in the separation zone. On the other hand, these particles may be concentrated either in right or left container, as if air turbulent exceeds and shift them to any of mentioned containers. Due to the described probabilities, the high ash content particles would have been accumulated in center / wrong container(s), due to they have no polarity while are introduced into the separation zone.

4.5 Dual Energy X-ray Transmission Sorting Technology

The cleaning performance of XRT technology on Korean anthracite coal was evaluated based on raw materials size fraction and separation criteria (setting). For the finest size range (31.75 mm x 19 mm), the cleaning performances of rougher, cleaner, and overall processing circuit (in which these two units are considered as a combined unit) will be assessed, over various employed settings. More clarification, for each three mentioned units, primary, the data achieved on three setting will be studied, and compared to each other. As a result, procedure of data analysis will be conducted in one stage which is more divided into three sub stages, recognized by units. During the process of analysis, the achieved experimental data will be interpreted based on separation efficiency indicators, termed as E_p , Cut Density, Organic Efficiency, products ash, clean coal yield, and combustible recovery. Throughout the first stage of analysis process, we will discuss potential reasons affecting the changing trend of afore-named factors. These reasons could be applied for analyzing cleaning performance of mentioned units on two other feed size ranges.

As previously explained, in the manual beneficiation process, to change the separation setting, a new calibration curve is generated by increasing the intensity of emitted x-ray

radiations. Hence, for a given particle, the number of red pixels increases with change of setting. Thus, higher ash content particles would have more chance to be ejected (as product) because of obtaining more percentage of red pixels. In XRT device, separation setting plays the same role as heavy medium in dense medium cyclone. Therefore, varying setting from 1 to 3 means as increasing the separation density. In this section, setting 1, 2, and 3 have been categorized as low, medium, and high setting, respectively.

4.5.1 31.75 mm x 19 mm size fraction of raw feed

4.5.1.1 Rougher Unit

This phase of data analysis focuses on studying the cleaning performance of rougher unit on 31.75 x 19 mm size Korean anthracite coal, over various separation settings varying from low to high. Regarding the effect of setting raise on treating process and data provided on Table 4.11, with changing setting from low to high, clean coal yield, product ash content, combustible recovery, and organic efficiency progressively increase, due to higher portions of feed material are recovered. Since the combustible materials were not completely liberated from impurities, the increase of mass recovery cause the combustible recovery and product ash content to be raised. In addition, based on the obtained organic efficiencies, the more intense settings provide more efficient cleaning processes.

Table 4.13 Analytical results achieved in rougher stage of DE-XRT over three separation settings

Setting	Product Yield (%)	Product Ash (%)	Combustible Recovery (%)	Organic Efficiency (%)
1	13.45	17.10	38.79	61.14
2	20.02	22.45	51.60	71.51
3	28.75	30.10	67.92	73.72

By plotting partitions curves associated to each separation setting (Figure 4.10), the cleaning performance of rougher stage on forgoing feed size range could be more comprehensively evaluated. As illustrated on Figure 3.16, while separation setting varies, cut density increases, due to greater amount of high ash-heavy particles are reported to product stream. Moreover, in each setting, several quantities of clean coal and tailings have misplaced to wrong streams. These phenomena occur due to the fluctuating motions of belt, which cause particles to bounce. Generally, the product bypass to reject stream is attributed to particle-particle overlapping, before reaching to detecting zone. In this case, two low density particles (which obtain high percentage of red pixels, as individually exposed to x-ray beam) are detected as a combined single particle which is thicker than each particle, individually. This combined particle would more attenuate x-ray radiation, and hence the majority of its pixels will be assigned blue color. As a result, both low ash content particles will be directed to tailing stream.

On the other hand, the tailing bypass to product stream could be associated to process of particles accumulation after passing detecting zone. More clarification, a low ash content particle is initially detected by unit operator. The selected particle, during its journey towards the end of belt, may be covered by a high ash content particle, due to the fluctuating motions of belt. Hence, when these accumulated particles reach to air valve, both are ejected as product. Clearly, the E_p values of various experiments are directly depended on the amount of low and high density particles which have misplaced to wrong stream. Thus, the E_p value is not only independent of separation settings, but is function of particles bouncing on the belt. As a result, the amount of product and reject misplacement to wrong streams is independent of separation setting (Table 4.12).

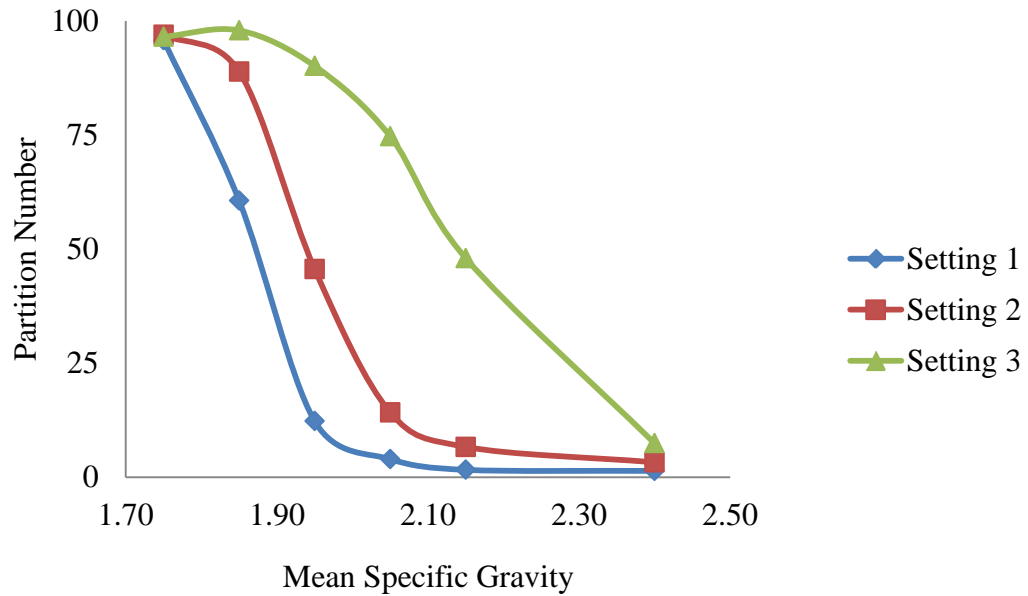


Figure 4.10 Partition curves obtained from performances of rougher stage of DE-XRT over three separation settings

Table 4.14 Partition curves parameters obtained from performances of rougher stage of DE-XRT over three separation settings

Setting	Product Bypass (%)	Reject Bypass (%)	Ep	Cut Density (tons/m ³)
1	4.23	1.41	0.055	1.870
2	3.05	3.29	0.060	1.940
3	3.48	7.47	0.070	2.140

4.5.1.2 Cleaner Unit

To evaluate cleaning performance of cleaner unit at a specific setting, we need to consider the performance of rougher unit working on conjunction with that cleaner unit. As explained previously, in rougher stage, the product ash content increases with elevation of separation setting. Therefore, in first setting, the rougher unit generated a

clean coal containing lowest ash content comparing to other settings. Then, this product was retreated in cleaner unit. As a result, in first setting, the cleaner unit produces a clean coal having the least amount of impurities rather than two other settings.

In addition, the amount of product yield, combustible recovery, and cut density are completely depended on the quantity of high ash content particles which have misplaced to product stream of rougher unit. As provided on table 4.12, in lower settings of rougher stage, the amount of Ep and reject bypass to product is less than higher settings. Hence, in lower settings, the raw feed of cleaner unit contains less percentage of heavy particles which should be ejected. As a result, on cleaning stage, the product yield decreases while setting elevates. Likewise, due the mentioned fact, the cut density of experiments conducted based on the lower settings, is less than ones which was run on higher settings. Because, in lower settings, the quantity of high ash particles is less, hence removing a small portion of them would bring about the cut density greatly decreases. In addition, rejecting greater amount of high ash particles in higher settings, would results in discarding more portions of combustible materials locking to impurities. Thus, the combustible recovery relies on a descending trend from weakest setting to the strongest one.

The Ep values and the amount of reject / clean coal bypass to wrong streams, change on a fluctuating trend independent of separation setting. As discussed earlier, during experiments, there was no possibility to control the amount of particles' misplacement to wrong stream. It is worth to be mentioned that, on the cleaning stage, particles would more easily bounce on the belt, due to the population of particles on the belt has decreased comparing to rougher stage. Furthermore, the organic efficiency of various settings have also set on a fluctuating trend in which initially increases and then decreases with elevation of setting from low to high. This trend could be directly associated with the quantity of clean coal bypass to reject stream, in various separation settings. Regarding provided results on tables 4.12 and 4.14, the lowest product bypass occurs in medium setting. As a result, at the specific product ash content, this setting recovers the

highest amount of feed mass. Hence, the greatest organic efficiency will be provided at this setting. The summary of discussed results has been provided on Tables 4.13 and 4.14. Likewise, the cleaning performance of cleaner in each setting has been visualized by plotting associated partition curves, as shown on Figure 4.11.

Table 4.15 Analytical results achieved by DE-XRT cleaner stage over three separation settings

Setting	Product Yield (%)	Product Ash (%)	Combustible Recovery (%)	Organic Efficiency (%)
1	92.69	12.38	97.98	99.67
2	88.95	15.46	96.96	99.94
3	81.98	20.24	93.6	98.77

Table 4.16 Partition curves parameters obtained from performances of cleaner stage of DE-XRT over three separation settings

Setting	Product Bypass (%)	Reject Bypass (%)	Ep	Cut Density (tons/m ³)
1	1.10	14.92	0.105	2.24
2	0.96	11.39	0.080	2.27
3	1.73	13.26	0.075	2.29

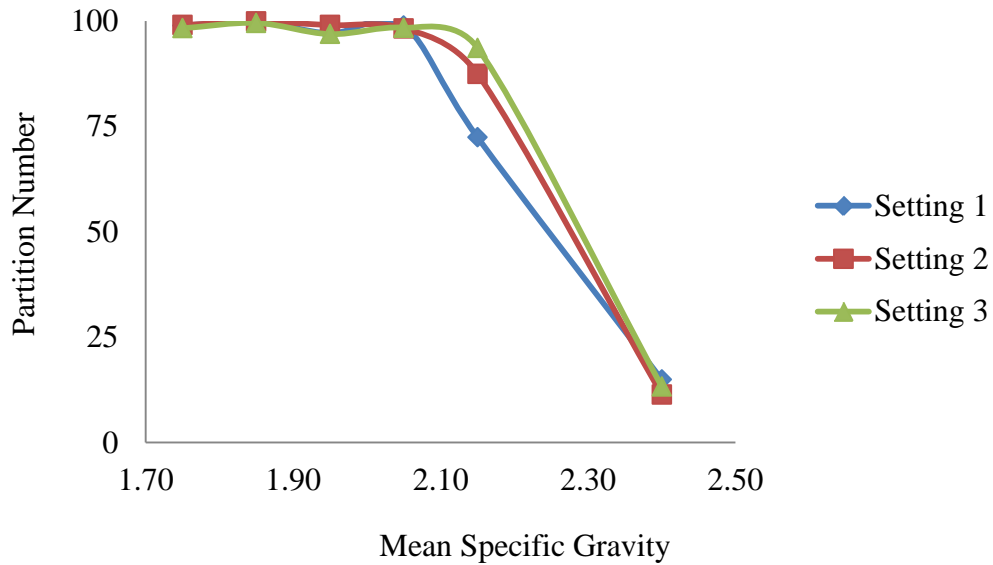


Figure 4.11 Partition curves obtained from performances of cleaner stage of DE-XRT over three separation settings

4.5.1.3 Overall circuit

To assess the cleaning performance of overall processing circuit, simultaneously, the cleaning performance of both units on anthracite beneficiation process needs to be considered. In this configuration, three products have been generated, which termed as rougher tailing, cleaner product, and cleaner tailing. Therefore, various analytical data and partition curves have been provided by means of the mentioned products.

As described before, on the rougher stage, the amount of mass recovery enhances while separation setting is set on the higher levels. At a specific setting, to assess overall product yield of processing circuit, the amount of mass recovery on cleaning stage also should be taken into account. Referring table 4.13, the product yield has been established on a descending trend with increasing separation setting. Although, the lower amount of feed mass were recovered at first setting of rougher stage, the great portion of which was recovered at corresponding setting of cleaning stage. However, as presented on Table 4.15, the product yield of overall circuit increasingly varies as settings rise. This implies

that the final clean coal yield is dependent on the amount of mass recovery at rougher stage. Since a large amount of raw material is fed into the rougher stage, any small differences what so ever in the percentage of product yield over various settings would cause cleaners' raw feeds to have significant differences in weight. At cleaning stage, the stronger settings recover lower amounts of feed mass. However, the overall yield of circuit would not be significantly declined, due to the raw feed mass of cleaner unit at higher settings was more than raw feed mass of which works on lower settings.

Similarly, the combustible recovery also is depended on quantity of feed mass which is recovered in each stage. Combustible recovery of total beneficiating process could be calculated by multiplying the amounts of combustible recoveries achieved on rougher and cleaner stages. In rougher process, combustible recovery grows with increases of separation setting (due to enhancement of product yield). On the other hand, in next processing stage, the amount of combustible recovery establishes on a descending trend with elevating setting, as discussed before. In addition, in first stage, the amounts of combustible recoveries largely differ from each other. While, in the next stage, almost equal portions of combustible materials have been concentrated throughout several settings. As a result, the overall circuit's combustible recovery is more dependent on percentage of combustible materials recovered by rougher rather than those of which concentrated by cleaner.

The final product of circuit is generated by cleaner unit. As mentioned on pervious section, at cleaning process, the weakest setting produces a clean coal containing lowest amount of mineral matters, due to the raw feed contents the least percentage of impurities. Moreover, organic efficiency increases while the process of coal treatment is conducted by means of more intense settings. The organic efficiency is directly affected by the portion of feed mass directed to product stream (clean coal yield). As discussed, the combination of both units results in enhancement of product yield, over several settings. Thus, at particular clean coal ash content, it would be expected that higher settings provide the greater values of organic efficiency. Due to the discussed facts, the

cleaning performance of overall circuit is greatly dependent on rougher stage rather than cleaner one.

Table 4.17 Analytical results achieved by DE-XRT overall circuit over three separation settings

Setting	Product Yield (%)	Product Ash (%)	Combustible Recovery (%)	Organic Efficiency (%)
1	12.80	12.38	38.00	85.33
2	18.18	15.46	50.03	86.33
3	24.44	20.24	63.57	97.76

Partition curve factors (provided in table 4.16) indicate that the cut density progressively increases as higher settings employed for coal treatment. Since the low portion of cleaner's raw feed is reported to cleaner reject stream, the cleaner product has as same characteristics as the rougher product. Thus, the overall cut density would be almost equal to cut density of rougher processing stage. Considering this fact, the cut density of entire circuit would be elevated with rising separation setting of rougher stage. The reason is attributed to high ash - heavy particles which are increasingly concentrated into rougher product stream.

Table 4.18 Partition curves parameters obtained from performance of DE-XRT overall circuit over three separation settings

Setting	Product Bypass (%)	Reject Bypass (%)	Ep	Cut Density (tons/m ³)
1	5.14	0.22	0.055	1.87
2	3.89	0.38	0.065	1.94
3	4.92	1.04	0.105	2.13

The entire clean coal bypass to reject stream is proportional to the amount of product which is misplaced in each processing stage. However, the rougher unit more significantly affects on overall bypass than cleaner unit, due to raw feed of first stage more weighs comparing to second stage's raw feed. Thereby, at first stage, any small percentage of bypass would result in high quantity of clean coal misplacement. In addition, the amount of clean coal bypass in second stage will increase the overall bypass of processing circuit. But, the effect of cleaner unit in rising total bypass is not as significant as rougher unit. As a result, in overall circuit, similar to rougher stage, the quantity of clean coal misplacement changes on the fluctuating trend with increasing separation setting.

Similarly, to interpret the changing trend of tailing bypass to product stream, the performance of both units needs to be considered. In this case, the entire reject bypass is more dependent on the performance of cleaner unit than rougher one. As stated earlier, greater amount of feed mass is processed by rougher unit, hence some portion of high density particles may be misplaced to the rougher product stream. However, the following processing stage discards the majority of the mentioned particles. Thereby, the overall circuit's product contains less quantity of high density particles than rougher stage's product. However, the final quantity of reject bypass is completely proportional to initial amount of tailing bypass. Due to this fact, the percentage of tailing misplacement increases while separation setting sets on the higher levels.

The provided E_p values could be analyzed based on changing trend of organic efficiency. As general rule, higher organic efficiency indicates that overall circuit has conducted more efficient treatment process, at a specific setting. As a result, the associated E_p value should be the least. As observed on the Table 4.15 and 4.16, the highest organic efficiency and E_p value were obtained on the last setting. Thereby, the provided E_p value is not reliable. Associated partition curves have been plotted on the Figure 4.12.

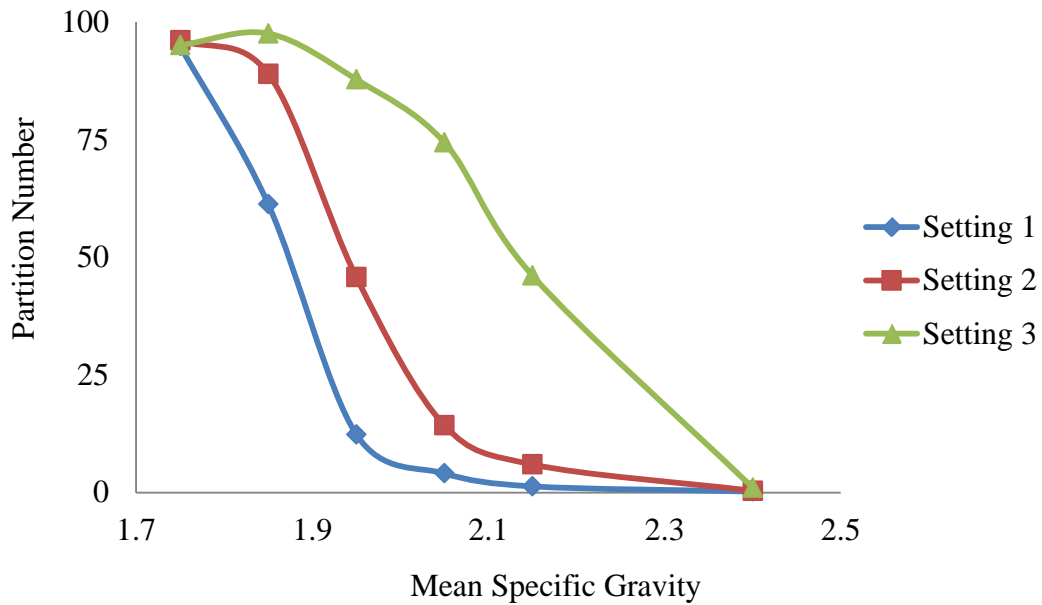


Figure 4.12 Partition curves parameters obtained from performances of DE-XRT overall circuit over three separation settings

Throughout the analysis process, we discussed potential reasons affecting the changing trend of separation efficiency indicators e.g. E_p and product yield. Since, the afore-discussed reasons could be used for analyzing cleaning performance of mentioned units on two other feed size ranges, experiential results associated to other size ranges will not be interpreted. However, the obtained data have been presented on appendices.

CHAPTER 5

SUMMARY AND CONCLUSION

The majority of boiler furnaces have been designed to utilize anthracite coal containing low amount of impurities. Run-out-of-mine (ROM) anthracite coal contains partially incombustible minerals which significantly decline coal quality and thus the combustible value of final product. Hence, coal preparation is needed to minimize the quantity of incombustible materials. To assess the potential of upgrading Korean anthracite coal, an investigation has been carried out utilizing four distinctly different processing technologies including an air table, dense medium cyclone, tribo-electric separator, and X-ray transmission sorting.

The aforementioned technologies have not been previously evaluated for the treating of Korean anthracite coal. In addition to the four technologies, the other technologies that have been most frequently used in anthracite cleaning have been reviewed. Cleaning performance and operational principles of various anthracite cleaning machines have been comprehensively discussed.

The samples utilized in the investigation were provided by KIGAM (Korean Institute of Geoscience and Mineral Resources). Particle size and cleanability properties were evaluated for each of the coal samples received. Regarding the type of employed machine, the experimental approach has been thoroughly discussed. The investigation generated performance data that can be used to project full-scale performance on a particle size-by-size basis. The ultimate goal of the project was to identify technologies that provide the best opportunity to economically upgrade Korean anthracite coal which has difficult cleaning characteristics.

The experimental program used to evaluate each technology was different. The cleaning performance of an air table was assessed by means of a statistically-designed set of experiments and the results used to develop empirical relationships describing product

quality, combustible recovery and product yield as a function of operating parameters. The goal was to determine the optimum conditions which provide the maximum mass yield at a given product ash content. Partition curves were not used to assess process of performance.

The separation performances of dense medium cyclone and XRT sorting were evaluated by means of all abovementioned factors plus partition curve factors and organic efficiency. The tribo-electric process did not provide a separation that could be used to provide an adequate statistical assessment. As such, performance assessment was limited to individual test results obtained from the performance of the experimental design tests.

The finding of this investigation can be summarized as follows:

1. The Korean coal samples were found to have very difficult cleaning characteristics. The level of difficulty varied between the coals samples received. In general, the majority of the clean coal exists in the specific gravity range of 1.6 to 1.8 which is significantly higher than lower rank coal. The cleaning difficult is revealed by the amount of coal in the intermediate gravity fractions between 1.8 to 2.0 which was 15 % of the total sample and higher.
2. Dense medium cyclone experiments were conducted using medium specific gravity values of 1.7, 1.75, 1.85 and 1.9. For the 1.9 specific gravity medium, an evaluated feed pressure of 6 psi was used to overcome viscosity effects apparent when using magnetite having a particle size that is 91 % passing 45 microns. The other tests with low specific gravity values were performed using a feed pressure of 4 psi.

For 6 x 1 mm coal, the dense medium cyclone produced a clean coal containing 6 % and 7 % ash under specific gravity values of 1.7 and 1.75, respectively. The ash content increased as expected when the medium gravity

was raised to 1.85. The probable error value obtained at a medium gravity of 1.85 was 0.03 which led to an organic efficiency of 96.36 %.

The test performed at a medium specific gravity of 1.90 and pressure of 6 psi was ineffective in providing an acceptable separation performance.

3. The potential of using a dry separation technique to upgrade the Korean coal was assessed using an air concentration table. A statistically designed test program involving 46 tests was conducted on 8 x 0.6 mm coal. The 6 x 1 mm coal was used in a separate set of 26 experiments to determine separation differences in the optimum operating parameter values. Feed rate was held constant for the fine particle tests.

When treating the coarse 8 x 0.6 mm size fraction, the air table produced clean coal containing varied amounts of ash from 18 % to 48 % over the 46 tests. Tailing ash values ranged from 45 % to 78 % when targeting the production of a clean coal containing 18 % ash. From a feed having 47 % ash, the maximum mass yield to the product was 10.8 %. The set of operating parameter values that provided the best separation efficiency resulted in an ash reduction from 47 % to 32 % while recovering 58 % of the feed mass and 70 % of the combustibles.

The dry processing of the finer fraction using the air table did not provide product ash contents significantly below 35 %. However, effective removal of high ash content materials was achieved as indicated in a test in which about 5 % of the feed reported to the reject which contained 80 % ash. Product ash content varied from 34 % to 42 % over the 27 tests while mass yield ranged from 12 % to 98 %.

Air flow rate through the table and transverse angle (downward slope from feed to light product stream) were significant for determining the separation performance for both the coarse and fine particle feed. The interaction between the two parameters was significant for determining both yield and product ash for the coarse feed. This finding is reasonable since both parameters are involved in the physics of particle transport across the table while levitating the light material which requires more energy for coarser particles.

4. Another dry cleaning technology tests for the treatment of 63 x 19 mm coal is the XRT sorting process. The technology utilizes x-ray transmission to identify particles of different density as they are transported across a moving conveyor belt. Air jets at the discharge of the belt direct a stream of air at particles pre-selected for ejecting into a stream away from the stream containing the majority of the belt discharge.

The separation performance achieved in a single cleaning stage was significantly more efficient than the air table performance. At a feed rate of 110 tons/hr, the ash content was reduced from 69.3 % to 22.45 % while recovering 51.6 % of the combustible. The organic efficiency was 71.5 % which reflects the difficult cleaning characteristics of the coal and about 3 % bypass of low and high density particles. The probable error value of 0.06 indicates an exceptional performance for a dry separation process.

In an effort to evaluate the potential to reduce ash content, the product from the first stage was re-cleaned. A high level of efficiency was achieved in the cleaner stage resulting in an ash reduction from 22.45 % to 15.46 % with a combustible recovery of 97.00 %.

When combining the performance, the rougher cleaner circuit reduced the ash content from 69.3 % to 15.46 % while recovering 50.00 % of combustibles. The organic efficiency was a very respectable 86.3 %, as a result of a sharp separation (0.065 Ep) and limited bypass (i.e., 0.38% high density and 3.89 % low density bypass).

5. The cleaning of material finer than 1 mm was evaluated using a dry tribo-electrostatic separator using a three-level design was conducted to identify the optimum operating conditions. The four parameters investigated include feed rate, charger rotational speed, charger voltage, and air flow velocity. The separation performances obtained under the broad range of test conditions in 29 experiments revealed very little upgrading.
6. The dense medium cyclone unit provided the most efficient separating for Korean anthracite coal as indicated by an organic efficiency of 96 % under a condition that resulted in a product ash content of 9.38 %. XRT sorting provided a performance that was slightly inferior to the dense medium cyclone but exceptional when compared to other dry cleaning technologies.

The air table provided an adequate performance but the product ash content was significantly higher than the clean coal products generated from the dense medium cyclone and XRT sorting units. Tribo-electrostatic separation technology appears to be ineffective in treating the -1 mm Korean coal.

7. The entire dry separation process was simulated by a circuit including XRT sorting technology, Air Concentration Table and Tribo-electrostatic separation technology. The cleaning circuit succeeded in recovering 15.49 % of total feed mass with producing a clean coal containing 18.90 % of mineral matters.

APPENDICES

A. Air table designed experinmets

Table A.1. Air table experiments conducted on the coarse sample

Run	Feed Rate (Kg/hr)	Air Frequency (Hz)	Table Frequency (Hz)	Longitudinal Angle (°)	Transverse Angle (°)
1	250	50	35	1	6.5
2	250	50	30	1.5	6.5
3	250	40	35	1	8
4	250	40	40	1.5	5
5	250	30	35	1.5	8
6	250	40	30	1	6.5
7	200	40	35	1.5	8
8	250	40	35	1.5	6.5
9	250	40	35	2	8
10	250	30	35	1.5	5
11	200	40	35	1	6.5
12	300	30	35	1.5	6.5
13	250	40	40	1.5	8
14	300	50	35	1.5	6.5
15	300	40	35	1	6.5
16	250	30	30	1.5	6.5
17	250	50	35	1.5	8
18	250	40	40	2	6.5
19	250	40	35	1.5	6.5
20	250	50	40	1.5	6.5
21	200	40	35	2	6.5
22	300	40	35	1.5	5
23	250	40	35	1.5	6.5
24	300	40	40	1.5	6.5
25	200	40	30	1.5	6.5

Continues of table A.1

26	250	50	35	2	6.5
27	250	50	35	2	6.5
28	300	40	35	1.5	8
29	200	50	35	1.5	6.5
30	250	40	35	1.5	6.5
31	250	40	35	2	5
32	200	40	40	1.5	6.5
33	250	30	40	1.5	6.5
34	250	40	30	1.5	8
35	300	40	35	2	6.5
36	250	50	35	1.5	5
37	300	40	30	1.5	6.5
38	200	40	35	1.5	5
39	200	30	35	1.5	6.5
40	250	40	35	1	5
41	250	40	35	1.5	6.5
42	250	40	30	2	6.5
43	250	40	30	1.5	5
44	250	30	35	1	6.5
45	250	40	35	1.5	6.5
46	250	40	40	1	6.5

Table A.2. Air table trials associated to fine sample

Run	Air Frequency (Hz)	Table Frequency (Hz)	Longitudinal Angle (°)	Transverse Angle (°)
1	40	40	1	6.5
2	50	35	1	6.5
3	40	30	1.5	5
4	40	30	1.5	8
5	40	30	1	6.5
6	30	30	1.5	6.5
7	40	35	1.5	6.5
8	40	40	1.5	8
9	40	40	2	6.5
10	40	35	2	5
11	40	35	1.5	6.5
12	40	35	1	5
13	30	35	1.5	5
14	50	35	1.5	5
15	30	35	1	6.5
16	30	35	2	6.5
17	40	35	1	8
18	50	35	2	6.5
19	40	30	2	6.5
20	50	30	1.5	6.5
21	40	35	1.5	6.5
22	50	40	1.5	6.5
23	50	35	1.5	8
24	30	35	1.5	8
25	30	40	1.5	6.5
26	40	35	2	8
27	40	40	1.5	5

B. Air table, achieved results

B.1. Analytical results associated to coarse sample

Run No.	Ash (%)		Product Yield (%)	Combustible Recovery (%)
	Tailings	Product		
1	62.72	40.50	74.57	86.57
2	61.89	43.74	77.15	75.75
3	55.57	41.52	52.00	52.93
4	45.93	27.26	10.60	13.45
5	52.02	23.14	27.67	41.59
6	45.51	42.19	42.95	43.31
7	76.93	44.74	91.97	100.00
8	58.10	33.17	44.58	55.60
9	61.70	43.49	62.55	68.83
10	51.77	18.06	7.13	10.83
11	71.67	40.70	87.59	96.60
12	58.24	28.34	38.75	50.67
13	72.96	43.13	86.86	98.83
14	75.78	43.45	92.70	100.00
15	67.97	43.90	77.64	85.56
16	62.80	47.69	61.61	65.10
17	72.56	43.12	95.83	98.60
18	72.87	40.67	79.96	90.75
19	66.54	43.50	77.19	88.19
20	66.48	44.61	81.14	92.19
21	68.81	37.89	88.65	100.00
22	49.56	34.49	52.02	68.51
23	58.18	39.95	75.71	78.82
24	66.55	48.57	73.56	79.06

Continues of table B.1

25	57.46	40.95	90.54	95.82
26	56.31	43.42	78.98	88.94
27	53.02	32.30	26.21	33.39
28	71.63	50.55	92.11	96.29
29	84.40	43.98	97.46	100.00
30	60.43	40.05	63.24	70.08
31	54.36	37.67	55.54	68.69
32	73.59	41.41	78.31	86.14
33	49.27	31.63	21.19	27.82
34	64.23	41.10	87.01	96.84
35	66.40	41.57	77.39	94.42
36	49.27	31.36	21.19	26.96
37	55.12	44.07	81.30	90.99
38	63.74	42.21	69.62	81.24
39	62.27	33.84	45.58	60.33
40	51.72	31.85	58.38	70.50
41	65.48	44.25	83.74	83.97
42	67.73	42.77	84.11	93.15
43	57.59	39.91	60.35	68.11
44	56.64	32.16	41.51	55.86
45	66.68	42.40	82.23	92.58
46	77.66	42.74	73.90	78.79

B.2. Analytical results associated to fine sample

Run No.	Ash (%)		Product Yield (%)	Combustible Recovery (%)
	Tailings	Product		
1	64.46	40.09	85.33	90.49
2	75.50	42.35	95.58	97.89
3	55.60	40.30	65.64	71.68
4	74.00	40.60	97.26	100.00
5	71.05	41.59	90.73	92.58
6	54.86	37.82	70.10	76.86
7	80.23	40.45	94.84	99.30
8	67.62	38.84	86.29	96.95
9	54.54	38.20	71.60	79.09
10	51.72	38.11	59.03	63.80
11	52.00	38.47	67.79	75.71
12	46.69	35.91	31.01	35.43
13	44.21	35.76	11.76	13.46
14	50.45	38.79	60.04	65.99
15	47.26	36.05	28.13	31.91
16	49.47	35.32	39.70	45.79
17	61.12	39.25	75.19	80.63
18	60.01	39.10	83.55	92.19
19	74.08	40.16	94.17	97.26
20	67.56	41.62	97.63	100.00
21	67.37	40.46	87.63	92.34
22	66.06	40.97	88.61	93.94
23	81.73	40.18	98.43	100.00
24	49.42	36.35	48.20	54.12
25	45.38	34.41	21.11	24.64
26	74.70	39.46	55.81	60.29
27	51.35	36.61	39.81	43.16

C. Rotary Tribo-electric Separator, designed experinmets

Run	Feed Rate (lb/hr)	Charger Rotation Speed (rpm)	Charger Voltage (V)	Air Flow Velocity (m/s)
1	12.5	5000	0	2.5
2	5	3000	0	2.5
3	12.5	1000	-3000	1.75
4	12.5	3000	-3000	2.5
5	20	3000	-3000	1.75
6	12.5	3000	3000	1
7	12.5	1000	0	1
8	12.5	1000	3000	1.75
9	12.5	3000	0	1.75
10	20	3000	0	1
11	5	1000	0	1.75
12	12.5	3000	-3000	1
13	12.5	5000	-3000	1.75
14	5	3000	3000	1.75
15	20	3000	0	2.5
16	20	1000	0	1.75
17	12.5	3000	0	1.75
18	12.5	5000	3000	1.75
19	12.5	3000	3000	2.5
20	12.5	3000	0	1.75
21	20	3000	3000	1.75
22	12.5	5000	0	1
23	5	3000	-3000	1.75
24	20	5000	0	1.75
25	12.5	3000	0	1.75
26	5	5000	0	1.75
27	12.5	1000	0	2.5
28	5	3000	0	1
29	12.5	3000	0	1.75

D. Analytical results associated to Rotary Tribo-electric Separator experiments

Test	Product Ash (%)			Sign of electrodes	
	Left	Center	Right	Left Electrode	Right Electrode
1	41.25	39.62	38.68	Positive	Negative
2	36.89	41.13	38.34	Positive	Negative
3	40.51	39.77	42.06	Positive	Negative
4	36.80	41.11	38.95	Positive	Negative
5	36.60	41.27	37.48	Positive	Negative
6	32.90	40.25	40.13	Positive	Negative
7	40.03	40.32	39.37	Positive	Negative
8	35.11	39.34	40.78	Negative	Positive
9	40.65	40.70	34.98	Positive	Negative
10	39.70	41.32	33.79	Positive	Negative
11	41.17	39.68	38.64	Positive	Negative
12	37.18	41.69	38.33	Positive	Negative
13	40.32	39.90	39.04	Positive	Negative
14	33.17	40.31	39.88	Negative	Positive
15	38.25	40.49	36.64	Positive	Negative
16	39.74	40.03	37.55	Positive	Negative
17	39.20	40.91	35.62	Positive	Negative
18	36.83	38.51	41.17	Negative	Positive
19	34.38	40.24	39.84	Negative	Positive
20	33.04	40.05	39.90	Positive	Negative
21	39.74	41.48	35.06	Negative	Positive
22	34.18	40.79	39.97	Positive	Negative
23	41.09	40.07	37.72	Positive	Negative
24	35.09	40.54	38.47	Positive	Negative
25	41.44	40.12	38.96	Positive	Negative
26	38.50	41.04	35.55	Positive	Negative
27	40.75	38.62	39.79	Positive	Negative
28	41.52	39.93	38.14	Positive	Negative
29	41.01	41.91	34.30	Positive	Negative

E. XRT cleaning performance data, raw feed size,60 mm x 30 mm

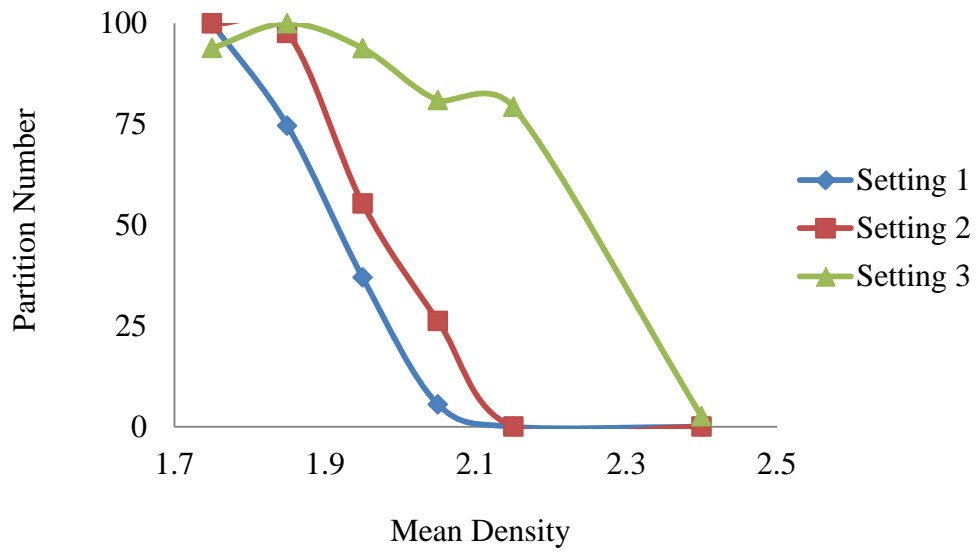
E.1 analytical results, rougher unit

Setting	Product Yield (%)	Product Ash (%)	Combustible Recovery (%)	Organic Efficiency (%)
1	13.10	13.81	42.08	97.04
2	18.19	16.99	54.42	90.96
3	24.55	24.98	69.08	90.93

E.2 partition curve factors, rougher unit

Setting	Product Bypass (%)	Reject Bypass (%)	Ep	Cut Density (tons/m ³)
1	0.00	0.00	0.065	1.91
2	0.00	0.00	0.07	1.97
3	6.17	2.53	0.08	2.25

E.3 partition curves, rougher unit



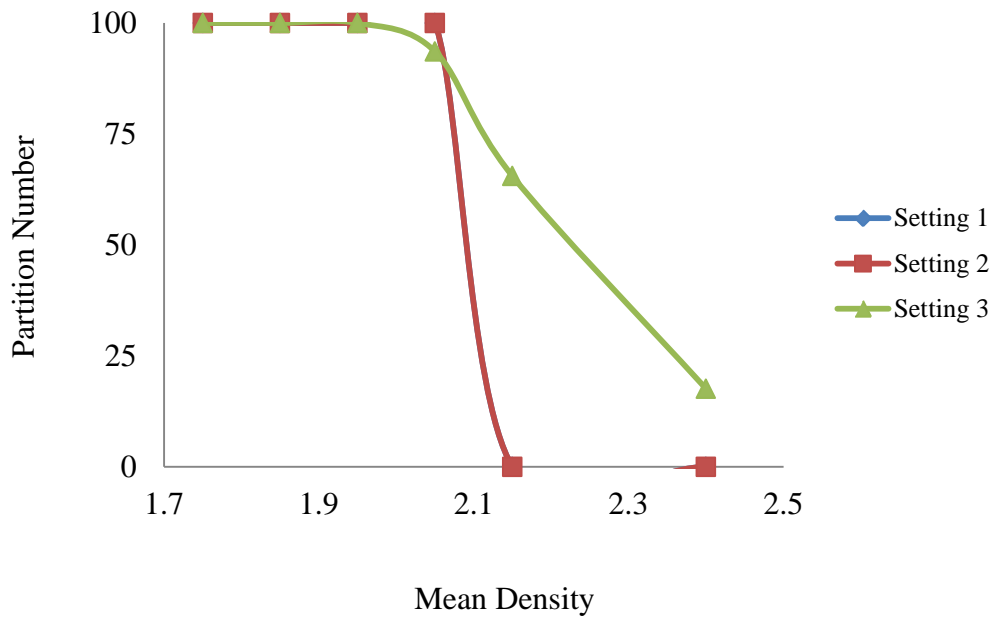
E.4 analytical results, cleaner unit

Setting	Product Yield (%)	Product Ash (%)	Combustible Recovery (%)	Organic Efficiency (%)
1	100.00	13.81	100.00	100.00
2	100.00	16.99	100.00	100.00
3	90.05	21.97	93.70	98.95

E.5 partition curve factors, cleaner unit

Setting	Product Bypass (%)	Reject Bypass (%)	Ep	Cut Density (tons/m ³)
1	0.00	0.00	0.02	2.09
2	0.00	0.00	0.02	2.09
3	0.00	17.59	0.125	2.23

E.6 partition curves, cleaner unit.



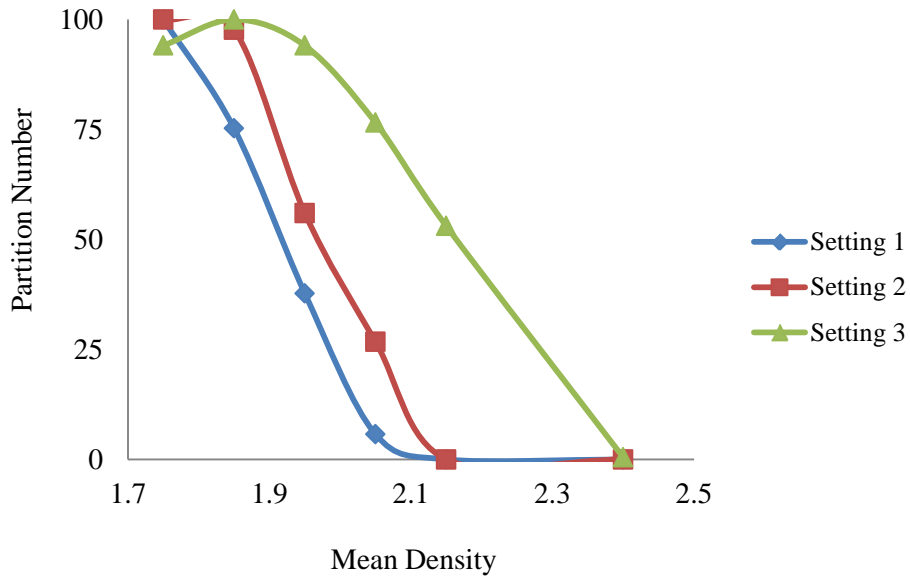
E.7 Analytical results, overall circuit.

Setting	Product Yield (%)	Product Ash (%)	Combustible Recovery (%)	Organic Efficiency (%)
1	13.48	13.81	42.08	97.68
2	18.62	16.99	54.42	93.09
3	22.94	21.97	64.73	99.75

E.8 partition curve factors, overall circuit.

Setting	Product Bypass (%)	Reject Bypass (%)	Ep	Cut Density (tons/m ³)
1	0.00	0.00	0.065	1.92
2	0.00	0.00	0.070	1.97
3	5.91	0.47	0.110	2.16

E.9 partition curves, overall circuit



F. XRT cleaning performance data, raw feed size, 60 mm x 20 mm

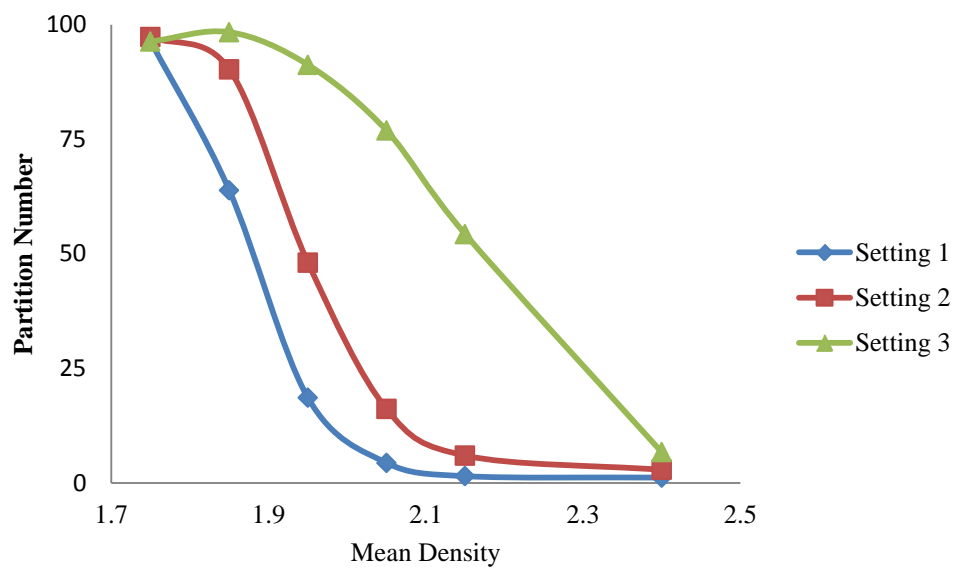
F.1 analytical results, rougher unit

Setting	Product Yield (%)	Product Ash (%)	Combustible Recovery (%)	Organic Efficiency (%)
1	13.72	16.53	39.73	65.33
2	20.12	21.65	52.3	80.48
3	28.73	29.36	68.58	73.66

F.2 partition curve factors, rougher unit

Setting	Product Bypass (%)	Reject Bypass (%)	Ep	Cut Density (tons/m ³)
1	3.62	1.17	0.06	1.88
2	2.72	2.87	0.06	1.94
3	3.68	6.71	0.12	2.17

F.3 partition curves, rougher unit



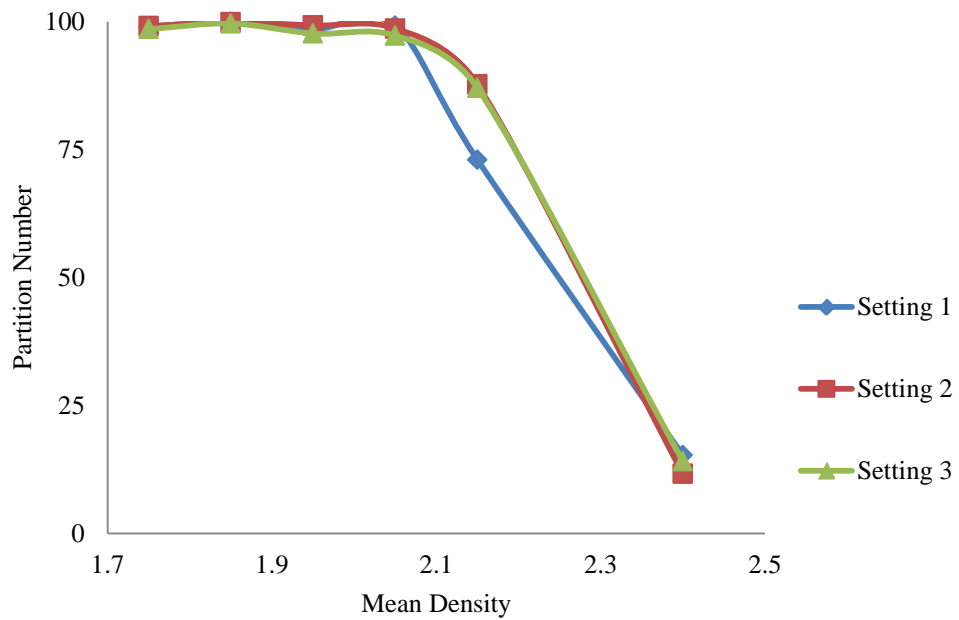
F.4 analytical results, cleaner unit

Setting	Product Yield (%)	Product Ash (%)	Combustible Recovery (%)	Organic Efficiency (%)
1	94.19	12.69	98.38	99.15
2	90.65	15.61	97.39	99.62
3	84.01	15.99	93.86	98.84

F.5 partition curve factors, cleaner unit

Setting	Product Bypass (%)	Reject Bypass (%)	Ep	Cut Density (tones/m ³)
1	0.93	15.32	0.105	2.25
2	0.85	11.67	0.105	2.25
3	1.44	14.15	0.085	2.23

F.6 partition curves, cleaner unit



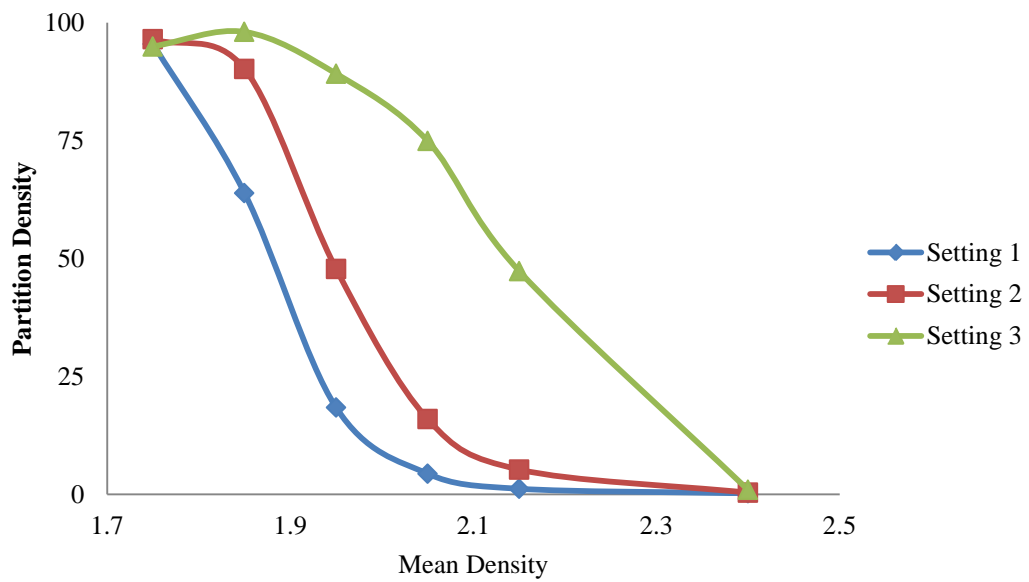
F.7 analytical results, overall circuit

Setting	Product Yield (%)	Product Ash (%)	Combustible Recovery (%)	Organic Efficiency (%)
1	12.93	12.69	39.09	83.94
2	18.24	15.61	50.93	86.85
3	24.14	20.52	64.37	93.55

F.8 partition curve factors, overall circuit

Setting	Product Bypass (%)	Reject Bypass (%)	Ep	Cut Density (tons/m ³)
1	4.51	0.17	0.06	1.88
2	3.54	0.33	0.06	1.94
3	5.05	0.92	0.11	2.14

F.9 partition curves, overall circuit



REFERENCES

Albrecht, M. C. (1980). Coal Preparation Processes. *American Society of Mechanical Engineers Annual Meeting*, (pp. 279-289). San Francisco, California.

Albrecht, M. C. (1982). Introduction to Coal Preparation. *4th Annual Symposium on Industrial Coal Utilization*. DOE, Cincinnati.

Alderman, J. K., & Snoby, R. J. (2001). Improving power plant performance and reducing emissions through the use of pneumatic dry cleaning for low rank coal. *In SME Annual Meeting*,. Denver, Colorado.

Alexis, J. (1980). Cleaning Coal and Refuse Fines With the Humphreys Spiral Concentrator. *Mining Engineering (Littleton, CO, USA)* , 32 (8), 1224-1226.

Arnold, B. J., Klima, M. S., & Bethell, P. J. (2007). Designing the Coal Preparation Plant of the Future. *SME*.

Ashmead, D. C. (1920). Advances in the Preparation of Anthracite. *American Institute of Mining Engineers Transactions* , 66, 422-508.

Atlantic Coal Plc. (2012). *Anthracite: The cleanest burning solid fossil fuel known to man*.

Ayres, W. S. (1909). A New Separator for the Removal of Slate from Coal. *Spokane Meeting* , 648-654.

Bada, S. O., Falcon, L. M., & Falcon, R. M. S. (2010). The potential of electrostatic separation in the upgrading of South African fine coal prior to utilization-a review. *The Journal of The Southern African Institute of Mining and Metallurgy* , 110, 691-702.

Bada, S. O., Falcon, L. M., Falcon, R. M. S., & Du Cann, V. M. (2012). Qualitative analysis of fine coals obtained from triboelectrostatic separation. *Journal of The Southern African Institute of Mining and Metallurgy* , 112 (1), 55-62.

Benusa, M. D., & Klima, M. S. (2009). An Evaluation of a Two-Stage Spiral Processing Fine Anthracite Refuse. *International Journal of Coal Preparation and Utilization* , 29 (2), 49-67.

Bimpong, C. (2008). *Alternative Materials for Dense Medium Separation*.

Cho, H., & Kim, J. (2002). Recovering carbon from anthracite using hindered settling column. *In SME Annual Meeting*, (pp. 02-064).

CIEŚLA, A. (2012). Theoretical consideration for oxygen enrichment from air using high-TC superconducting membrane. *Carbon* , 1461 (121.4), 3-8.

Coal Age-The challenge of coal's new growth era. (1961). 66 (10).

De jong, T. P. R., & Dalmijn, W. L. (2003). Dual Energy X-ray Transmission Imaging: Applications in Metal Processing. *TMS (The Minerals, Metals & Materials Society)* , 463-471.

Dennen, W. L., & Wilson, V. H. (1948). Cleaning Anthracite Silt For Boiler Fuel with Humphreys Spiral Separator. *Coal Technology* .

Dieudonné, V., Jonkers, A., & Loveday, G. (2006). An approach to confidently predicting jigging performance. *The Journal* , 18, 20.

Drummond, R., Nicol, S., & Swanson, A. (2002). Teetered bed separators—the Australian experience. *Journal of the South African Institute of Mining and Metallurgy (South Africa)* , 102 (7), 385-391.

Dube, R. M. (2012). *Collectors for Enabling Flotation of Oxidized Coal*.

Dwari, R. K., & Rao, K. H. (2007). Dry beneficiation of coal-a review. *Mineral Processing and Extractive Metallurgy Review* , 28 (3), 177-234.

Eckerd, J. W., & Spencer, J. D. (1971). Anthracite Preparation-Past and Present. *Presented at the AIME Centennial Annual Meeting*. New York, New York.

Eichas, K., & Schonert, K. (1993). A Double Drum Separator for Triboelectric Separation of Very Fine Materials. *18th International Mineral Processing Congress* , 417-423.

Fuerstenau, D. W., & Raghavan, S. (1976). Some aspects of the thermodynamics of flotation. *Flotation--A. M. Gaudin Memorial* .

Gaber, A. J. (1969). Removal of Pyrite from Pulverized Coal by Induced Roll Magnetic Separator. *Presented at the Annual Meeting of American Institute of Mining, Metallurgical and Petroleum Engineers*. Washington, D. C .

Ghosh, T. (2013). Modeling of An Ai-based Density Separator.

Gouri Charan, T. R., Chattopadhyay, U. S., Singh, K. P., Kabiraj, S. K., & Haldar, D. D. (2011). Beneficiation of high-ash, Indian non-coking coal by dry jigging. *Minerals & Metallurgical Processing Journal* , 28 (1), 21-23.

Hall, R. D., Given, I. A., Edwards, J. H., Wooton, P., & McCarthy, L. C. (1936). Coal Age-A quarter century of progress in coal mining. 41 (10).

- He, Y. B., & Laskowski, J. S. (1993). The Effect of Dense Media Properties on the Performance of A Dense Medium Cyclone. *Presented at the SME Annual Meeting*. Reno, Nevada.
- Honaker, R. Q., & Mondal, K. (1999). Dynamic modelling of fine particle separations in a hindered bed classifier. *Society for Mining, Metallurgy, and Exploration*. Denver, Colorado.
- Honaker, R. Q., & Patil, D. P. (2002). Parametric evaluation of a dense-medium process using an enhanced gravity separator. *Coal Preparation* , 22 (1), 1-17.
- Honaker, R. Q., Akram, Z., & Groppo, J. (2009). Recovery and utilization of bottom ash magnetics for coal cleaning medium. *In SME Annual Meeting*. Denver, Colorado.
- Honaker, R., Das, A., & Nombe, M. (2005). Fine Coal Cleaning Using A Centrifugal Fluidized Bed Separator . *SME Annual Meeting*. Salt Lake City, Utah.
- Houwelingen, J. A., & De Jong, T. P. R. (2004). Dry cleaning of coal: review, fundamentals and opportunities. *Geologica Belgica* .
- Jiang, X. K., Ban, H., Li, T. X., Schaefer, J. L., Neathery, J. K., & Stencel, J. M. (1999). Quantifying the recovery of beneficiated products from pneumatic triboelectrostatic processing. *SME Annual Meeting*. Denver, Colorado.
- Klima, M., Chander, S., & Subbarayan, S. (1995). Recovery Of Anthracite From Preparation Plant Tailings. *SME Annual Meeting*. Denver, Colorado.
- Knuutila, K. (2006). Carpc Model MIH(13)111-5 Laboratory High-intensity Induced-roll Magnetic Separator.
- Koca, S., Bektas, Y., & Koca, H. (2010). Contact Angle Measurements On Lignite Surface. *25th International Mineral Processing Congress (IMPC) Proceedings*. Brisbane, QLD, Australia.
- Kohmuench, J. N. (2000). *Improving Efficiencies in Water-Based Separators Using Mathematical Analysis Tools* (Doctoral dissertation, Virginia Polytechnic Institute and State University).
- Kohmuench, J. N., Mankosa, M. J., Honaker, R. Q., & Bratton, R. C. (2006). Applications of the CrossFlow teeter-bed separator in the US coal industry. *SME Annual Meeting*. St. Louis, MO.
- Kohmuench, J., Mankosa, M., Yan, E., Wyslouzil, H., Christodoulou, L., & Luttrell, G. (2010). Advances In Coarse Particle Recovery-Fluidised-bed Flotation. *25th International Mineral Processing Congress (IMPC) Proceedings*. Brisbane, QLD, Australia.

- Lawver, J. E., Taylor, J. B., & Knoll, F. S. (1986). Laboratory Testing For Electrostatic Concentration Circuit Design. In *Design and Installation of Concentration and Dewatering Circuits* (pp. 454-477).
- Leonard, J. W. (Ed.). (1979). *Coal Preparation* (4 ed.). The American Institute of Mining, Metallurgical, and Petroleum Engineers .
- Lotz, C. W. (1960). *Notes on the Cleaning of Bituminous Coal*. School of Mines of West Virginia University.
- Luttrell, G. H., Kohmuench, J. N., Stanley, F. L., & Trump, G. D. (1998). Improving Spiral Performance Using Circuit Analysis. *SME Annual Meeting*. Orlando, Florida.
- Manouchehri, H. R., Hanumantha Rao, K., & Forssberg, K. S. E. (2000). Review of electrical separation methods, Part 1 : Fundamental aspects. *Minerals and Metallurgical Processing* , 17 (1).
- Mao, L., & Yoon, R. H. (1997). First-order Flotation Rate Equation Incorporating Hydrodynamic And Surface Forces. *SME Annual Meeting*. Denver, Colorado.
- Meister, W. G. (2009). Anthracite Production and Exports A World Map. *World Coke and Anthracite Conference*. Krakow, Poland.
- Metso Minerals Industries, Inc. (2006). *Brochure of High Gradient Magnetic Separators*.
- Mitchell, D. R. (Ed.). (1950). *Coal Preparation*.
- Mitchell, D. R. (1942). Progress in Air Cleaning of Coal. *Trans. AIME* , 149, 115.
- Mitchell, D. R., & Hewes, R. B. (1943). *Miscellaneous Processes*.
- Officer, E. W. A., & Hamlin, M. (1993). Emission Factor Documentation for AP-42 Section 1.2 Anthracite Coal Combustion.
- Osborne, D. (Ed.). (2013). *The coal handbook Towards cleaner production* (Vol. 1: Coal production).
- Price, J. D., & Bertholf, W. M. (1949). Coal Washing in Colorado and New Mexico. In *AIME Transactions* (Vol. 184, p. 413).
- Srinivasa, V. P. (1981). Heavy Media Separation. *AIME Annual Meeting*. Chicago, Illinois.
- Strydom, H. (2010). The Application of Dual Energy X-ray Transmission Sorting to the Separation of Coal from Torbanite.

- Tao, D., & Al-Hwaiti, M. (2010). Beneficiation study of Eshidiya phosphorites using a rotary triboelectrostatic separator. *Mining Science and Technology (China)* , 20 (3), 357-364.
- Tao, D., Fan, M., & Jiang, X. (2008). An innovative rotary triboelectrostatic separator for fly ash purification. *SME Annual Meeting*. Salt Lake City, Utah.
- Tao, D., Sobhy, A., Li, Q., & Honaker, R. (2010). Dry Fine Coal Cleaning Using Rotary Triboelectrostatic Separator(RTS). *SME Annual Meeting*. Phoenix, AZ.
- Tao, Y., Li, Z., Wang, L., & Zhao, Y. (2011). Applied Research On Teeter Bed Separator In Chengjiao Coal Preparation Plant. *SME Annual Meeting*. Denver, CO.
- Tiernon, C. H. (1980). Concentrating Tables for Fine Coal Cleaning. *Mining Engineering* .
- Tong, Y. (2012). Technical amenability study of laboratory-scale sensor-based ore sorting on a mississippi valley type lead-zinc ore.
- Utz, B. R. (1993). Overview of coal preparation research conducted at the DOE Pittsburgh energy technology center. *SME Annual Meeting*. Reno, Nevada.
- Von Ketelhodt, L., & Bergmann, C. (2010). Dual energy X-ray transmission sorting of coal. *Journal of The Southern African Institute of Mining and Metallurgy* , 110 (7), 371.
- Weiss, N. L. (Ed.). (1985). *SME Mineral Processing Handbook* (Vol. 1). Society of Mining Engineers of the American Institute of Mining, Metallurgical, and Petroleum Engineers.
- Weitkaemper, L., & Wotruba, H. (2010). Effective Dry Density Beneficiation of Coal. *XXV International Mineral Processing Congress (IMPC)*, (pp. 3687-3693). Brisbane, QLD, Australia.
- Zhang, X. X., Duan, D. Y., Tian, B., Wang, J. S., Deng, F., & Zhang, S. (2010). Triboelectrostatic Producing Ultra-Clean Coal. *XXV International Mineral Processing Congress (IMPC) proceedings*. Brisbane, Australia.

VITA

Majid Mahmoodabadi was born in Tehran, Iran. He obtained his bachelor's degree in Mining Engineering from Islamic Azad University South Azad University, Tehran, Iran in January 2008. Upon graduation, he worked as Tunnel Engineer for around 4 years. He joined the program of Master of Science in Mining Engineering Department of University of Kentucky in August 2012.